MRI

EXTENDED EVALUATION OF UNPAVED ROAD DUST SUPPRESSANTS IN THE IRON AND STEEL INDUSTRY

FINAL REPORT

EPA Contract No. 68-02-3177, Assignment No. 14
MRI Project No. 4862-L(14)

Date Prepared: October 7, 1983

Prepared for

Industrial Environmental Research Laboratory
U.S. Environmental Protection Agency
Research Triangle Park, North Carolina 27711

Attn: Mr. Robert McCrillis (MD-63)

EXTENDED EVALUATION OF UNPAVED ROAD DUST SUPPRESSANTS IN THE IRON AND STEEL INDUSTRY

by

Gregory E. Muleski, Thomas Cuscino, Jr., and
Chatten Cowherd, Jr.
Midwest Research Institute
425 Volker Boulevard
Kansas City, Missouri 64110

FINAL REPORT

EPA Contract No. 68-02-3177, Assignment No. 14
MRI Project No. 4862-L(14)

Date Prepared: October 7, 1983

Prepared for

Industrial Environmental Research Laboratory
U.S. Environmental Protection Agency
Research Triangle Park, North Carolina 27711

Attn: Mr. Robert McCrillis (MD-63)

PREFACE

This report was prepared by Midwest Research Institute for the Environmental Protection Agency's Industrial Environmental Research Laboratory under EPA Contract No. 68-02-3177, Work Assignment No. 14. Mr. Robert McCrillis was the project officer. The report was prepared in Midwest Research Institute's Air Quality Assessment Section (Dr. Chatten Cowherd, Head). The authors of this report were Dr. Gregory E. Muleski, Mr. Thomas Cuscino, Jr., task leader, and Dr. Chatten Cowherd. Exposure profiling was conducted in the field under the direction of Mr. Frank Pendleton and Dr. Gregory Muleski with assistance from Mr. David Griffin, Ms. Julia Poythress, Mr. Steve Cummins, and Mr. Thomas Cuscino. Chemical analysis of the captured particulate was performed by Dr. Lloyd Petrie.

Approved for:

MIDWEST RESEARCH INSTITUTE

M. P. Schrag, Director
Environmental Systems Department

October 7, 1983

ABSTRACT

This study was directed to measurement of the long-term control effectiveness of various dust suppressants used to mitigate particulate emissions from vehicular traffic on unpaved roads in the iron and steel industry. Control effectiveness values were determined by emission measurements, utilizing the exposure profiling technique, before and after control application. Control effectiveness was determined for total particulate (TP) and for three particle size (aerodynamic diameter) fractions: ≦ 15 μm, inhalable particulate (IP); ≦ 10 μm (PM_{10}); and ≦ 2.5 μm, fine particulate (FP). Parameters affecting the cost-effectiveness of unpaved road dust suppressants were also quantified, and the trace element composition of uncontrolled unpaved road surface material and airborne dust emissions was examined.

Three dust suppressants used to reduce unpaved road emissions were evaluated during the study: (1) a 20% solution of Petro Tac (an emulsified asphalt) applied at an intensity of 3.2 ℓ/m^2 (0.70 gal/yd^2); (2) water applied at an intensity of 2.0 ℓ/m^2 (0.43 gal/yd^2); and (3) a 20% solution of Coherex® (a petroleum resin) applied at an intensity of 3.8 ℓ/m^2 (0.83 gal/yd^2) followed by a repeat application of 4.5 ℓ/m^2 (1.0 gal/yd^2) of 12% solution 44 days later. Twenty-nine tests of controlled and uncontrolled particulate emissions from vehicular traffic on unpaved roads were conducted.

A decay in control effectiveness, as a function of vehicle passes after application, was measured for the dust suppressants tested. The asphalt emulsion showed an effective lifetime ranging from about 50,000 vehicle passes for control of FP emissions to over 100,000 vehicle passes for control of TP emissions. Unlike the asphalt emulsion, the petroleum resin appeared to control particulate emissions of different size fractions in a consistent manner throughout its lifetime of about 7,500 vehicle passes for the first application. The tests of the reapplication of the petroleum resin provided strong indication of a residual effect from the initial application. The lifetime of the repeat application ranged from 17,000 passes for FP to 45,000 passes for TP. The tests of watering of unpaved roads indicated high initial control efficiency which decreased at a rate of approximately 8%/hr. The rate of control efficiency decay was found to decrease with decreasing particle size.

Comparison of optimal cost-effectiveness values for the dust suppressants evaluated in this study and for the road conditions tested indicates that the chemical techniques are capable of controlling unpaved road PM_{10} emissions for 1/20 to 1/2 the cost of using water. Essentially linear relationships were found between downwind airborne and surface aggregate mass concentrations for the majority of the trace elements detected in the chemical analysis of uncontrolled, unpaved road dust emissions.

CONTENTS

CONTENTS (Concluded)

FIGURES

FIGURES (Concluded)

TABLES

TABLES (Continued)

TABLES (Concluded)

SUMMARY AND CONCLUSIONS

The purpose of this study was to measure the long term control efficiency (effectiveness) of various dust suppressants used in the iron and steel industry to mitigate particulate emissions from vehicular traffic on unpaved roads. Control efficiency values were determined not only for total particulate (TP), but also for particles less than 15 μm in aerodynamic diameter (inhalable particulate, IP), less than 10 μm in aerodynamic diameter (PM_{10}), and less than 2.5 μm in aerodynamic diameter (fine particulate, FP). In addition to control efficiency determination, parameters affecting the cost-effectiveness of unpaved road dust suppressants were quantified, and the trace element composition of uncontrolled unpaved road surface material and airborne dust emissions was examined. Vehicular traffic on unpaved roads was the sole concern of this study because this source was estimated to contribute 56% of the open source suspended particulate emissions in the iron and steel industry.

The exposure profiling method developed by MRI was the technique utilized to measure uncontrolled and controlled emission factors for vehicular traffic on unpaved roads. Exposure profiling of roadway emissions involves direct isokinetic measurement of the total passage of open dust emissions approximately 5 m downwind of the edge of the road by means of simultaneous sampling at four points distributed vertically over the effective height of the dust plume. Downwind particle size distributions were measured at the 1.5 and 4.5 m heights utilizing cyclone precollectors followed by parallel slot cascade impactors. Upwind size distributions were also determined using a cyclone/impactor combination.

Twenty-nine tests of controlled and uncontrolled particulate emissions from vehicular traffic on unpaved roads were conducted. Six of these tests provided uncontrolled, baseline emissions data necessary to determine control efficiency and cost-effectiveness values.

Three dust suppressants used to reduce unpaved road emissions were evaluated during the study:

1. A 20% solution of Petro Tac (an emulsified asphalt) applied at an intensity of 3.2 ℓ/m^2 (0.70 gal/yd^2).

2. Water applied at an intensity of 2.0 ℓ/m^2 (0.43 gal/yd^2).

3. A 20% solution of Coherex® (a petroleum resin) applied at an intensity of 3.8 ℓ/m^2 (0.83 gal/yd^2) followed by a repeat application of 4.5 ℓ/m^2 (1.0 gal/yd^2) of 12% solution 44 days later.

The results presented in this report are directly applicable only to these dilution ratios and application intensities. The chemical dust suppressants

were applied in quantities recommended by the manufacturers. These quantities were, in general, much higher than those currently used at iron and steel plants.

Table SC-1 presents estimated lifetimes and source/control parameters for the dust suppressants evaluated during this study. The lifetimes given are applicable only to situations with the same source/control parameters. The lifetime is the time at which a sufficient number of vehicle passes have caused the control efficiency to decay to zero.

TABLE SC-1. CONTROL EFFICIENCY DECAY RATES

Dust suppressant	Mean vehicle weight (Mg)	Mean No. of wheels	Particle size range	Estimated lifetime (vehicle passes)
Asphalt Emulsion (initial application) 3.2 ℓ/m^2 of 20% solution in water	27	9.2	TP	125,000
			IP	77,000
			PM_{10}	91,000
			FP	53,000
Petroleum Resin (initial application) 3.8 ℓ/m^2 at 20% solution in water	34	6.2	TP	7,100
			IP	7,100
			PM_{10}	7,700
			FP	7,700
Petroleum Resin (reapplication) 4.5 ℓ/m^2 of 12% solution in water	39	6.0	TP	45,000
			IP	26,000
			PM_{10}	23,000
			FP	17,000
Water 1.9 ℓ/m^2	44	6.0	TP	480
			IP	530
			PM_{10}	560
			FP	620

The asphalt emulsion was tested over a period of approximately four months and nearly 50,000 vehicle passes. Although TP emissions showed the lowest initial control efficiency, the control efficiency values associated with particulate emissions in the smaller size ranges showed a much greater rate of decay than that for TP. For example, initial FP control efficiency was substantially greater than that of TP, but the FP control efficiency decay rate was much greater, so that FP emissions nearly matched the uncontrolled state at a time when TP emissions were still controlled at the 50% level.

The tests of watering of unpaved roads indicated high initial control efficiency which decreased at a rate of approximately 8% per hour. The rate of control efficiency decay was found to decrease with decreasing particle size.

The tests of an initial application of a petroleum resin product did not indicate significant variation in the control efficiency decay rate as a function of particle size range. During each test in the 41 day period after application, the measured control efficiency increased with decreasing particle size. Unlike the asphalt emulsion, the petroleum resin appeared to control particulate emissions of different size fractions in a consistent manner throughout its lifetime. In other words, the decay rate for the initial application of the petroleum resin was nearly identical regardless of the particle size.

The tests of the reapplication of the petroleum resin provided strong indication of a residual effect from the initial application. Figure SC-1 compares the PM_{10} control efficiency decay functions for those associated with the initial and repeat applications. The rate of decay for the repeat application was found to be roughly one order of magnitude less than that associated with the initial application. Comparison of the surface aggregate size distribution before and after chemical retreatment suggests that the bonding characteristics of the reapplication are enhanced by a residual effect of the initial treatment.

Comparison of optimal cost-effectiveness values for the dust suppressants evaluated in this study indicates that the chemical techniques are capable of controlling unpaved road PM_{10} emissions for 1/20 to 1/2 the cost of using water. However, it must be noted that direct comparisons between suppressants are difficult at best, even when tests are conducted at the same site, because of changes in vehicle characteristics, traffic rate and the like. Comparisons between suppressants evaluated at different sites are an even more formidable task because there are additional uncontrollable variations in road structure and surface characteristics. Consequently, there are situations where watering, for example, may be more cost-effective than chemical dust suppressants.

Essentially linear relationships were found between downwind airborne and surface aggregate mass concentrations for the majority of the trace elements detected in the chemical analysis of uncontrolled, unpaved road dust emissions. Because of these relationships, it appears possible to economically estimate airborne elemental mass concentrations by examining the corresponding concentrations in the surface material. However, more data are required to substantiate such an approach.

In a comparison designed to accentuate the variation between measurement-based emission factors using 10 m and 6 m profiling towers, the percent difference ranged from 10 to 17%. Because the small differences found in this worst-case comparison are within the experimental accuracy of the profiling method, the difficulties in erecting and operating a 10 m tower at a 5 m distance from the edge of the road are not justified.

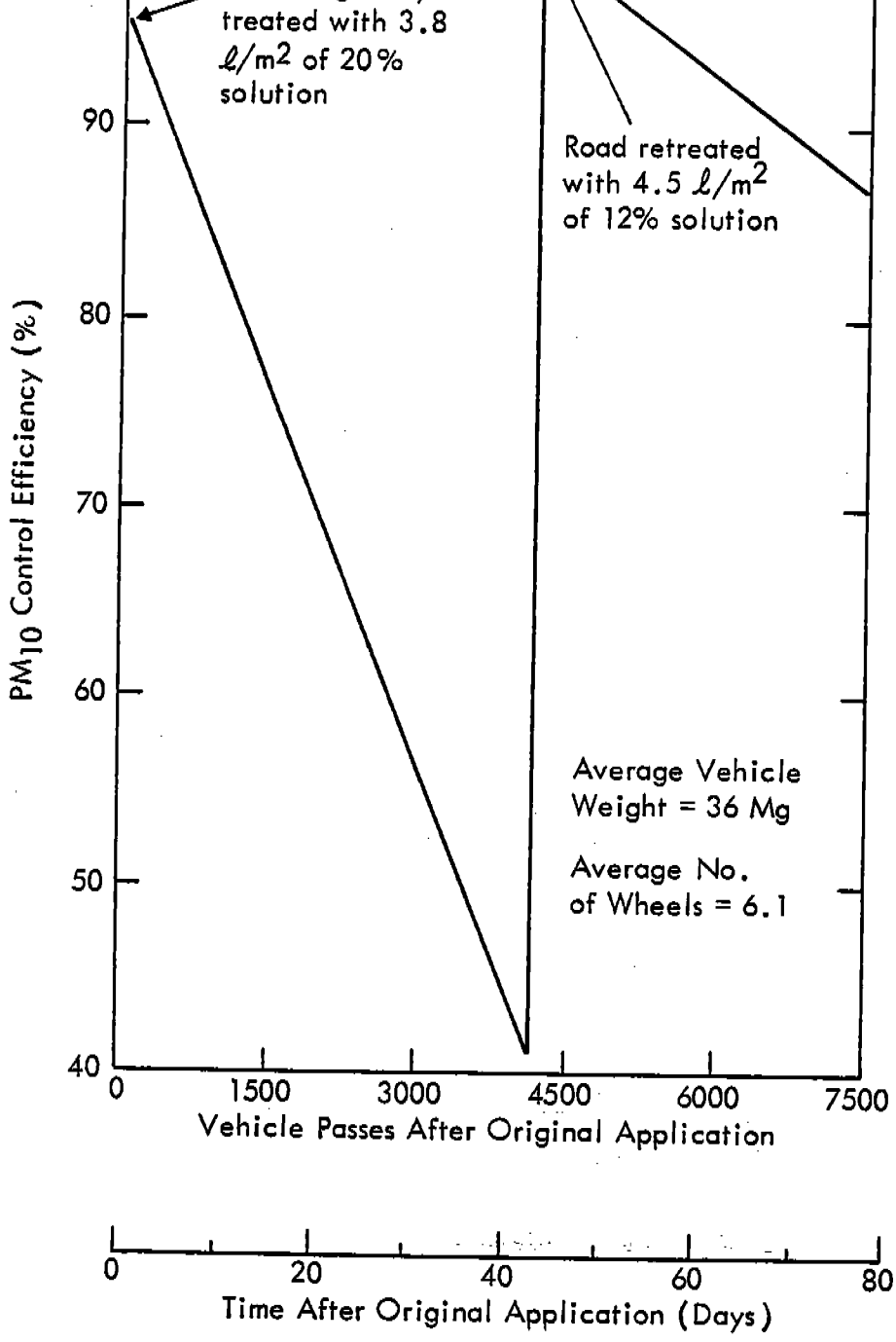

Figure SC-1. Comparison of the control performance for PM_{10} of an initial and a repeat application of a petroleum resin illustrating the residual effect.

Additional work is needed in the area of open dust control evaluation. To truly optimize the cost-effectiveness of a control program designed to meet a minimally acceptable level of average control, a range of application intensities and dilution ratios should be examined. Ideally, enough data should be collected to support a mathematical relationship between average control efficiency and application parameters. The values of application parameters tested should span the ranges commonly employed in the iron and steel industry for the most prevalent dust suppressants. To provide optimization of control performance for a given dust suppressant, each control efficiency decay function should be based on a minimum of three application intensities.

In order to reduce the expense in conducting the field investigations required to characterize dust suppressant performance in the iron and steel industry, effort should be made to identify readily quantifiable source parameters which can be used as measures of control effectiveness. This would enable the tracking of control performance without the need for labor-intensive source testing.

As an additional measure to reduce the amount of costly field testing, a laboratory screening procedure should be developed and implemented. The laboratory procedure could center around wind tunnel exposure of representative samples of aggregate materials. In addition to wind forces, the testing may involve simulation of the forces of vehicle tire/road surface contact. Control performance could be measured as resistance to loss of exposed surface materials. Ideally, the program adopted for the laboratory simulation should produce the same effectiveness ranking for the typical chemicals as that determined by field tests of these chemicals. This would establish the usefulness of the laboratory-based ranking for application to field conditions.

SECTION 1.0

INTRODUCTION

Previous studies have provided strong evidence that open dust sources (such as vehicular traffic on unpaved and paved roads, aggregate material handling, and wind erosion) should occupy a prime position in control strategy development in the iron and steel industry.[1,2,3] This conclusion has been based on comparisons between industry-wide uncontrolled emissions from open dust sources and typically controlled fugitive emissions from major process sources such as steel-making furnaces, blast furnaces, coke ovens, and sinter machines. In addition, preliminary cost-effectiveness (dollars expended per unit mass of reduced particulate emissions) analysis of promising control options for open dust sources has indicated that control of these sources might result in significantly improved air quality at a lower cost compared to the control of process sources.

These preliminary conclusions warranted this study to gather additional data on control performance and costs for open dust sources in the steel industry. Although testing was conducted at iron and steel plants, the control efficiencies presented in this report are applicable to unpaved roads in other industries, providing that the roads have similar traffic and road surface characteristics.

With the publication of the Bubble Policy (Alternative Emissions Reduction Options) in the Federal Register on December 11, 1979 (proposed revisions published April 7, 1982), the economy of controlling open dust sources as compared to implementing more costly controls on stack and process fugitive sources of particulate emissions has been recognized. At the time of this writing, five emission reduction plans (bubbles) in the iron and steel industry involving open dust sources have been published in the Federal Register. The affected plants and the dates of the proposed or final rules are shown below:

Plant	Date	Status
Armco-Middletown Works	March 31, 1981	Final Rule
Shenango-Neville Plant	December 29, 1981	Final Rule
National-Weirton Steel Division	December 9, 1982	Final Rule
National-Granite City Steel Division	December 17, 1982	Proposed Rule
National-Great Lakes Steel Division	December 17, 1982	Proposed Rule

As a requirement of the Bubble Policy, it must be demonstrated that no net gain in emissions occurs from an imaginary bubble surrounding the plant. The emission reduction rate for a controlled open dust source is estimated using the following equation:

$$\Delta R = Me(C)/2{,}000 \qquad (1\text{-}1)$$

where: ΔR = reduction in mass emission rate (tons/year)
M = annual source extent
e = uncontrolled emission factor, i.e., pounds of uncontrolled emissions per unit of source extent
C = average control efficiency expressed as a fraction.

Values for the uncontrolled emission factor (e) in Equation 1-1 can be calculated using the predictive emission factor equations shown in Table 1-1. These predictive equations are the outcomes of numerous prior MRI field tests.[1,2,4,5,6] In those tests, parameters which affect particulate emission levels from open sources, such as moisture and silt contents of the emitting material or equipment characteristics, were identified and measured during the testing process. For those sources with a sufficient number of tests, multiple linear regression formed the basis upon which significant variables were identified and then used in developing the predictive equation.

The annual source extent (M) in Equation 1-1 can be estimated by plant management from plant records and discussions with operating personnel. The variable with the least accurate data to support an estimate of the emission reduction is the control efficiency (C).

Table 1-2 presents a summary of open dust source controls that are or have been used in the iron and steel industry. Control efficiency values are needed for all the techniques shown in Table 1-2. This report focuses on control efficiency quantification for categories IA and IB in Table 1-2.

1.1 VARIABLES AFFECTING CONTROL EFFICIENCY

Control efficiency values for unpaved roads can be affected by four broad categories of variables: (a) time-related variables, (b) control application variables, (c) vehicle characteristics, (d) characteristics of the surface to be treated, and (e) particle size range being considered.

1.1.1 Time-Related Variables

Because of the finite durability of all surface-treatment control techniques, ranging from hours (watering) to years (paving), it is essential to relate an efficiency value to a frequency of application (or maintenance). For measures of lengthy durability, the maintenance program required to sustain control effectiveness should be indicated. One likely pitfall to be avoided is the use of field data collected soon after control measure application to represent the average control efficiency over the lifetime of the measure.

Table 1-1

OPEN DUST EMISSION FACTORS EXPERIMENTALLY DETERMINED BY MRI

Source Category	Measure of Extent	Emission Factor[a] (lb/unit of source extent)
1. Unpaved roads	Vehicle-miles traveled	$5.9 \left(\frac{s}{12}\right) \left(\frac{S}{30}\right) \left(\frac{W}{3}\right)^{0.7} \left(\frac{w}{4}\right)^{0.5} \left(\frac{d}{365}\right)$
2. Paved roads	Vehicle-miles traveled	$0.09\,I \left(\frac{4}{N}\right) \left(\frac{s}{10}\right) \left(\frac{L}{1{,}000}\right) \left(\frac{W}{3}\right)^{0.7}$
3. Batch load-in (e.g., front-end loader, railcar dump)	Tons of material loaded in	$0.0018 \frac{\left(\frac{s}{5}\right) \left(\frac{U}{5}\right) \left(\frac{h}{5}\right)}{\left(\frac{M}{2}\right)^2 \left(\frac{Y}{6}\right)^{0.33}}$
4. Continuous load-in (e.g., stacker, transfer station)	Tons of material loaded in	$0.0018 \frac{\left(\frac{s}{5}\right) \left(\frac{U}{5}\right) \left(\frac{h}{10}\right)}{\left(\frac{M}{2}\right)^2}$
5. Active storage pile wind erosion	Acre-days of exposed storage pile surface	$1.7 \left(\frac{s}{1.5}\right) \left(\frac{d}{235}\right) \left(\frac{F}{15}\right)$
6. Batch load-out (e.g., front-end loader, railcar dump)	Tons of material loaded out	$0.0018 \frac{\left(\frac{s}{5}\right) \left(\frac{U}{5}\right) \left(\frac{h}{5}\right)}{\left(\frac{M}{2}\right)^2 \left(\frac{Y}{6}\right)^{0.33}}$
7. Wind erosion of exposed areas	Acre-years of exposed land	$3{,}400 \frac{\left(\frac{e}{50}\right) \left(\frac{s}{15}\right) \left(\frac{i}{25}\right)}{\left(\frac{P\text{-}E}{50}\right)^2}$

Correction Parameters

- s = Silt content of aggregate or road surface material (%)
- S = Average vehicle speed (mph)
- W = Average vehicle weight (tons)
- L = Surface dust loading on traveled portion of road (lb/mile)
- U = Mean wind speed at 4 m above ground (mph)
- M = Unbound moisture content of aggregate or road surface material (%)
- Y = Dumping device capacity (yd^3)
- d = Number of dry days per year
- i = Percentage of time wind speed exceeds 12 mph at 1 ft above the ground
- e = Surface erodibility (tons/acre/year)
- P-E = Thornthwaite's Precipitation-Evaporation Index
- N = Number of active travel lanes
- I = Industrial road augmentation factor[b]
- w = Average number of vehicle wheels
- h = Drop height (ft)
- F = Percentage of time unobstructed wind speed exceeds 12 mph at mean pile height

a Represents particulate smaller than 30 μm in diameter based on particle density of 2.5 g/cm^3.

b
- Equals 7.0 for trucks coming from unpaved to paved roads and releasing dust from vehicle underbodies;
- Equals 3.5 when 20% of the vehicles are forced to travel temporarily with one set of wheels on an unpaved road berm while passing on narrow roads;
- Equals 1.0 for traffic entirely on paved surface.

TABLE 1-2. SUMMARY OF POTENTIAL OPEN DUST SOURCE CONTROL TECHNIQUES

Source	Control technique
I. Unpaved roads and parking lots.	A. Watering B. Chemical treatment[a] C. Paving D. Oiling
II. Paved roads and parking lots.	A. Sweeping 1. Broom a. Wet b. Dry 2. Vacuum B. Flushing
III. Material handling and storage pile wind erosion.	A. Watering B. Chemical treatment[a]
IV. Conveyor transfer stations.	A. Enclosures B. Water sprays C. Chemical sprays[a]
V. Exposed area wind erosion.	A. Watering B. Chemical treatment[a] C. Vegetation D. Oiling

[a] For example: (1) salts, (2) lignin sulfonates, (3) petroleum resins (4) wetting agents, (5) latex binders, and (6) asphalt emulsions.

The climate, for the most part, accelerates the decay of control performance adversely through weathering. For example, freeze-thaw cycles break up the crust formed by binding agents; heavy precipitation washes away water-soluble chemical treatments like lignin sulfonates or salts; and solar radiation dries out watered surfaces. On the other hand, light precipitation might improve the efficiency of water extenders and hygroscopic chemicals like calcium chloride.

The average control efficiency, C(T), is given by:

$$C(T) = \frac{1}{T} \int_0^T c(t)\, dt \qquad (1\text{-}2)$$

where: $C(T)$ = Average control efficiency during period ending T days after application (percent)

$c(t)$ = Instantaneous control efficiency at t days after application (percent)

T = Time period over which average control efficiency is desired (days)

It must be emphasized that the average control efficiency, in addition to being a function of averaging time, is also heavily dependent upon the variables discussed in the following sections.

1.1.2 Control Application Variables

The control application variables affecting control performance are: (a) application intensity; (b) application frequency; (c) dilution ratio; and (d) application procedure. Application intensity is the volume of solution placed on the surface per unit area of surface. The higher the intensity, the higher the anticipated control efficiency. However, this relationship applies only to a point, because too intense an application will begin to run off the surface. The point where runoff occurs depends on the slope and porosity of the surface.

1.1.3 Vehicle Characteristics

The decay in control efficiency occurs largely because vehicles traveling over the surface impart energy to the treated surface which breaks the adhesive bonds that keeps fine particulate composing the surface from becoming airborne. For example, an increase in vehicle weight and speed serves to accelerate the decay in efficiency for chemical treatment of unpaved roads. Figure 1-1 is a general plot portraying the change in rate of decay of the instantaneous control efficiency for a chemical suppressant applied to an unpaved road as a function of vehicle speed, weight, and traffic rate.

1.1.4 Characteristics of Surface to be Treated

Any surface characteristics which contribute to the breaking of a surface crust will adversely affect the control efficiency. For example, for unpaved road controls, road structure characteristics affect the performance of chemical controls. These characteristics are: (a) combined subgrade and base bearing strength, as measured by the California Bearing Ratio (CBR); (b) amount of fine material (silt and clay) on the surface of the road; and (c) the friability of the road surface material. Low bearing strength causes the road to flex and rut in spots with the passage of heavy trucks; this destroys the compacted surface enhanced by the chemical treatment. A lack of fine material in the wearing surface deprives the chemical

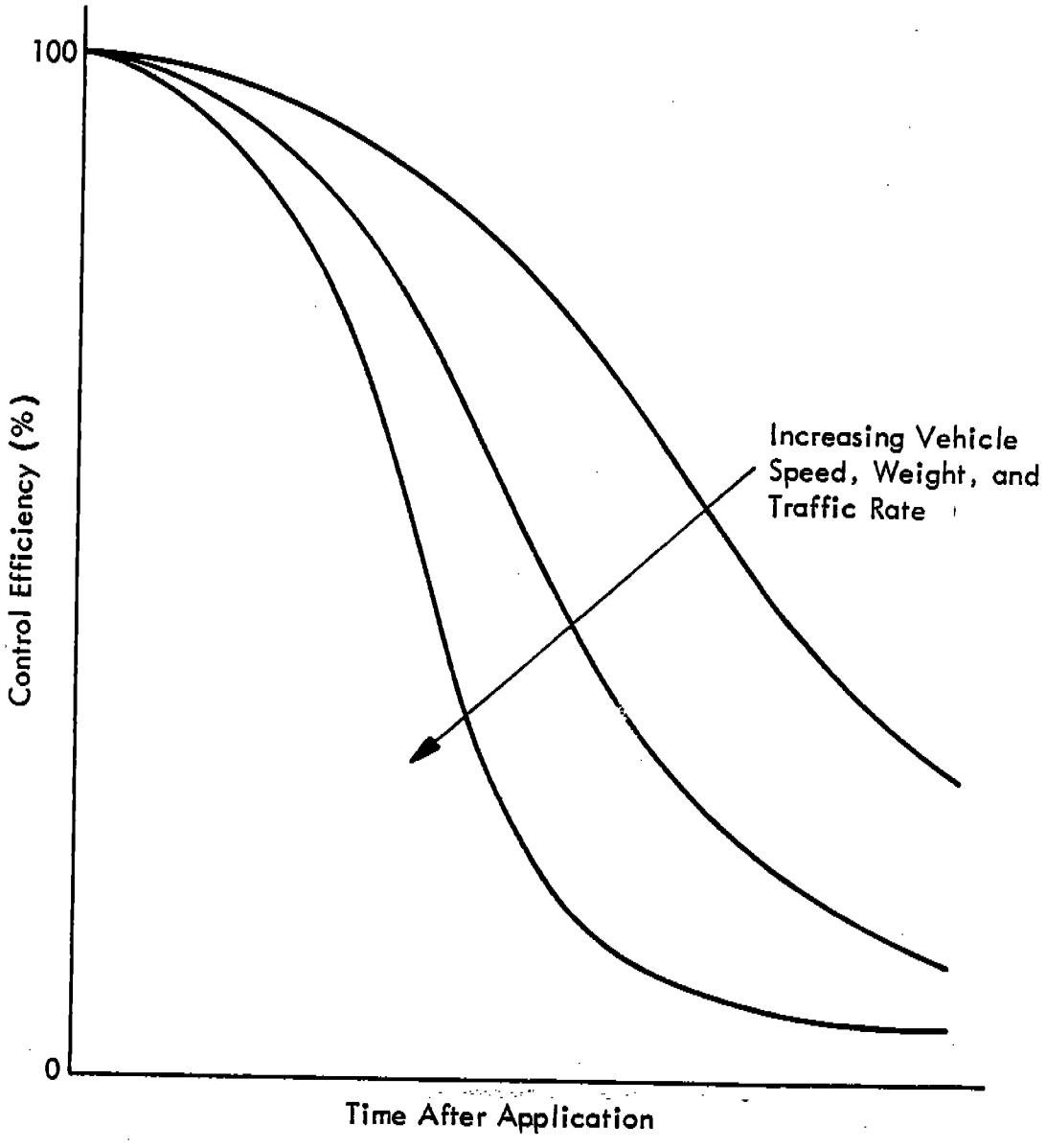

Figure 1-1. Effect of vehicle speed, weight, and traffic rate on control performance.

treatment of the increased particle surface area necessary for interparticle bonding. Finally, the larger particles of a friable wearing surface material simply break up under the weight of the vehicles and cover the treated road with a layer of untreated dust.

1.1.5 Particle Size Range

Another factor affecting the performance of a control measure is the airborne particle size range being considered. On a microscopic level, variation in control efficiency for different size ranges may be viewed as a result of variation of bonding forces for particles with different surface area to volume ratios. Although there are very few data available to predict how the efficiency of a specific control measure will vary with particle size, prior MRI testing suggests that the control efficiency associated with finer particles is less than that for larger particles.[3]

The particle size ranges to be studied in this report are:

- TP Total airborne particulate matter.
- IP Inhalable particulate matter consisting of particles smaller than 15 μm in aerodynamic diameter.
- PM_{10} Particulate matter consisting of particles smaller than 10 μm in aerodynamic diameter.
- FP Fine particulate matter consisting of particles smaller than 2.5 μm in aerodynamic diameter.

1.2 PROJECT OBJECTIVES

The overall objective of this study was to provide data that document the mass of particulate emissions (in several size ranges) generated by vehicular traffic on controlled, unpaved roads in the iron and steel industry. The majority of the data was to provide control efficiencies for common road dust suppressants over the lifetime of each control measure. Thus, the long-term control efficiency decay function associated with each dust suppressants applied to unpaved roads formed the primary goal of this study. It must be emphasized that the chemical control measures were applied following the manufacturer's recommendations for dilution ratio and application intensity, and as such, data presented in this report are directly applicable only to the dilution ratios and application intensities tested.

There were several secondary objectives in this study which follow: (a) calculation of the cost-effectiveness of measures designed to reduce unpaved road dust emissions; (b) comparison of the emission factors obtained with simultaneously operated 6-m and 10-m profiling towers; and (c) determination of the trace elemental composition of particulate emissions from unpaved roads in the iron and steel industry.

1.3 REPORT STRUCTURE

The report is structured as follows: (a) Section 2.0 focuses on the methodology used to quantify pertinent control measures in the iron and steel industry; (b) Section 3.0 presents and discusses the results of source testing with exposure profiling; (c) Section 4.0 presents cost data associated with unpaved road dust control; and (d) Section 5.0 presents the results of special studies conducted during this project. Sections 6.0 through 8.0 present references, glossary, and English to metric conversion units, respectively.

This report contains both metric and English units. In the text, most numbers are reported in metric units with English units in parentheses. For numbers commonly expressed in metric units in the air pollution field, no English equivalent is given, i.e., particle size is in μm, density is in g/cm^3, and concentration is in $\mu g/m^3$.

Numbers in this report are generally rounded to three significant figures; therefore, columns of numbers may not add to the exact total listed. Rounding to three significant figures produces a rounding error of less than 0.5%.

SECTION 2.0

SELECTION OF CONTROL MEASURES, TEST SITES, STUDY DESIGN, AND DESCRIPTION OF TEST METHODOLOGY

This section describes how the unpaved road dust control measures to be tested were selected. Also, the selection criteria for test sites and study design are given. Finally the detailed test methodology is described, including air and surface material sampling, laboratory analysis, and calculation procedures.

2.1 CONTROL MEASURE SELECTION

Historically, the most widely used control measure for unpaved roads, besides watering, has been Coherex® (a petroleum resin). However, because of the sharp rise in prices of petroleum-based products over the past decade, the iron and steel industry has expressed interest in less expensive, alternative chemical controls. These control measures may be either petroleum resin products similar to Coherex® but with lower delivery costs, or products of another nature (such as asphalt emulsions, salts, or lignin sulfonates).

In order to assess the current interest in chemical control of unpaved road dust within the steel industry, a survey was conducted through corporate officials from eight of the largest companies representing 30 of the 45 major steel plants in the country. The results of this survey representing the year 1981 and the first half of 1982 are shown in Table 2-1. The survey results show a strong general interest in unpaved road dust control and a specific interest in petroleum resins. The commitment to watering was not surveyed.

As can be seen, salts and asphalt emulsions rank behind petroleum resin products, in order of preference. The salts mentioned in Table 2-1 are not the conventional products but originate with oil drillers in Ohio who contract the removal of brine water from their fields. The contractor in turn offers to apply this product on unpaved roads at nearby plants at a low cost. No plant surveyed was found to be using conventional salt products on a large scale. Even the brine water was used only during 1981 at iron and steel plants.

Since the future of brine water was uncertain in early 1982 when this testing began, and taking into account the above survey results, Coherex®, the most used petroleum resin, and Petro Tac, the most used asphalt emulsion, were selected as the chemical dust suppressants to be tested. In

TABLE 2-1. SURVEY OF DUST SUPPRESSANT USE ON UNPAVED ROADS IN THE IRON AND STEEL INDUSTRY

Range of interest	Distribution of plant responses				
	Petroleum resins	Asphalt emulsions	Lignin sulfonates	Salts	Total
Committed to use	5	2		3	10
Testing	4		1		5
Considering	5				5
No plans to use chemical controls					10

addition, watering was also selected to be tested, so that its cost-effectiveness could be compared to that of the various dust suppressants and to expand the control efficiency data base.

2.2 TEST SITE SELECTION

Four iron and steel plants were surveyed by MRI personnel for possible test sites. Candidate sites were examined using criteria of: (a) road length and orientation with respect to prevailing winds; (b) traffic mix and rate; (c) upwind/downwind flow obstructions; (d) general meteorology such as mean wind speed, prevailing direction and frequency of precipitation; (e) availability of chemical dust suppressants and application equipment; and (f) proximity to MRI.

The original test plan required the testing of both chemical dust suppressants on contiguous road segments at a single plant. However, it became clear during the site surveys that no candidate test site had road lengths amenable to concurrent testing of different chemical controls on contiguous segments. MRI used the criterion that 240 to 300 m (800 to 1,000 ft) of usable road length was needed per chemical to avoid the tracking of dust from an untreated segment onto the center of the treated segment where testing would occur. However, no candidate test site had a usable road length greater than 340 m (1,100 ft). As a result, it was necessary to test only one chemical per plant. Consequently, two plant sites had to be selected.

The test sites selected were Jones and Laughlin's (J&L's) Indiana Harbor Works and Armco's Kansas City Works. J&L's Indiana Harbor Works was the only candidate test site with enough natural traffic to permit the performance of a complete test during a single period of acceptable daytime winds.

The J&L plant had an additional advantage in that a control program using Petro Tac was just being implemented. The major disadvantage of the J&L plant was a low frequency of acceptable wind direction and speed. The fact that natural traffic at the J&L site was ideal for testing in terms of rate and mix far outweighed any time lost waiting for appropriate winds.

Armco's Kansas City Works was selected as the second test site from the remaining three candidate sites. Because the remaining three sites all required leased traffic in order to generate a measurable 1-day emission rate, it was decided that the increased cost due to traffic leasing could be offset if time lost in the field were reduced by testing close to MRI. Armco's Kansas City site was selected since it is only ten miles from MRI.

2.3 SELECTION OF STUDY DESIGN

In developing a study design to characterize the control performance of unpaved road dust suppressants, both a sampling methodology and a control application plan must be chosen. The sampling method must be able to accurately characterize the dust emissions, and the control application plan must be developed with attention paid to possible interference effects which could impact control efficiency determination.

Unpaved road dust emissions are especially difficult to characterize for the following reasons:

1. Both uncontrolled and controlled emission rates have a high degree of temporal variability.

2. Emissions are comprised of a wide range of particle size (including coarse particles which deposit immediately adjacent to the source) and the control efficiency for different size ranges can vary substantially.

The scheme for quantification of emission factors must effectively deal with these complications to yield source-specific emission data needed to evaluate the priorities for emission control and the effectiveness of control measures.

Two basic techniques have been used in quantifying particulate emissions from vehicular traffic on unpaved roads:

1. The upwind/downwind method involves measurement of concentrations upwind and downwind of the source, utilizing ground-based samplers (usually hi-vol samplers) under known meteorological conditions. Atmospheric dispersion equations are used to back-calculate the emission rate which most nearly produces the measured concentrations. The Gaussian dispersion equations are often applied to cases of near-roadway dispersion. However, the equations generally used were not formulated for such an application.

2. MRI's exposure-profiling method involves direct measurement of the total passage of open dust source emissions immediately downwind of the source by means of simultaneous multipoint sampling over the effective cross section of the open dust source emission plume. This technique uses a

mass-balance calculation scheme similar to EPA Method 5 rather than requiring indirect calculation through the application of a generalized atmospheric dispersion model.

In addition to the above measurement techniques, the study design must also include a control application plan. Two major types of plans have been used:

1. Testing is conducted on two or more contiguous road segments. One segment is left untreated and the others are treated with a separate dust suppressant.

2. Uncontrolled testing is initially performed on one or more road segments. Each segment is then treated with a different chemical; there is no segment left untreated as a reference. A normalization of emissions is required to allow for differences in vehicle characteristics during the uncontrolled and controlled tests as they do not occur simultaneously.

Because of the two choices each for sampling method and control application plan, there are a total four possible study designs. Although the first control application plan allows concurrent testing of both controlled and uncontrolled emissions, it is necessary that a long road be available in order to accommodate the additional uncontrolled segment and to ensure that the control efficiency associated with a treated segment is not affected by the track-on of dust from neighboring uncontrolled segments. As noted in Section 2.2, none of the candidate test sites had road lengths amenable to this plan.

A measurement technique was then required to complete the study design. Because the cost-effectiveness of a control measure cannot be calculated without reliable uncontrolled emission factors, an accurate technique is required to quantify particulate emissions. The most suitable and accurate technique for quantifying unpaved road emissions in the iron and steel industry has been shown to be exposure profiling.[1] The method is source-specific and its increased accuracy over the upwind/downwind method is a result of the fact that emission factor calculation is based on direct measurement of the variable sought, i.e., mass of emissions per unit time.

Thus, the study design used in this testing program employed exposure profiling to first quantify uncontrolled particulate emissions from vehicular traffic on unpaved roads and to then determine control efficiency from normalized controlled emission factors. For a given control measure, uncontrolled and controlled tests were run sequentially on one road segment. This design allowed the determination of not only the control performance but also the cost-effectiveness of the dust suppressants evaluated.

The sampling and analysis procedures followed in this field testing program were subject to certain quality assurance (QA) guidelines. These guidelines will be discussed in conjunction with the activities to which they apply. These procedures met or exceeded the requirements specified in the reports entitled "Quality Assurance Handbook for Air Pollution Measurement Systems, Volume II - Ambient Air Specific Methods" (EPA 600/4-77-027a)

and "Ambient Monitoring Guidelines for Prevention of Significant Deterioration" (EPA 450/2-78-019).

As part of the QA program for this study, routine audits of sampling and analysis procedures were performed. The purpose of the audits was to demonstrate that measurements were made within acceptable control conditions for particulate source sampling and to assess the source testing data for precision and accuracy. Examples of items audited include gravimetric analysis, flow rate calibration, data processing, and emission factor and control efficiency calculation. The mandatory use of specially designed reporting forms for sampling and analysis data obtained in the field and laboratory aided in the auditing procedure. Further detail on specific sampling and analysis procedures are provided in the following sections.

2.4 AIR SAMPLING TECHNIQUES AND EQUIPMENT

The exposure profiling technique utilized in this study is based on the isokinetic profiling concept that is used in conventional source testing. The passage of airborne pollutant immediately downwind of the source is measured directly by means of simultaneous multipoint sampling over the effective cross section of the open dust source plume. This technique uses a mass-balance calculation scheme similar to EPA Method 5 stack testing rather than requiring indirect calculation through the application of a generalized atmospheric dispersion model.

The air samplers used in the field testing are listed in Table 2-2, and the deployment schemes are shown in Figures 2-1 and 2-2, respectively. For measurement of particulate emissions from unpaved roads, profiling sampling heads were distributed over a vertical network positioned just downwind (about 5 m) from the edge of the road. The downwind distance of 5 m was chosen for a number of reasons. This distance is far enough that traffic-generated turbulence does not interfere with sampling, but close enough to the source that a 6-m profiling tower samples substantially all of the mass flux (cf. Section 5.3). In a similar manner, the 10 m distance upwind from the road's edge is far enough from the source that (a) turbulence does not affect sampling, and (b) a sudden gust of wind would not substantially impact the upwind samplers. (Problems of this sort are also minimized by employing directional samplers upwind.) The 10-m distance is, however, close enough to the road to provide the representative background concentration values needed to determine the net (i.e., due to the source) mass flux.

The MRI exposure profiler, originally developed with MRI funds for a 1972 U.S. EPA contract as reported in Reference 5, was used in this study. The profiler (Figure 2-3) consists of a portable tower (6 to 10 m height) supporting an array of sampling heads. During testing, each sampling head was operated as an isokinetic exposure sampler directing passage of the flow stream through a settling chamber and than upward through a standard 20.3-cm by 25.4-cm (8-in. by 10-in.) glass fiber filter positioned horizontally. Sampling intakes were pointed into the wind, and sampling velocity of each intake was adjusted to match the local mean wind speed, as electronically determined by 10-min averages prior to and during the test.

TABLE 2-2. AIR SAMPLING EQUIPMENT

Sampler	Uncontrolled tests		Controlled tests	
	Intake height (m)	Location	Intake height (m)	Location
Profiling head	1.5[a]	downwind	1.5	downwind
	3.0	downwind	3.0	downwind
	4.5	downwind	4.5	downwind
	6.0	downwind	6.0	downwind
Cyclone/impactor	1.5	downwind	1.5	downwind
	4.5	downwind	4.5	downwind
	3.0	upwind	1.5	upwind
Cyclone	1.5[a]	downwind	4.5	upwind
37 mm cassette	1.5	downwind	1.5	downwind
	4.5	downwind	4.5	downwind
	3.0	upwind	1.5	upwind
			4.5	upwind

[a] Spectral™ grade glass fiber filters were used.

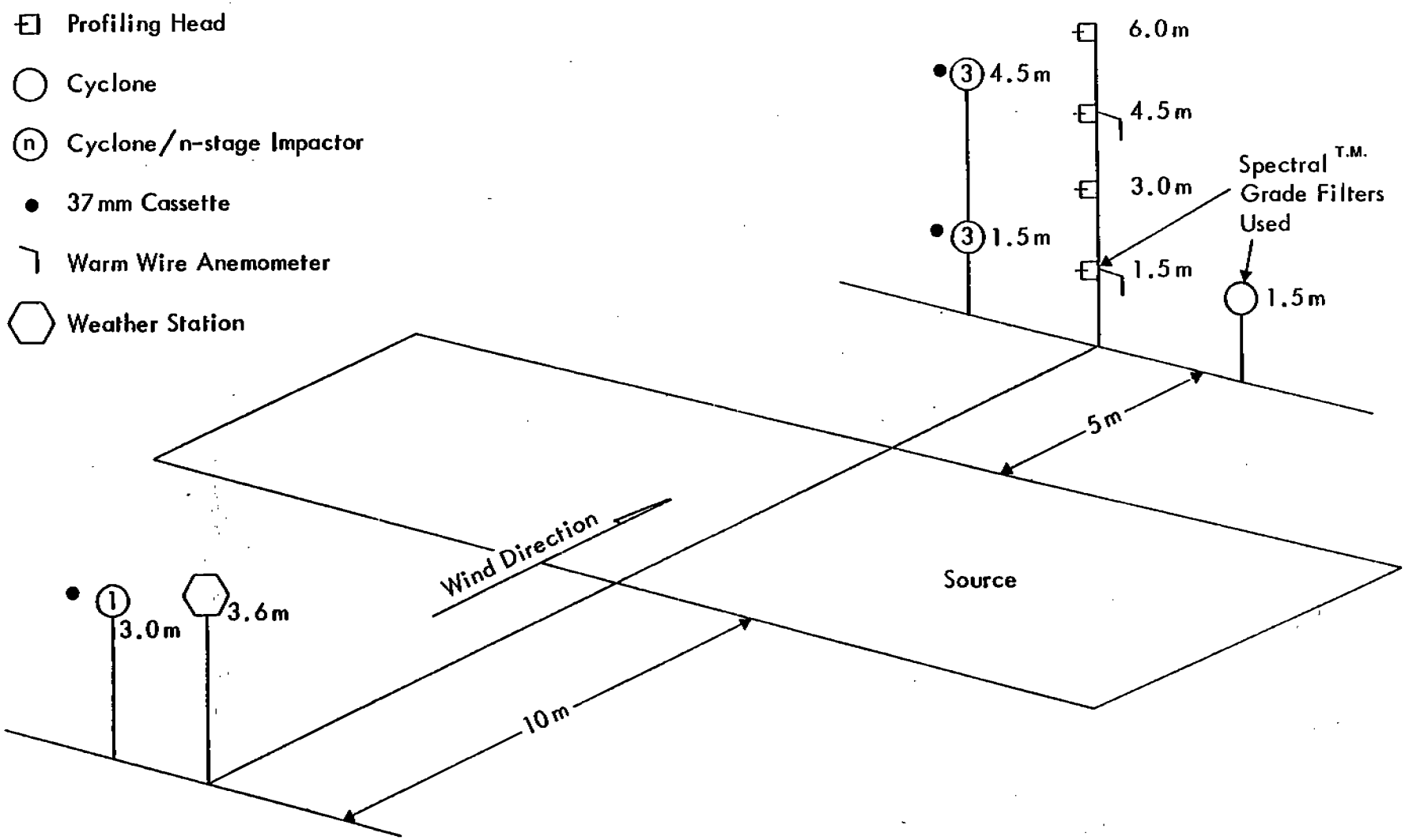

Figure 2-1. Equipment deployment diagram for uncontrolled tests.

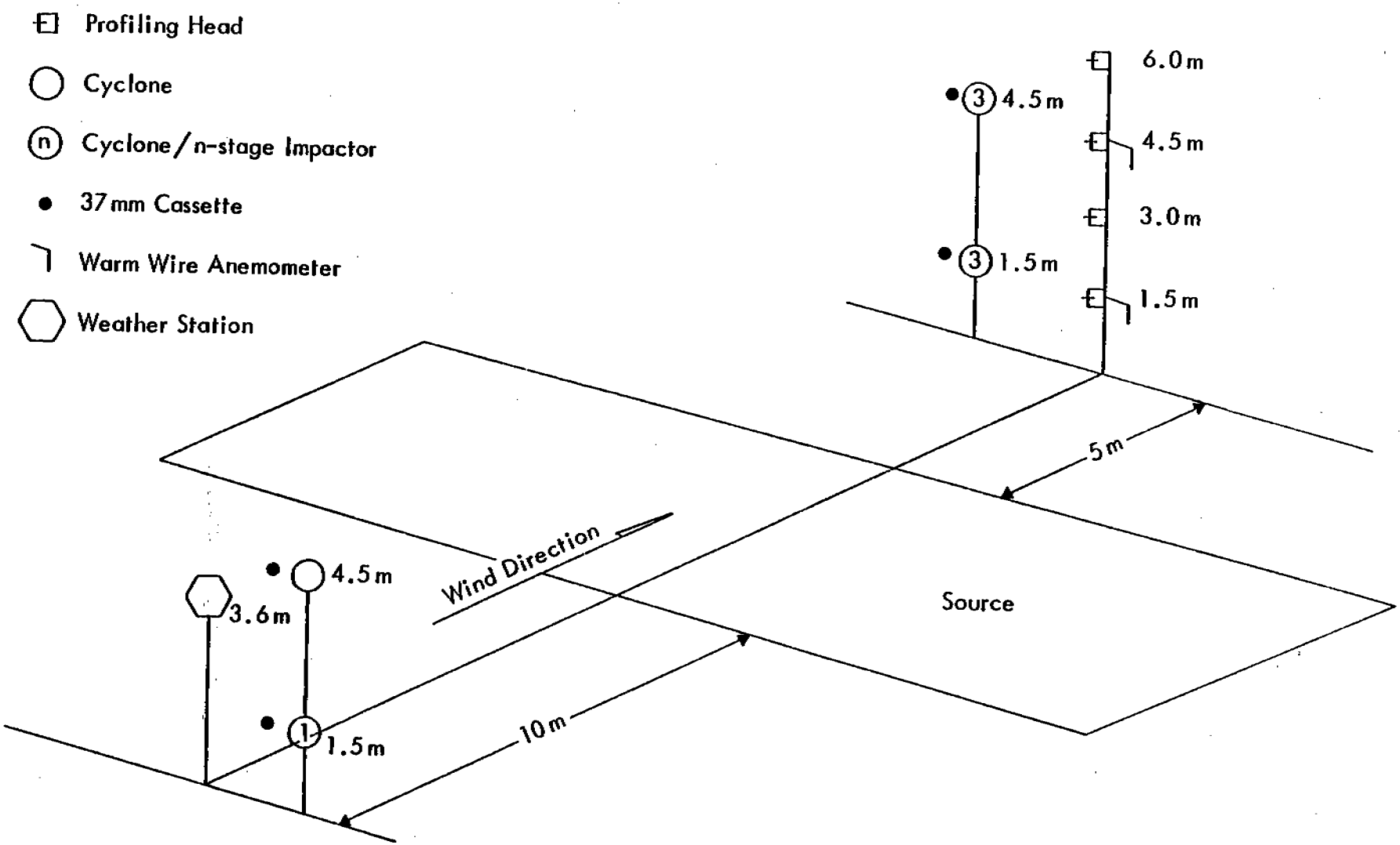

Figure 2-2. Equipment deployment diagram for controlled tests.

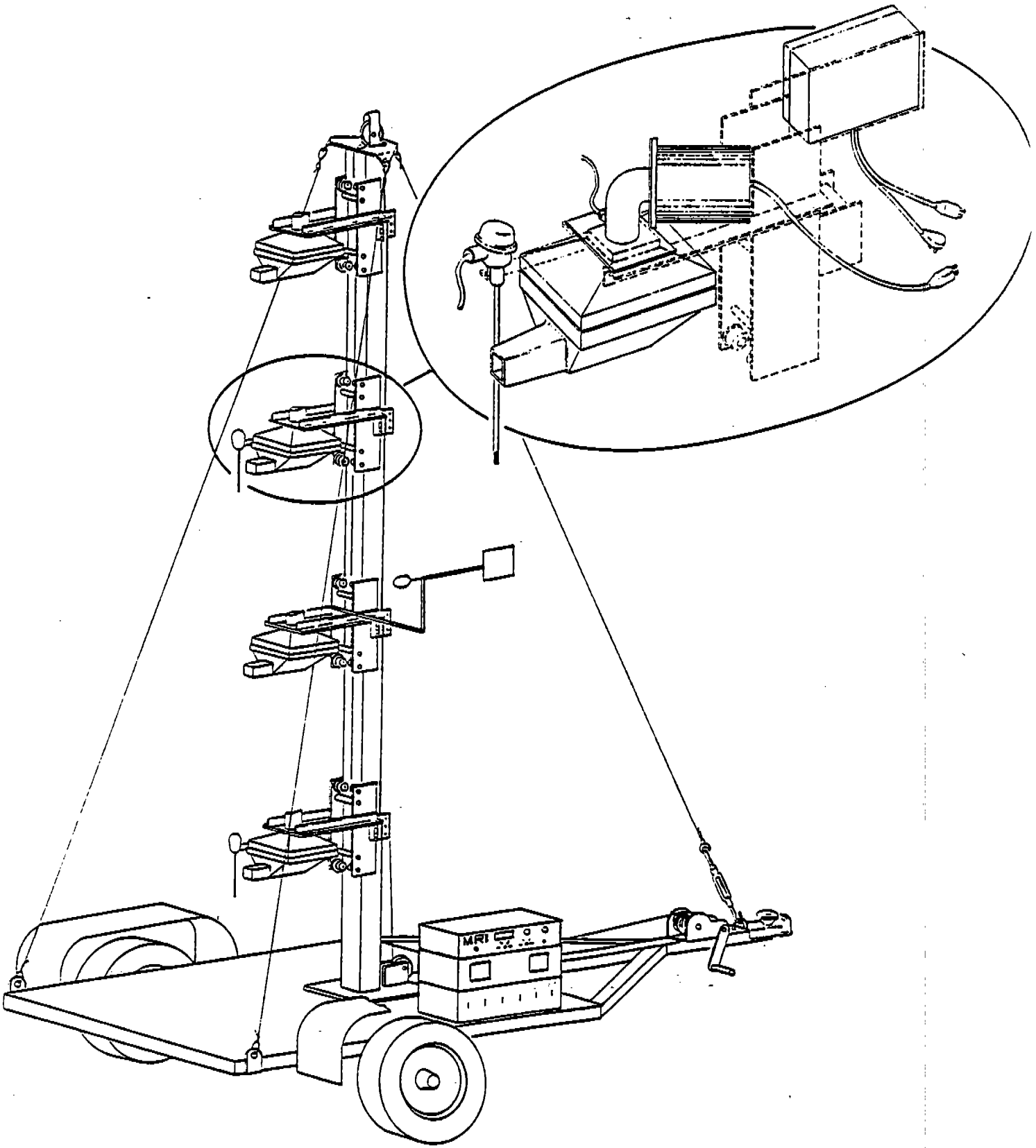

Figure 2-3. MRI exposure profiler.

Throughout each test, wind speed was monitored by warm-wire anemometers at two heights, and the vertical wind speed profile was determined by assuming a logarithmic distribution. Horizontal wind direction was monitored by a wind vane at a single height, and 10-min averages were determined electronically prior to and during the test. The sampling intakes were adjusted for proper directional orientation at 10-min intervals based on the average wind direction.

High volume five-stage slotted cascade impactors (Sierra Instruments, Model No. 230) with 24 m^3/hr (20 cfm) flow controllers were used to measure the downwind particle size distribution at two heights alongside the exposure profiler. Each impactor unit (Figure 2-4) was equipped with a Sierra Model No. 230CP cyclone preseparator to remove coarse particles which otherwise would tend to bounce off the glass fiber impaction substrates, causing fine particle measurement bias. The cyclone preseparator exhibited an effective cutpoint (50% collection efficiency) of 15 microns in aerodynamic diameter (μmA) at 20 ACFM. To further reduce particle bounce problems, each stage of the impactor substrates was sprayed with a stopcock grease solution to provide a sticky impaction surface.

Provision was also made to measure the upwind particle size distribution using a cyclone/impactor combination. Prior testing has shown that a knowledge of the background size distribution is essential in determining control efficiencies for fine particulate emissions. Arrangements were also made to determine whether the upwind particle size distribution varied with height.

The downwind impactors used the first three of the five impaction stages (50% cut-off diameters of 10.2 μmA, 4.2 μmA, and 2.1 μmA at 20 ACFM) while a single stage (3.5 μmA at 20 ACFM) slotted impactor was employed upwind. This special single-stage impactor was used to allow upwind size characterization to be performed in a reasonable amount of time.

In order to determine the particle size distribution of the coarse end of the spectrum, a 37 mm (1.5 in.) cassette sampler was deployed alongside each cyclone/impactor. Optical microscopic analyses of these filters provided information only about largest particle diameters at different heights. However, these values must be considered estimates because shape (in the unseen third dimension) and density are difficult to determine.

Finally, it should be noted that Spectral™ grade glass fiber filters were employed in selected samplers during the uncontrolled tests because these samples were subjected to trace metal analysis.

2.5 EMISSION TESTING PROCEDURE

2.5.1 Preparation of Sample Collection Media

Particulate samples were collected on Type A slotted glass fiber impactor substrates and on Type AE and Spectral™ grade glass fiber filters. As noted in the last section, all glass fiber cascade impactor substrates were greased to reduce the problem of particle bounce. The grease solution

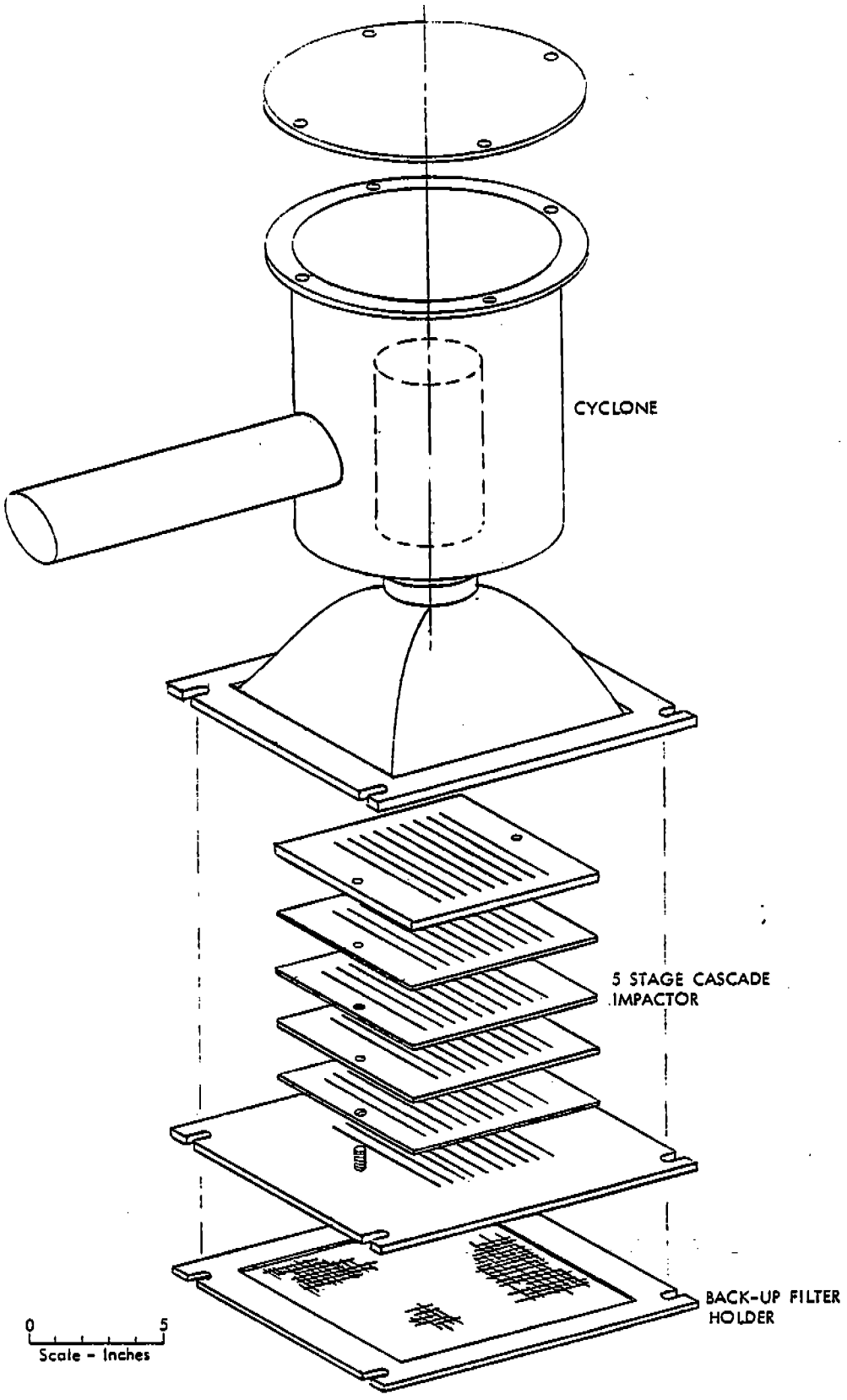

Figure 2-4. Cyclone/cascade impactor combination.

was prepared by dissolving 140 g (4.9 oz) of stopcock grease in 1 liter (0.26 gal) of reagent grade toluene. No grease was applied to the borders and backs of the substrates. The substrates were handled, transported, and stored in specially designed frames which protected the greased surfaces.

Prior to the initial weighing, the filters and greased substrates were equilibrated for 24 hr at constant temperature and humidity in a special weighing room. During weighing, the balance was checked at frequent intervals with standard (Class S) weights to assure accuracy. The filters and substrates remained in the same controlled environment for another 24 hr, after which a second analyst reweighed them as a precision check. If a substrate or filter could not pass audit limits, the entire lot was reweighed. Ten percent of the substrates and filters taken to the field were used as blanks. The quality assurance guidelines pertaining to preparation of sample collection media are presented in Table 2-3.

2.5.2 Pretest Procedures/Evaluation of Sampling Conditions

Prior to equipment deployment, a number of decisions were made as to the potential for acceptable source testing conditions. These decisions were based on forecast information obtained from the local U.S. Weather Service office. Sampling was not planned if there was a high probability of measurable precipitation.

If conditions were considered acceptable, the sampling equipment was transported to the site, and deployment was initiated. The deployment procedure normally took 1 to 2 hr to complete. During this time, the sampling flow rates were set for the various air sampling instruments. The quality control guidelines governing this activity are found in Table 2-4.

Once the source testing equipment was set up and the filters inserted, air sampling commenced. Information was recorded on specially designed reporting forms for quality assurance and included:

a. Exposure profiler - Start/stop times, wind speed profiles, and sampler flow rates (10-min average), and wind direction relative to the roadway perpendicular (10-min average).

b. Other samplers - Start/stop times and flow rates.

c. Traffic count by vehicle type and speed.

d. General meteorology - Wind speed, wind direction, and temperature.

From the information in (a), adjustments could be made to insure isokinetic sampling of both profiler heads (by changing the intake velocity and orientation) and cyclone preseparators (by changing intake nozzles and orientation). Table 2-5 outlines the pertinent QA procedures.

Sampling time was long enough to provide sufficient particulate mass and to average over several units of cyclic fluctuation in the emission rate (i.e., vehicle passes on the road).

TABLE 2-3. QUALITY ASSURANCE PROCEDURES FOR SAMPLING MEDIA

Activity	QA check/requirement
Preparation	Inspect and imprint glass fiber media with identification numbers.
Conditioning	Equilibrate media for 24 hr in clean controlled room with relative humidity of less than 50% (variation of less than ± 5%) and with temperature between 20 C and 25 C (variation of less than ± 3%).
Weighing	Weigh hi-vol filters and impactor substrates to nearest 0.1 mg.
Auditing of weights	Independently verify final weights of 10% of hi-vol filters and impactor substrates (at least four from each batch). Reweigh batch if weights of any hi-vol filters or impactor substrates deviate by more than ± 2.0 mg and ± 1.0 mg, respectively. For tare weights, conduct a 100% audit. Reweigh tare weight of any hi-vol filters or impactor substrates that deviate by more than ± 1.0 mg, and ± 0.5 mg, respectively.
Correction for handling effects	Weigh and handle at least one blank for each 1 to 10 hi-vol filters or impactor substrates of each type for each test.
Calibration of balance	Balance to be calibrated once per year by certified manufacturer's representative. Check prior to each use with laboratory Class S weights.

TABLE 2-4. QUALITY ASSURANCE PROCEDURES FOR SAMPLING FLOW RATES

Activity	QA check/requirement
Calibration	
• Cyclone/impactors	Calibrate flows in operating ranges using calibration orifice upon arrival and every 2 weeks thereafter at each plant prior to testing.
• Profiler heads	Calibrate flows in operating ranges using electronic calibration (Kurz Model 341 warm-wire anemometer) upon arrival and every 2 weeks thereafter at each regional site prior to testing.
• Orifice and electronic calibrator	Calibrate against displaced volume test meter annually.
Single-point flowrate checks	
• Primary procedure for profilers, hi-vols, and impactors	Check 25% of units with rotameter, calibration orifice, or electronic calibrator (warm-wire anemometer) once at each site within the plant prior to testing (different units each time). If any flows deviate by more than 7%, check all other units of same type and recalibrate non-complying units. (See alternative below.)

TABLE 2-5. QUALITY ASSURANCE PROCEDURES FOR SAMPLING EQUIPMENT

Activity	QA check/requirement
Maintenance	
· All samplers	Check motors, gaskets, timers, and flow measuring devices at each plant prior to testing.
Operation	
· Timing	Start and stop all samplers during time span not exceeding 1 min.
· Isokinetic sampling (profilers only)	Adjust sampling intake orientation whenever mean (10 min average) wind direction changes by more than 30°.
	Adjust intake velocity whenever mean (10 min average) wind speed approaching sampler changes by more than 20%.
· Isokinetic sampling (cyclone/impactors)	Adjust sampling intake orientation whenever adjustments are made to the exposure profiler intake orientation.
	Change the cyclone intake nozzle whenever the mean (10 min average) wind speed approaching the sampler falls outside of the suggested bounds for that nozzle. This technique allocates no nozzle for wind speeds ranging from 0-6 mph, and unique nozzles for each of the wind speed ranges 6-8, 8-11, 11-15, and 15-20 mph.
· Prevention of static mode deposition	Cap sampler inlets prior to and immediately after sampling.

Sampling lasted from 31 min to over 4 hr depending on the source and control measure (if any). Occasionally, sampling was interrupted due to occurrence of unacceptable meteorological conditions and then restarted when suitable conditions returned. Table 2-6 presents the criteria used for suspending or terminating a source test.

TABLE 2-6. CRITERIA FOR SUSPENDING OR TERMINATING AN EXPOSURE PROFILING TEST

A test may be suspended or terminated if:[a]

1. Rainfall ensues during equipment setup or when sampling is in progress.
2. Mean wind speed during sampling moves outside the 1.8 to 8.9 m/s (4 to 20 mph) acceptable range for more than 20% of the sampling time.
3. The angle between mean wind direction and the perpendicular to the path of the moving point source during sampling exceeds 45° for two consecutive 10 min averaging periods.
4. Daylight is insufficient for safe equipment operation.
5. Source condition deviates from predetermined criteria (e.g., occurrence of truck spill, or accidental water splashing prior to uncontrolled testing).

[a] "Mean" denotes a 10-min average.

2.5.3 Sample Handling and Analysis

To prevent particulate losses, the exposed media were carefully transferred at the end of each run to protective containers within the MRI instrument van. In the field laboratory, exposed filters were placed in individual glassine envelopes and then into numbered file folders. Impactor substrates were replaced in the protective frames. Particulate that collected on the interior surfaces of profiler intakes and cyclone preseparators was rinsed with distilled water into separate sample jars which were then capped and taped shut.

When exposed substrates and filters (and the associated blanks) were returned to the MRI laboratory, they were equilibrated under the same conditions as the initial weighing. After reweighing, 10% were audited to check weighing accuracy.

To determine the sample weight of particulate collected on the interior surfaces of samplers, the entire wash solution was passed through a 47 mm (1.8 in) Buchner type funnel holding a glass fiber filter under suction. This water was passed through the Buchner funnel ensuring collection of all suspended material on the 47 mm filter which was then dried in an oven at

100°C for 24 hr. After drying, the filters were conditioned at constant temperature and humidity for 24 hr.

All wash filters were weighed with a 100% audit of tared and a 10% audit of exposed filters. Blank values were determined by washing "clean" (unexposed) profiler intakes in the field and following the above procedures.

2.5.4 Emission Factor Calculation Procedure

To calculate emission rates using the exposure profiling technique, a conservation of mass approach is used. The passage of airborne particulate (i.e., the quantity of emissions per unit of source activity) is obtained by spatial integration of distributed measurements of exposure (mass/area) over the effective cross section of the plume. Exposure is the point value of the flux (mass/area-time) of airborne particulate integrated over the time of measurement, or equivalently, the net particulate mass passing through a unit area normal to the mean wind direction during the test. The steps in the calculation procedure are described below.

Particulate Concentrations--

The concentration of particulate matter measured by a sampler is given by:

$$C = 10^3 \frac{m}{Qt}$$

where: C = particulate concentration ($\mu g/m^3$)
m = particulate sample weight (mg)
Q = sampler flow rate (m^3/min)
t = duration of sampling (min)

The specific particulate matter concentrations were determined from the various particulate catches as follows:

Size range	Particulate catches
TP	Profiler filter + intake or cyclone + impactor substrates + backup filter
IP	Impactor substrates + backup filter
PM_{10}	Impactor substrates + backup filter
FP	Impactor substrates + backup filter

To be consistent with the National Ambient Air Quality Standard for total suspended particulate (TSP), all concentrations and flow rates were expressed in standard conditions (25°C and 101 kPa or 77°F and 29.92 in Hg).

Isokinetic Flow Ratio--

The isokinetic flow ratio (IFR) is the ratio of a directional sampler's intake air speed to the mean wind speed approaching the sampler. It is given by:

$$IFR = \frac{Q}{aU}$$

where: Q = sampler flow rate (m^3/min)
a = intake area of sampler (m^2)
U = mean wind speed at height of sampler (m/min)

This ratio is of interest in the sampling of TP, since isokinetic sampling assures that particles of all sizes are sampled without bias. In this study, profilers and cyclone preseparators were the directional samplers used.

Occasionally it is necessary to sample at a superisokinetic flow rate (IFR > 1.0), to obtain sufficient sample under light wind conditions, the following multiplicative factors can be used to correct measured exposures and concentrations to corresponding isokinetic values:

	Small particles (d < 5 μmA)	Large particles (d > 50 μmA)
Exposure Multiplier	1/IFR	1
Concentration Multiplier	1	IFR

A separate IFR is calculated for each profiler head based on the measured values of Q and U.

These correction factors for nonisokinetic TP concentrations are based on a relationship developed by Davies.[8] The relationship as applied to exposure profiling in the ambient atmosphere is as follows:

$$\frac{C_n}{C_t} = \frac{1}{IFR} - \frac{(1/IFR) - 1}{4Y + 1}$$

where

C_n = Nonisokinetic concentration of particles of diameter d
C_t = True concentration of particles of diameter d
Y = Inertial impaction parameter = d^2 c (ρ_p - ρ) U/18μ D
D = Diameter of probe
d = Diameter of particle
ρ = Density of air
μ = Viscosity of air
ρ_p = Density of particle
c = Cunningham correction factor

From Davies' equation, it is clear that, for very small d, $C_n = C_t$, and that, for large values of d, $C_n = C_t/IFR$. These observations lead to the simplified correction factors presented in the above table.

Using the simplified MRI approach for a particle-size distribution containing a mixture of small, intermediate, and large particles, the isokinetic correction factor is an average of the above multipliers weighted by the relative proportion of large and small particles. For example, if the mass of small particles in the distribution equals twice the mass of the large particles, the weighted isokinetic correction for exposure would be:

$$(1 + 2/IFR)/3$$

A more rigorous value for the average ratio ($\bar{R}$) of nonisokinetic to true concentration can be found by integrating the product of the particle size distribution and Davies' relationship over all possible particle diameters. An isokinetically corrected concentration can then be calculated as

$$C_t = C_n/\bar{R}$$

Using a log-normal distribution of particle diameters, the isokinetically corrected concentrations obtained by the $\bar{R}$-method and by MRI's simplified multiplicative correction factor method differ by less than 20% for IFR values between 0.2 and 1.5, by less than 30% in the range of 1.5 to 2.0, and by less than 60% for IFR values between 2.0 and 3.0.

Because the particle-size distribution and the isokinetic corrections are interrelated, isokinetic corrections are of an iterative nature. In the present study, isokinetic corrections based on the two methods described above were iterated until a convergence criterion of 1% difference between successive TP concentration values was satisfied. An average of the two methods was then employed.

Downwind Particle-Size Distributions--

Particle-size distributions were determined by plotting ratios of the cumulative concentrations measured by each impactor stage to the total concentration against the 50% cutoff diameters presented in Section 2.4.2. The total concentration measured by the profiler was used in place of that measured by the cyclone/impactor combination because the profiler was generally closer to the isokinetic condition. This was true simply because the intake velocity of the profiler is infinitely adjustable while discrete nozzle sizes must be used for the cyclone. These data were fitted to a log-normal mass size distribution after correction for particle bounce. The distributions obtained at two heights in the source plume were then used to determine the mass fractions corresponding to various particle-size ranges as a function of height. The mass fractions were assumed to vary linearly with height.

The technique used in this study to correct for the effects of particle bounce has been discussed in earlier MRI studies.[1,2,3] Simultaneous cascade

impactor measurements of airborne particle-size distribution with and without a cyclone precollector indicate that the cyclone precollector is quite effective in reducing fine particle measurement bias. However, even with the cyclone precollector, a monotonic decrease in collected particle weight on each successive impaction stage is frequently followed by a several-fold increase in weight collected on the back-up filter. But, because the assumed value (0.2 μm) for the effective cutoff diameter of the glass fiber back-up filter fits the progression of cutoff diameters for the impaction stages, the weight collected on the back-up filter should be consistent with the decreasing pattern shown by the weight collected on the impactor stages.[2] The excess particulate on the back-up filter is postulated to consist of coarse particles that penetrated the cyclone (with small probability) and bounced through the impactor. Although particle bounce is further reduced by greasing impaction substrates, it is not completely eliminated. A more complete discussion of techniques used to reduce the effects of particle bounce is presented in Appendix C.

To correct the measured particle size distribution for the effects of residual particle bounce, the following procedure was used in approximately 40% of the cases:

1. The calibrated cutoff diameter for the cyclone preseparator is used to fix the upper end of the particle-size distribution.

2. The lower end of the particle size distribution is fixed by the cutoff diameter of the last stage used (Stage 3) and the measured (or corrected, if necessary) mass fraction collected on the back-up filter. The corrected fraction collected on the back-up filter is calculated as the average of the fractions measured on the two preceding stages (Stages 2 and 3).

When a corrected mass is required, excess particulate mass is effectively removed from the back-up filter. However, because no clear procedure existed for apportioning the excess mass back onto the impaction stages, the size distribution determined from tests with particle bounce problems was constructed using the log-normal assumption and two points--the mass fraction collected in the cyclone and the corrected mass fraction collected on the back-up filter. The mass fraction associated with the first impaction stage lies very near this line.

Particulate Exposures and Profile Integration--

For directional samplers operated isokinetically, total particulate exposures are calculated by:

$$E = 10^{-7} \times CUt$$

where: E = total particulate exposure (mg/cm^2)
C = net TP concentration ($\mu g/m^3$)
U = approaching wind speed (m/s)
t = duration of sampling (s)

The exposure values vary over the height of the plume. If exposure is integrated over the height of the plume, then the quantity obtained represents the total passage of airborne particulate matter due to the source per unit length of the line source. This quantity is called the integrated exposure A and is found by:

$$A = \int_0^H E \, dh$$

where: A = integrated exposure (m-mg/cm^2)
E = particulate exposure (mg/cm^2)
h = vertical distance coordinate (m)
H = effective extent of plume above ground (m)

The effective height of the plume is found by linear extrapolation of the uppermost net TP concentrations to a value of zero.

Because exposures are measured at discrete heights of the plume, a numerical integration is necessary to determine A. The exposure must equal zero at the vertical extremes of the profile (i.e., at the ground where the wind velocity equals zero and at the effective height of the plume where the net concentration equals zero). However, the maximum TP exposure usually occurs below a height of 1 m, so that there is a sharp decay in TP exposure near the ground. To account for this sharp decay, the value of exposure at the ground level is set equal to the value at a height of 1 m. The integration is then performed using Simpson's rule.

Particulate Emission Factor--

The emission factor for total airborne particulate generated by vehicular traffic on a straight road segment expressed in grams of emissions per vehicle-kilometer-traveled (VKT) is given by:

$$e = 10^4 \frac{A}{N}$$

where: e = total particulate emission factor (g/VKT)
A = integrated exposure (m-mg/cm^2)
N = number of good vehicle passes (dimensionless)

Other Emission Factors--

Particulate emission factors for IP, PM_{10}, and FP are found in a manner analogous to that described above for TP. The concentrations corresponding to these size ranges are determined from the particle size distribution discussed earlier. A linear fit of the mass fractions at 1.5 m and 4.5 m is used to determine mass fractions at the other heights of the profile. Once net concentrations are determined, exposure values and emission factors are obtained in a manner identical to that for TP.

2.5.5 Control Efficiency Calculation Procedure

Although controlled and uncontrolled tests were conducted at the same site, it was necessary to obtain normalized values of emission factors in

order to make meaningful comparisons. This is true simply because the vehicle mix on the test road varied not only from day to day but also during different shifts during individual days. Thus, measurement-based emission factors required normalization in order that a change in vehicle mix was not mistakenly interpreted as part of the efficiency of the control measure being tested.

The method used in this study to normalize emission factors is based on MRI's experimentally determined predictive emission factor equation for uncontrolled unpaved roads and is identical to the process used in an earlier report.[3] The emission factors are scaled by:

$$e_n = e_i\left(\frac{S_n}{S_i}\right)\left(\frac{W_n}{W_i}\right)^{0.7}\left(\frac{w_n}{w_i}\right)^{0.5}$$

where: e_n = normalized value of the emission factor corresponding to run i

e_i = measured emission factor from run i

S_n = normalizing value for average vehicle speed

S_i = average vehicle speed during run i

W_n = normalizing value for average vehicle weight

W_i = average vehicle weight during run i

w_n = normalizing value for average number of wheels per vehicle pass

w_i = average number of wheels per vehicle pass during run i

The control efficiency in percent (c) is then found as

$$c = \left(1 - \frac{e_c}{\bar{e}_u}\right) \times 100\%$$

where: e_c = normalized emission factor for controlled road

$\bar{e}_u$ = geometric mean of normalized emission factors for uncontrolled roads

The normalization process varied slightly for the testing at J&L's Indiana Harbor Works. At the onset of testing approximately 1 month after application, it was found that the north and south portions of the road exhibited different rates of control efficiency decay. This was possibly due to the queuing of 18-wheel trucks on the south half of the road to use the

weigh station. When there were several trucks waiting in the line at the scale, the south side of the road was subjected to stop and go traffic. It is believed that the larger friction forces associated with braking and accelerating caused the much more rapid decay of control observed on the south side of the road. Because of the different rates of decay, it was necessary to apportion emissions between the two halves of the road.

The procedure used in the apportionment was based on the observation that the surface dust loading on each side of the road steadily increased during the course of testing. This quantity is an indication of the amount of material capable of becoming airborne. Furthermore, because unpaved road dust emissions are known to have a strong, positive correlation with the silt content (particles < 74 μm in diameter) of the surface aggregate, the apportionment process was based on the amount of silt available for re-entrainment.

The total emission rate is given by:

$$E_T (N_1 + N_2) = N_1 E_1 + N_2 E_2$$

where: E_T = measurement-based (overall) emission factor (mass/length-vehicle)

i = index for north or south side of road

N_i = number of vehicle passes on side i

E_i = emission factor for side i (mass/length-vehicle)

The total emission factor was apportioned to each side of the road by the number of vehicle passes and the silt loading for that side by use of the following equation:

$$E_i = \frac{s_i L_i (N_1 + N_2)}{s_1 L_1 N_1 + s_2 L_2 N_2} E_T$$

where: s_i = silt content for side i (%)
L_i = surface loading (mass/length)

In order to corroborate the apportionment technique, the traffic during one test was restricted to only one side of the road. The measurement-based emission factors for this test could then be compared to the corresponding apportioned emission factors from the previous tests.

Once the overall emission factor was apportioned over the two sides of the road, the two apportioned as well as the overall emission factors were then normalized following the procedure described above.

2.6 AGGREGATE MATERIAL SAMPLING AND ANALYSIS

Samples of the loose road surface were taken from lateral strips of known area (generally, the width of the road by 30 cm) during the course of

this study. These were analyzed for silt (those particles passing a 200 mesh screen) and moisture contents and to determine road surface loading values. Detailed steps for collection and analysis of samples for silt and moisture are given in a previous report.[5] An abbreviated discussion is presented below.

Roadway dust samples were collected by sweeping the loose layer of soil, slag, or crushed rock from the hardpan road base with a broom and dust pan. Sweeping was performed so that the road base was not abraded by the broom, and so that only the naturally occurring loose dust was collected. The sweeping was performed slowly so that dust was not entrained into the atmosphere.

Once the field sample was obtained, it was prepared for analysis. The field sample was split (if necessary) with a riffle to a sample size amenable to laboratory analysis. The basic procedure for moisture analysis was determination of weight loss upon oven drying. Table 2-7 presents a step-by-step procedure for determining moisture content. Moisture analysis was usually performed in the field laboratory on the same day as sample collection. In this fashion, the measured value was a more reliable estimate of the field conditions at the time of the test.

The basic procedure for silt analysis was mechanical, dry sieving. A step-by-step procedure is given in Table 2-8. The silt analysis was performed upon return to the main MRI laboratories.

The surface aggregate samples collected during the uncontrolled tests at the two plants were subjected to an additional analysis. After mechanical sieving, these samples were then sieved using a sonic sifter (ATM Sonic Sifter, Model L3PF). The purpose of this additional sieving was twofold: (a) to determine the size distribution of the silt content; and (b) to provide surface aggregate samples of different size ranges for trace metal analysis. Table 2-9 outlines the procedure followed in sonic sieving.

2.7 AUXILIARY EQUIPMENT AND SAMPLES

Provision was made to quantify additional parameters which affect the performance of a control measure applied to unpaved roads. As discussed in Section 1.1, these parameters include:

1. Intensity of the control application;
2. Number of vehicle passes following application; and
3. Vehicle mix of traffic on the controlled road.
4. Vehicle speed measured by a hand-held radar gun.

Because the efficiency associated with a control measure is only directly applicable to a particular dilution ratio and application intensity, arrangement was made to better quantify these variables.

TABLE 2-7. MOISTURE ANALYSIS PROCEDURES

1. Preheat the oven to approximately 110°C (230°F). Record oven temperature.

2. Tare the laboratory sample containers which will be placed in the oven. Tare the containers with the lids on if they have lids. Record the tare weight(s). Check zero before weighing.

3. Record the make, capacity, smallest division, and accuracy of the scale.

4. Weigh the laboratory sample in the container(s). Record the combined weight(s). Check zero before weighing.

5. Place sample in oven and dry overnight.[a]

6. Remove sample container from oven and (a) weigh immediately if uncovered, being careful of the hot container; or (b) place tight-fitting lid on the container and let cool before weighing. Record the combined sample and container weight(s). Check zero before weighing.

7. Calculate the moisture as the initial weight of the sample and container minus the oven-dried weight of the sample and container divided by the initial weight of the sample alone. Record the value.

8. Calculate the sample weight to be used in the silt analysis as the oven-dried weight of the sample and container minus the weight of the container. Record the value.

[a] Dry materials composed of hydrated minerals or organic materials like coal and certain soils for only 1-1/2 hr. Because of this short drying time, material dried for only 1-1/2 hr must not be more than 2.5 cm (1 in.) deep in the container.

TABLE 2-8. SILT ANALYSIS PROCEDURES

1. Select the appropriate 8-in. diameter, 2-in. deep sieve sizes. Recommended U.S. Standard Series sizes are: 3/8-in., No. 4, No. 20, No. 40, No. 100, No. 140, No. 200, and a pan. Comparable Tyler Series sizes can also be utilized. The No. 20 and the No. 200 are mandatory. The others can be varied if the recommended sieves are not available or if buildup on one particular sieve during sieving indicates that an intermediate sieve should be inserted.

2. Obtain a mechanical sieving device such as a vibratory shaker or a Roto-Tap (without the tapping function).

3. Clean the sieves with compressed air and/or a soft brush. Material lodged in the sieve openings or adhering to the sides of the sieve should be removed (if possible) without handling the screen roughly.

4. Obtain a scale (capacity of at least 1,600 g) and record make, capacity, smallest division, date of last calibration, and accuracy.

5. Tare sieves and pan. Check the zero before every weighing. Record weights.

6. After nesting the sieves in decreasing order with the pan at the bottom, dump dried laboratory sample (probably immediately after moisture analysis) into the top sieve. The sample should weigh between 800 and 1600 g (1.8 and 3.5 lb).[a] Brush fine material adhering to the sides of the container into the top sieve and cover the top sieve with a special lid normally purchased with the pan.

7. Place nested sieves into the mechanical device and sieve for 10 min. Remove pan containing minus No. 200 and weigh. Repeat the sieving in 10 min intervals until the difference between two successive pan sample weighings (where the tare of the pan has been subtracted) is less than 3.0%. Do not sieve longer than 40 min.

8. Weigh each sieve and its contents and record the weight. Check the zero before every weighing.

9. Collect the laboratory sample and place the sample in a separate container if further analysis is expected.

10. Calculate the percent of mass less than the 200 mesh screen (75 μm). This is the silt content.

[a] This amount will vary for finer textured materials; 100 to 300 grams may be sufficient when 90 percent of the sample passes a No. 8 (2.36 mm) sieve.

TABLE 2-9. SONIC SIFTING ANALYSIS PROCEDURE

1. Obtain a sonic sieving apparatus.

2. Select the appropriate sieves that are optionally available for use with the above machine. The sieves commonly utilized are the 53 μm, 20 μm, and 10 μm sieves.

3. Obtain an analytical balance with the smallest division being 0.01 mg.

4. The material to be sieved on this machine is bottom pan (< 75 μm) catch from the mechanical silt analysis procedure (Table 2-8).

5. Clean the sieves in a low wattage (< 800 watts) ultra-sonic bath, taking care to immerse the seives edgewise only in the solvent. The use of Freon T.F. as a solvent is recommended because of its fast drying time. Once the sieves are clean, handle them only with cloth gloves to prevent contamination and static charge buildup. Latex gloves are not recommended.

6. Tare weigh the sieves and the catch pan. Weigh each sieve and the catch pan three times, alternating sieves between each weighing, and record each weight. Calibrate the balance with Class S weights prior to each weigh period, and periodically check the balance during its use.

7. After nesting the sieves in decreasing order of size, place the sample into the top sieve. The sample should weigh between 0.5 and 1.0 g. The sample weigh boat must be tare weighed prior to receiving the sample and again after the sample is introduced to the top sieve. The difference is subtracted from the sample weight and is recorded as material lost due to handling. Due to the hygroscopic nature of oven dried soils, the sample will gain moisture. Thus, the work must be done quickly without stopping for any length of time during the entire test cycle.

8. Once the material is placed on the top sieve, cover the top sieve with the sound wave generating diaphragm and place the sieves in the sonic shaker. The total sieving time is 5.0 min. With the sonic shaker in the sieve mode and the amplitude set on 2, sieve the material. Increase the amplitude to 5 after 1 min. After 1.5 min (elapsed time) switch the machine to the sift/pulse mode until the end of the test. If during the sift/pulse mode appreciable amounts of material collect on the sieve wall, carefully tap the sides where the particulate is adhering using a wooden stick.

(continued)

TABLE 2-9. (concluded)

9. After the 5 min sieving, remove the sieves and promptly weigh each sieve as rapidly as possible. Repeat the weighing two more times. Record each weight and do not interrupt this procedure.

10. Calculate the average tare and final weights of each sieve and pan. Subtract the tare from the final weight to find the average amount retained on each sieve and pan. Calculate both the mass and the percentage retained. Record these values on the data sheet.

By either working closely with plant personnel or actually contracting the work, MRI was able to directly oversee the mixing and application of the solution. To measure the application intensity, tared sampling pans (20 cm x 20 cm x 5 cm) were placed at various locations on the road surface prior to application. Special attention was paid to the problem associated with the solution bouncing off the bottom of the pan. To reduce this potential source of error, an absorbent material was used to line the bottom of the pan. A cross-sectional view is given in Figure 2-5.

After the control was applied, the sample pans were reweighed and the density of the solution determined. The application intensity measured by each pan is given by:

$$a = \frac{m_f - m_t}{\rho A}$$

where: a = application intensity (volume/area)

m_f = final weight of the pan and solution (mass)

m_t = tare weight of the pan (mass)

ρ = weight density of solution (mass/volume)

A = area of the pan (area)

Application intensities measured by each pan were examined for any significant spatial variation.

Decay in control efficiency for chemical dust suppressants is dependent upon the number of vehicle passes after application, although, for watering, time is the more important variable. In order to define decay as a function of traffic rate as well as time, pneumatic tube axle counters were deployed at the site after control application. In addition to vehicle counts during testing, independent counts determining the distribution of vehicles by number of axles were taken during each shift at the plant. This information was used to convert axle counts into the number of vehicle passes.

In order to determine the number of vehicle passes from axle count data, a simple calculation is necessary. If A represents the total number of axle counts, and N_j the number of passes by vehicles with j axles, then

$$A = \sum_j jN_j$$

If N is the total number of vehicle passes (regardless of the number of axles), then:

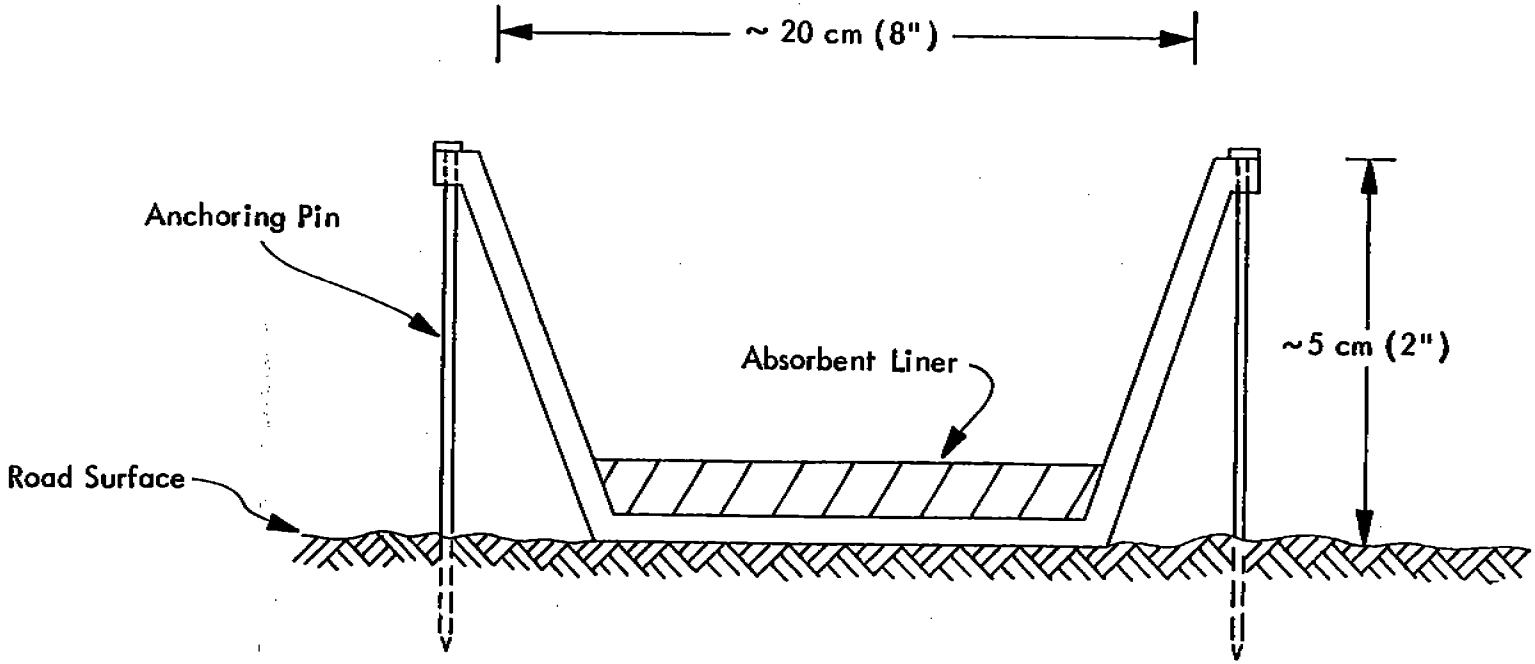

Figure 2-5. Cross-sectional view of the sampling pan used in measuring application intensity.

$$N = \frac{A}{\sum_j j f_j}$$

where: $f_j = \frac{N_j}{N}$ = fraction of vehicles with j axles

SECTION 3.0

RESULTS OF TESTING

The following field tests were performed at two iron and steel plants - J&L's Indiana Harbor Works (designated as plant AG), and Armco's Kansas City Works (designated as plant AJ):

Plant AG

- Three uncontrolled tests followed by
- Eight tests on a road treated with an asphalt emulsion

Plant AJ

- Three uncontrolled tests at Plant AJ, followed by
- Three tests on a watered road, followed by
- Eight tests on a road treated with a petroleum resin, followed by
- Four tests on a road retreated with a petroleum resin

Maps of the test sites at Plants AG and AJ are shown in Figures 3-1 and 3-2, respectively.

This section presents the results of the field tests and discusses the control efficiency of the techniques evaluated.

3.1 RESULTS OF EXPOSURE PROFILING TESTS

Twenty-nine tests of unpaved road dust emissions were conducted during the course of this study. Table 3-1 presents the site parameters associated with these exposure profiling tests.

Three separate control measures were evaluated--(a) a 20% solution of Petro Tac (an emulsified asphalt) applied at an intensity of 3.2 liter/m^2 (0.70 gal/ $yard^2$); (b) water applied at an intensity of 2.0 liter/m^2 (0.43 gal/$yard^2$); and (c) a 20% solution of Coherex® (a petroleum resin) applied at an intensity of 3.8 liter/m^2 (0.83 gal/$yard^2$) followed by a repeat application of 4.5 liter/m^2 (1.0 gal/$yard^2$) of 12% solution 44 days later. Tests to evaluate watering and Coherex® were performed at Plant AJ, while Petro Tac was tested at Plant AG.

Table 3-2 compares for each run, the raw TP concentration measured by the profiler sampler at a height of 3 m, with interpolated values of TP concentrations measured by the cyclone/impactor samplers operated both upwind and downwind of the test road.

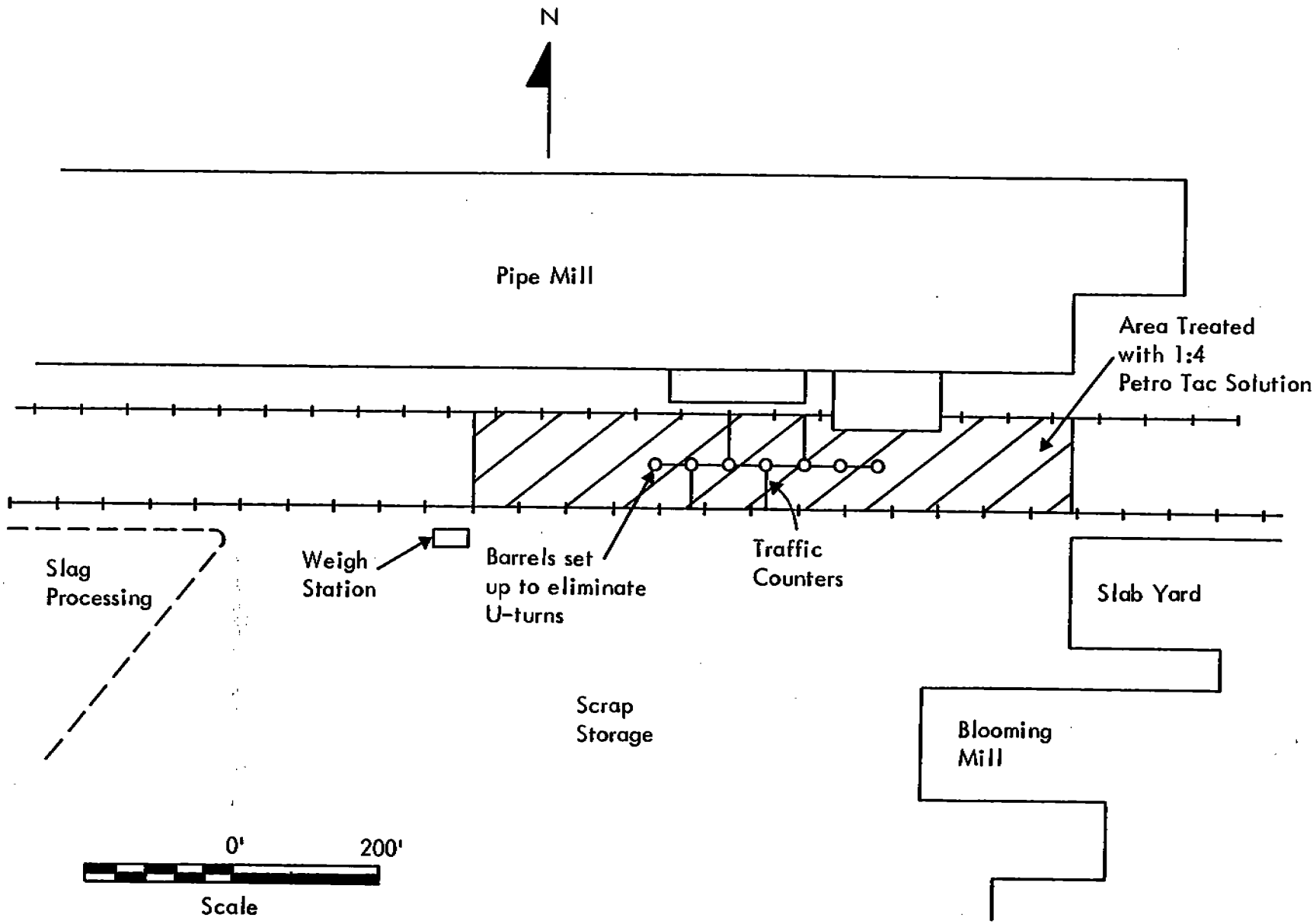

Figure 3-1. The test site at plant AG.

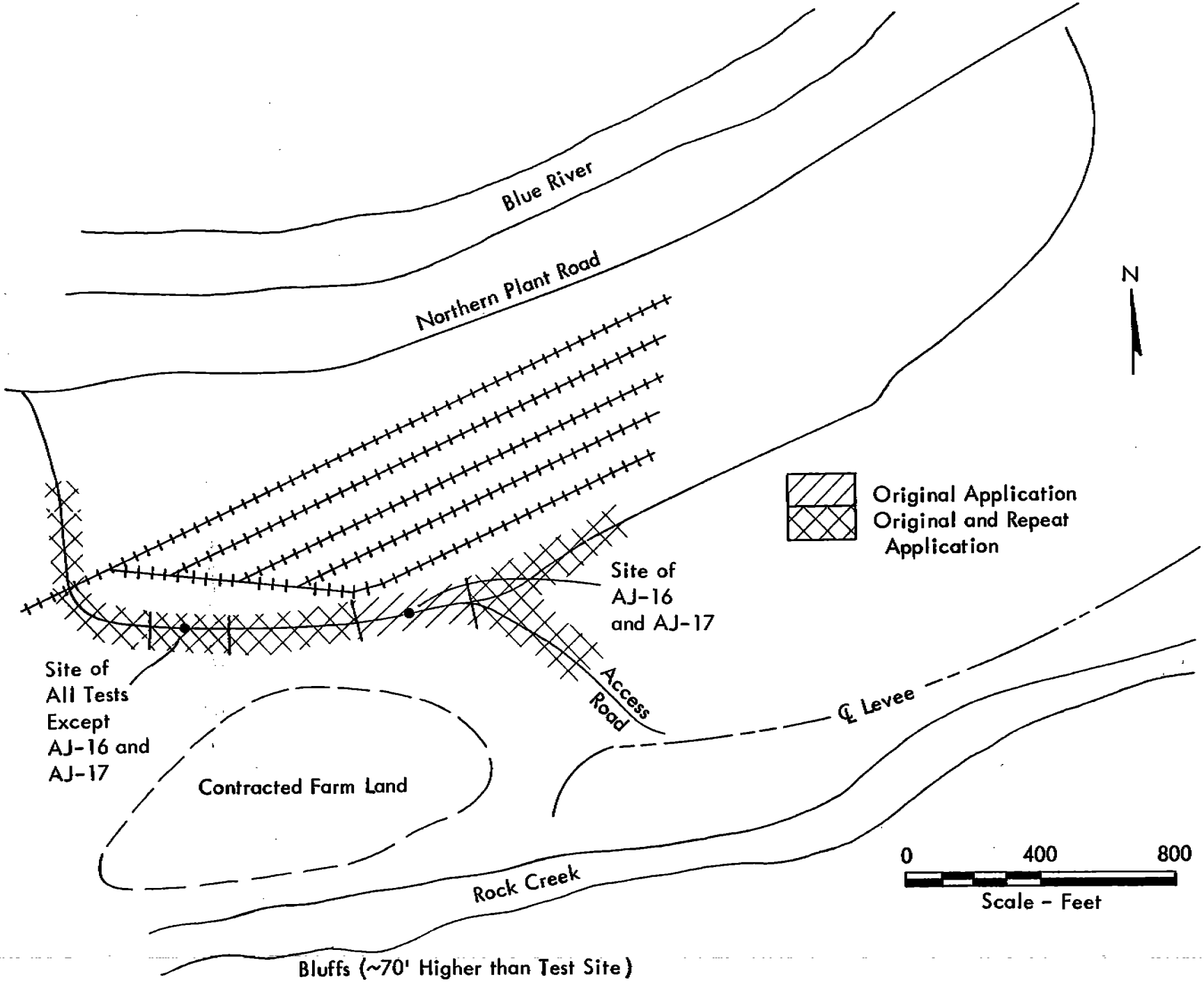

Figure 3-2. Test sites at plant AJ.

TABLE 3-1. EXPOSURE PROFILING TEST SITE PARAMETERS

Run	Control measure	Date	Time after control application	Test start	Sampling duration (min)	No. of vehicle passes during testing	Cumulative vehicle passes after control application	Ambient air temperature (°C)	Ambient air temperature (°F)	Mean wind speed[a] (m/s)	Mean wind speed[a] (mph)	Cumulative rainfall after application (mm)	Cumulative rainfall after application (in.)
AG-1	None	6/10/82	-	11:19	31	27	-	22	71	1.9	4.2	-	-
AG-2	None	6/11/82	-	14:23	106	30	-	21	69	3.3	7.4	-	-
AG-3	None	6/12/82	-	14:28	99	22	-	21	70	2.6	5.8	-	-
AG-4	Petro Tac	6/16/82	2 days	13:28	107	79	780	11	52	1.2	2.7	25	0.97
AG-5	Petro Tac	6/17/82	3 days	11:23	128	120	1,300	21	69	2.2	4.8	25	0.97
AG-6	Petro Tac	7/6/82	23 days	11:36	166	160	9,400	31	87	2.9	6.6	92	3.63
AG-7	Petro Tac	7/9/82	26 days	10:40	202	84	11,000	22	71	1.0	2.2	113	4.46
AG-8	Petro Tac	7/13/82	30 days	09:58	100	93	12,000	21	70	1.4	3.2	147	5.78
AG-9	Petro Tac	10/7/82	115 days	13:44	75	31	47,000	21	69	2.8	6.3	382	15.02
AG-10	Petro Tac	10/8/82	116 days	09:34	76	49	48,000	18	65	1.5	3.4	388	15.26
AG-11	Petro Tac	10/8/82	116 days	12:07	62	62	48,000	23	74	1.2	2.6	388	15.26
AJ-1	None	9/8/82	-	12:48	48	45	-	25	77	1.5	3.3	-	-
AJ-2	None	9/8/82	-	14:34	46	47	-	24	76	0.91	2.0	-	-
AJ-3	None	9/9/82	-	11:34	50	50	-	27	80	1.9	4.2	-	-
AJ-4	Watering	9/10/82	1.0 hr	15:11	79	86	43	31	90	2.7	6.1	0	0
AJ-5	Watering	9/10/82	2.8 hr	17:06	67	71	120	29	85	2.5	5.6	0	0
AJ-6	Watering	9/10/82	4.8 hr	19:28	46	49	180	26	78	2.0	4.4	0	0
AJ-7	Coherex®	9/22/82	7 days	12:53	90	68	660	19	66	1.6	3.6	6	0.24
AJ-8	Coherex®	9/23/82	8 days	14:22	89	120	750	21	70	2.6	5.8	6	0.24
AJ-9	Coherex®	9/27/82	12 days	11:30	126	120	1,100	21	69	2.4	5.3	6	0.24
AJ-10	Coherex®	10/25/82	40 days	12:31	50	44	3,800	17	62	1.2	2.8	66	2.60
AJ-11	Coherex®	10/25/82	40 days	14:00	65	61	3,800	18	65	1.4	3.1	66	2.60
AJ-12	Coherex®[b]	10/26/82	41 days	14:24	68	60	3,900	16	61	3.4	7.7	66	2.60
AJ-13	Coherex®[b]	11/2/82	4 days	12:15	190	150	580	14	57	3.7	8.2	0	0
AJ-14	Coherex®[b]	11/3/82	5 days	11:10	240	250	690	5.6	42	5.5	12	0	0
AJ-15	Coherex®	11/15/82	17 days	14:08	131	107	1,800	9.4	49	3.9	8.8	25	0.99
AJ-16	Coherex®	11/30/82	76 days	12:15	140	140	7,200	13	55	2.2	4.9	139	5.49
AJ-17	Coherex®[b]	12/1/82	77 days	12:45	125	120	7,400	18	65	3.5	7.9	139	5.49
AJ-18	Coherex®[b]	12/3/82	35 days	12:50	119	115	3,300	6.1	43	2.2	5.0	59	2.32

[a] At a height of 3 m.

[b] Test of retreated surface.

TABLE 3-2. REPRESENTATIVE TP CONCENTRATIONS (UNCORRECTED)

Run	TP concentration at 3 m above ground (µg/m³)		
	Upwind Cyclone/Cascade Impactor[a]	Downwind Profiler	Downwind Cyclone/Cascade Impactor[b]
AG-1	1,160	2,560[c]	2,540
AG-2	478	1,890	1,930
AG-3	247	1,500	1,290
AG-4	225	501[c]	216
AG-5	172	507	418
AG-6	374	964	1,090
AG-7	192	737[c]	497
AG-8	160	1,120[c]	958
AG-9	92	725[c]	650
AG-10	204	2,630	1,690
AG-11	204	1,660	940
AJ-1	205	7,580	7,020
AJ-2	205	9,450[c]	9,700
AJ-3	91	7,620	5,860
AJ-4	110	208	268
AJ-5	110	1,280[c]	1,350
AJ-6	110	2,570	1,990
AJ-7	72	1,320	2,330
AJ-8	84	308[b,c]	667
AJ-9	84[d]	3,660[b]	3,670
AJ-10	187	3,910[c]	3,340
AJ-11	187	2,780[c]	2,830
AJ-12	148	4,500	4,860
AJ-13	123	224	176
AJ-14	184	486	1,110
AJ-15	50	350	342
AJ-16	59	522[c]	200
AJ-17	38	264	242[e]
AJ-18	16	689	141

[a] Values for controlled tests interpolated from 1.5 m and 4.5 m concentrations.
[b] Interpolated from 1.5 m and 4.5 m concentrations.
[c] This value required correction for non-isokinesis.
[d] 4.5 m value.
[e] 1.5 m value.

There was good agreement in the downwind concentrations, except when the values were low; in those cases, the fairly uniform wall losses in the cyclone are believed to account for the observation that the cyclone/impactor values were consistently lower than the profiler values of TP concentration.

As indicated in Table 3-2, eleven of the profiler concentrations required correction for non-isokinesis. In most of these cases, the mean wind speed was low, resulting in an isokinetic ratio exceeding the acceptable upper limit of 1.2. This is illustrated in Table 3-3, which gives the isokinetic correction parameters for the 1.5 m and 4.5 m profiling heights. These values, in conjunction with the aerodynamic particle size data shown in Table 3-4, were used to determine isokinetically corrected concentrations and exposures according to the procedure described in Section 2.5.4. The isokinetic ratios for the cyclone/impactor samplers also exceeded 1.2 under light wind conditions; but no isokinetic corrections were made to particulate concentrations measured by the impactor stages, all of which had cut-points below 10 μm aerodynamic diameter.

Table 3-5 lists, for each run, the individual point values of isokinetically corrected exposure (net mass per sampling intake area) within the open dust source plume as measured by the exposure profiling equipment. These point values were integrated over the height of the plume to determine emission factors, as described in Section 2.5.4.

Table 3-6 presents the isokinetic emission factors for TP, IP, PM_{10}, and FP. Table 3-7 presents vehicle and site parameters which have been found in previous studies to have a significant effect on the emission factors from uncontrolled unpaved roads.

In order to determine control efficiencies, it was necessary to determine normalized TP, IP, PM_{10} and FP emission factors. However, as discussed in Section 2.5.5, an additional step was necessary in the case of Plant AG. Because the north and south sides of the test road exhibited different rates of control efficiency decay, the overall emissions were apportioned over the two sides for Runs AG-6 through AG-10. The values used to apportion the emission factors are given in Table 3-8. Note that AG-11 was run solely with traffic on the north side of the road in order to test the validity of the apportionment procedure.

Normalized emission factors are presented in Tables 3-9 and 3-10 for Plants AG and AJ, respectively. Note that the normalized, apportioned emission factors for TP, IP and PM_{10} for AG-11 follow the expected trend shown in AG-9 and AG-10. Because run AG-11 was conducted to test the validity of the apportionment, it appears that the procedure works well for particulate emissions in these size ranges.

3.2 CONTROL EFFICIENCIES

From the normalized emission factors, overall control efficiencies were determined using the procedure described in Section 2.5.5. Figures 3-3 through 3-5 present the control efficiencies associated with Petro Tac for TP, IP, and PM_{10} emissions, respectively.

TABLE 3-3. ISOKINETIC CORRECTION PARAMETERS

Run	Mean wind speed				Profiler mean intake velocity				Mean measured isokinetic ratio (IFR)	
	Ht = 1.5 m		Ht = 4.5 m		Ht = 1.5 m		Ht = 4.5 m			
	(cm/s)	(fpm)	(cm/s)	(fpm)	(cm/s)	(fpm)	(cm/s)	(fpm)	Ht = 1.5 m	Ht = 4.5 m
AG-1	197	388	177	349	353	695	396	779	2.10	2.84
AG-2	306	603	355	698	319	628	297	584	1.05	0.86
AG-3	237	467	271	533	260	511	289	568	1.10	1.07
AG-4	98	192	133	262	232	456	207	407	2.38	1.55
AG-5	147	289	220	434	232	457	246	484	1.61	1.12
AG-6	207	407	304	598	223	439	339	667	1.11	1.16
AG-7	83	164	109	214	207	407	201	396	2.49	1.85
AG-8	123	242	155	305	183	360	201	396	1.49	1.30
AG-9	274	539	284	559	169	332	192	378	0.61	0.67
AG-10	132	260	162	319	119	234	125	246	0.90	0.79
AG-11	118	233	114	224	119	234	119	234	1.01	1.05
AJ-1	91	180	172	339	183	360	201	395	2.00	1.13
AJ-2	65	128	107	210	183	360	183	360	2.82	1.71
AJ-3	98	192	240	473	183	360	233	458	1.88	0.97
AJ-4	176	346	333	656	200	394	399	785	1.14	1.21
AJ-5	150	296	312	614	183	360	421	828	1.22	1.36
AJ-6	120	236	244	480	183	360	238	468	1.52	0.98
AJ-7	128	252	171	336	196	386	208	410	1.53	1.22
AJ-8	203	400	279	549	220	434	296	582	1.09	1.07
AJ-9	200	394	261	514	231	454	255	501	1.16	0.99
AJ-10	112	221	130	255	183	360	183	360	1.63	1.41
AJ-11	119	234	147	289	183	360	183	360	1.54	1.25
AJ-12	290	570	373	735	334	658	398	784	1.15	1.08
AJ-13	301	592	404	795	343	675	458	902	1.13	1.12
AJ-14	518	1,020	564	1,110	480	944	579	1,140	0.92	1.03
AJ-15	341	671	421	829	299	588	374	737	0.87	0.89
AJ-16	169	333	299	589	213	420	336	661	1.28	1.12
AJ-17	280	551	390	767	278	548	397	781	1.00	1.02
AJ-18	186	367	243	478	205	404	259	509	1.11	1.06

TABLE 3-4. AERODYNAMIC PARTICLE SIZE DATA

Run/ Height	Largest particle diameter[a] (μm)					Downwind Cascade impactor data					
	Upwind[b]			Downwind		% < 15 μm		% < 10 μm		% < 2.5 μm	
	1.5 m	3 m	4.5 m	1.5 m	4.5 m	1.5 m	4.5 m	1.5 m	4.5 m	1.5 m	4.5 m
AG-1	-	140	-	114	153	16	16	15	15	5	5
AG-2	-	153	-	114	136	35	39	28	32	11	14
AG-3	-	47	-	114	57	31	27	25	22	9	8
AG-4	57	-	40	57	81	16[c]	15[c]	14[c]	13[c]	8[c]	7[c]
AG-5	141	-	57	81	57	32[c]	36	25[c]	29	8[c]	10
AG-6	81	-	58	68	68	16	22	13	17	5	6
AG-7	40	-	40	81	81	13	13	10	10	3	3
AG-8	40	-	81	47	45	18	24	14	20	4	6
AG-9	57	-	57	40	57	44	44	31	31	6	6
AG-10	47	-	114	68	40	21	20	16	16	5	6
AG-11	47	-	114	57	57	20	19	16	16	6	6
AJ-1	-	81	-	57	40	37	34	27	26	6	6
AJ-2	-	81	-	47	40	13	20	9	15	2	4
AJ-3	-	24	-	53	47	20	21	14	16	3	4
AJ-4	114	-	47	55	55	39	47	23	40	14	23
AJ-5	114	-	47	57	57	19	30	13	24	2	9
AJ-6	114	-	47	28	d	12[c]	14	8[c]	11	< 1[c]	5
AJ-7	114	-	172	81	57	11	16	8	12	1	3
AJ-8[e]	81	-	57	114	81	12	16	8	12	1	3
AJ-9	40	-	108	129	57	13	16	8	12	1	3
AJ-10	57	-	57	47	68	15	23	12	18	4	6
AJ-11	57	-	57	47	40	16	36	12	22	3	9
AJ-12	24	-	68	308	57	17	32	11	19	2	1
AJ-13	40	-	257	81	57	17	33	12	20	2	< 1[c]
AJ-14	57	-	108	81	57	15	18	11	14	4	5
AJ-15	47	-	47	138	114	23	d	18	d	7	d
AJ-16	d	-	d	47	68	26	19	18	16	7	7
AJ-17	47	-	33	40	81	22	f	17	f	6	f
AJ-18	100	-	45	68	68	g	30	g	25	g	9

[a] Determined by optical microscopy.

[b] Blanks indicate that no sampler was deployed at that height.

[c] Suspect values, light substrate or backup filter loadings.

[d] Sample lost.

[e] Because of light loadings, size data of AJ-7 and AJ-9 used.

[f] Unit not deployed.

[g] Sampler malfunction.

TABLE 3-5. PLUME SAMPLING DATA

Run	Sampling height (m)	Sampling rate (m^3/hr)	Sampling rate (cfm)	Net TP exposure[a] (mg/cm^2)
AG-1	1.5	33	19	1.68
	3.0	32	19	1.31
	4.5	37	22	1.00
	6.0	31	18	0.678
AG-2	1.5	30	17	4.42
	3.0	31	18	3.00
	4.5	28	16	2.22
	6.0	36	21	1.36
AG-3	1.5	24	14	1.94
	3.0	25	15	1.94
	4.5	27	16	1.94
	6.0	29	17	1.30
AG-4	1.5	22	13	0.301
	3.0	18	10	0.420
	3.4	19	11	0.190
	6.0	18	10	0.278
AG-5	1.5	22	13	0.582
	3.0	21	13	0.551
	4.5	23	13	0.542
	6.0	24	14	0.514
AG-6	1.5	21	12	2.00
	3.0	30	17	1.81
	4.5	32	18	1.85
	6.0	40	24	1.95
AG-7	1.5	19	11	1.37
	3.0	18	10	1.43
	4.5	19	11	1.24
	6.0	35	20	0.968
AG-8	1.5	17	10	1.73
	3.0	19	11	1.67
	4.5	19	11	1.47
	6.0	18	10	1.08

(continued)

TABLE 3-5 (continued)

Run	Sampling height (m)	Sampling rate (m^3/hr)	Sampling rate (cfm)	Net TP exposure[a] (mg/cm^2)
AG-9	1.5	16	9.2	0.529
	3.0	17	9.8	0.597
	4.5	18	10	0.475
	6.0	19	11	0.376
AG-10	1.5	11	6.5	1.73
	3.0	11	6.5	1.67
	4.5	12	6.8	1.30
	6.0	12	7.0	1.18
AG-11	1.5	11	6.5	1.04
	3.0	11	6.5	0.929
	4.5	11	6.5	0.536
	6.0	11	6.5	0.485
AJ-1	1.5	17	10	2.46
	3.0	17	10	3.11
	4.5	18	11	2.78
	6.0	20	12	1.75
AG-2	1.5	17	10	4.96
	3.0	17	10	3.80
	4.5	17	10	3.00
	6.0	19	11	3.69
AJ-3	1.5	17	10	3.67
	3.0	18	11	4.23
	4.5	22	13	3.04
	6.0	25	14	1.36
AJ-4	1.5	19	11	0.188
	3.0	29	17	0.128
	4.5	37	22	0.00948
	6.0	43	26	0.00
AJ-5	1.5	17	10	1.47
	3.0	31	18	1.47
	4.5	39	23	1.08
	6.0	46	27	0.474

(continued)

TABLE 3-5 (continued)

Run	Sampling height (m)	Sampling rate (m^3/hr)	Sampling rate (cfm)	Net TP exposure[a] (mg/cm^2)
AJ-6	1.5	17	10	1.71
	3.0	19	11	1.34
	4.5	22	13	0.822
	6.0	27	16	0.434
AJ-7	1.5	18	11	2.87
	3.0	19	11	1.08
	4.5	19	11	1.10
	6.0	21	12	0.596
AJ-8	1.5	21	12	1.07
	3.0	23	14	0.872
	4.5	27	16	0.475
	6.0	30	18	0.367
AJ-9	1.5	21	13	9.47
	3.0	b	b	6.61
	4.5	24	14	3.76
	6.0	26	15	2.49
AJ-10	1.5	17	10	2.83
	3.0	17	10	1.86
	4.5	17	10	1.26
	6.0	17	10	0.789
AJ-11	1.5	17	10	2.84
	3.0	17	10	1.66
	4.5	17	10	0.763
	6.0	17	10	0.477
AJ-12	1.5	31	18	7.05
	3.0	34	20	5.60
	4.5	37	22	2.22
	6.0	39	23	0.474
AJ-13	1.5	32	19	0.495
	3.0	35	21	0.342
	4.5	43	25	0.0224
	6.0	46	27	0.00

(continued)

TABLE 3-5 (concluded)

Run	Sampling height (m)	Sampling rate (m^3/hr)	Sampling rate (cfm)	Net TP exposure[a] (mg/cm^2)
AJ-14	1.5	45	26	4.18
	3.0	47	30	2.37
	4.5	54	32	1.01
	6.0	56	33	0.273
AJ-15	1.5	28	16	1.82
	3.0	32	19	0.924
	4.5	35	20	0.553
	6.0	36	21	0.142
AJ-16	1.5	20	12	0.597
	3.0	23	14	0.916
	4.5	31	18	0.179
	6.0	33	19	0.168
AJ-17	1.5	26	15	0.542
	3.0	29	17	0.569
	4.5	37	22	0.217
	6.0	41	24	0.152
AJ-18	1.5	19	11	1.06
	3.0	19	11	1.07
	4.5	24	14	0.375
	6.0	25	15	0.190

[a] Isokinetically corrected when necessary.

[b] The 3 m sampler malfunctioned during AJ-9. The exposure value is interpolated from 1.5 m and 4.5 m data.

TABLE 3-6. EMISSION FACTORS

Run	Control Measure	Emission factor TP (g/VKT)	TP (lb/VMT)	IP (g/VKT)	IP (lb/VMT)	PM_{10} (g/VKT)	PM_{10} (lb/VMT)	FP (g/VKT)	FP (lb/VMT)
AG-1	None	3,380	12.0	389	1.38	378	1.34	33.0	0.117
AG-2	None	6,850	23.4	2,110	7.47	1,560	5.55	280	0.994
AG-3	None	5,980	21.2	1,490	5.30	1,080	3.82	137	0.485
AG-4	Petro Tac	272	0.963	4.26	0.0151	2.73	0.00969	-	-
AG-5	Petro Tac	409	1.45	106	0.375	69.9	0.248	-	-
AG-6	Petro Tac	1,020	3.63	39.5	0.140	9.98	0.0354	-	-
AG-7	Petro Tac	1,590	5.63	91.1	0.323	38.4	0.136	-	-
AG-8	Petro Tac	1,280	4.52	226	0.803	172	0.610	11.8	0.0420
AG-9	Petro Tac	1,320	4.67	632	2.24	434	1.54	73.0	0.259
AG-10	Petro Tac	2,500	8.88	426	1.51	313	1.11	68.5	0.243
AG-11	Petro Tac	922	3.27	131	0.466	94.4	0.335	4.34	0.0154
AJ-1	None	3,890	13.8	1,450	5.15	1,180	4.17	257	0.915
AJ-2	None	6,040	21.4	1,010	3.58	738	2.62	206	0.732
AJ-3	None	4,170	14.8	829	2.94	603	2.14	140	0.498
AJ-4	Watering	71.9	0.255	24.3	0.0861	14.3	0.0508	7.67	0.272
AJ-5	Watering	1,050	3.73	220	0.781	159	0.563	34.4	0.122
AJ-6	Watering	1,640	5.81	165	0.585	139	0.493	59.2	0.210
AJ-7	Coherex®	1,650	5.85	252	0.895	138	0.490	14.2	0.0504
AJ-8	Coherex®	460	1.63	13.2	0.0469	6.12	0.0217	-	-
AJ-9	Coherex®	3,550	12.6	462	1.64	296	1.05	33.5	0.119
AJ-10	Coherex®	3,020	10.7	536	1.90	420	1.49	127	0.449
AJ-11	Coherex®	1,820	6.45	395	1.40	255	0.904	70.7	0.251
AJ-12	Coherex®	4,680	16.6	1,010	3.57	629	2.23	47.1	0.167
AJ-13	Coherex®	108	0.384	17.9	0.0634	1.60	0.00568	-	-
AJ-14	Coherex®	606	2.15	80.1	0.284	51.6	0.183	10.3	0.0367
AJ-15	Coherex®	629	2.23	114	0.404	88.2	0.313	36.6	0.130
AJ-16	Coherex®	226	0.801	40.6	0.144	27.7	0.0982	6.40	0.0227
AJ-17	Coherex®	225	0.798	26.9	0.0953	18.5	0.0656	1.38	0.00489
AJ-18	Coherex®	386	1.37	129	0.457	105	0.373	30.4	0.108

TABLE 3-7. VEHICULAR TRAFFIC DATA AND ROAD SURFACE CHARACTERISTICS

Run	Control measure	Silt (%)	Mean vehicle speed (kph)	Mean vehicle speed (mph)	Mean vehicle weight (Mg)	Mean vehicle weight (tons)	Mean No. of wheels per vehicle pass
AG-1	None	7.5	24	15	24	27	9.8
AG-2	None	5.8	27	17	23	25	7.3
AG-3	None	7.2	26	16	25	28	6.6
AG-4	Petro Tac	0.28	24	15	21	23	9.2
AG-5	Petro Tac	0.29	23	14	29	32	10
AG-6	Petro Tac	5.0	24	15	27	30	13
AG-7	Petro Tac	4.9	26	16	31	34	10
AG-8	Petro Tac	5.3	23	14	28	31	9.1
AG-9	Petro Tac	8.2	21	13	25	28	6.1
AG-10	Petro Tac	8.5	21	13	28	31	8.1
AG-11	Petro Tac	13	23	14	24	26	5.8
AJ-1	None	6.3	24	15	49	54	6.0
AJ-2	None	7.4	24	15	47	52	6.0
AJ-3	None	7.7	24	15	45	50	7.1
AJ-4	Watering	4.9	24	15	44	48	6.1
AJ-5	Watering	5.3	24	15	45	50	6.0
AJ-6	Watering	a	24	15	44	48	5.9
AJ-7	Coherex®	1.9	24	15	44	49	5.9
AJ-8	Coherex®	5.5	24	15	31	34	7.2
AJ-9	Coherex®	7.1	24	15	45	50	6.4
AJ-10	Coherex®	6.1	32	20	26	29	6.0
AJ-11	Coherex®	4.3	31	19	24	27	6.0
AJ-12	Coherex®	5.7	34	21	40	44	6.0
AJ-13	Coherex®	b	29	18	34	38	6.0
AJ-14	Coherex®	0.034	35	22	51	56	6.0
AJ-15	Coherex®	1.6	27	17	49	54	6.0
AJ-16	Coherex®	2.1	37	23	29	32	6.0
AJ-17	Coherex®	1.5	32	20	31	34	6.0
AJ-18	Coherex®	1.7	35	22	28	31	6.0

[a] Darkness prevented sample from being taken.

[b] A complete size distribution is given in Table 3-16. The mass of the silt collected was so small as to be undetectable.

TABLE 3-8. EMISSION APPORTIONMENT DATA FOR PLANT AG

Run	Side of road	Percent of traffic	Surface loading (kg/km)	Silt content (%)	Apportioning factor	Average vehicle parameters: Weight (Mg)	Average vehicle parameters: Wheels
AG-6	North	51	726	1.1	0.0121	28	12
	South	49	26,200	5.1	2.03	28	14
AG-7	North	59	949	2.5	0.0222	32	10
	South	41	51,400	5.0	2.41	30	11
AG-8	North	40	3,290	3.0	0.107	30	8.6
	South	60	26,800	5.5	1.60	27	9.4
AG-9	North	52	4,360	9.7	0.162	23	6.2
	South	48	61,400	8.1	1.91	29	5.9
AG-10	North	47	6,140	12	0.226	19	8.6
	South	53	67,000	8.2	1.69	35	7.6
AG-11	North	100	8,380	13	1.00	23	5.8

TABLE 3-9. NORMALIZED EMISSION FACTORS FOR PLANT AG

Run	Side of Road[a]	Normalized[b,c] emission factors (g/VKT) TP	IP	PM_{10}	FP
AG-1	O	3,190	367	355	31.3
AG-2	O	7,050	2,170	1,610	288
AG-3	O	6,490	1,620	1,170	148
AG-4	O	299	4.71	3.02	-
AG-5	O	364	93.9	62.0	-
AG-6	N	9.73	0.375	0.0947	-
	S	1,490	57.2	14.5	-
	O	764	29.3	7.44	-
AG-7	N	26.0	1.49	0.628	-
	S	2,850	163	68.8	-
	O	1,180	67.6	28.5	-
AG-8	N	132	23.4	17.8	1.45
	S	2,060	364	278	22.6
	O	1,260	224	170	13.8
AG-9	N	302	145	99.8	16.8
	S	3,160	1,510	1,040	174
	O	1,750	840	578	97.0
AG-10	N	804	136	100	21.9
	S	4,170	708	522	114
	O	2,820	482	352	77.6
AG-11	N	1,250	179	128	5.89

[a] Emissions are reported for the North and South sides of the road (where apportionment was necessary) as well as Overall.

[b] Normalizing values are 24 kph (15 mph), 26 Mg (28 tons) and 8.5 wheels.

[c] Blank entries denote net mass fluxes too small to accurately sample.

TABLE 3-10. NORMALIZED EMISSION FACTORS FOR PLANT AJ

Run	Normalized[a,b] emission factors (g/VKT)			
	TP	IP	PM_{10}	FP
AJ-1	3,720	1,390	1,120	247
AJ-2	5,920	993	728	203
AJ-3	3,890	770	561	130
AJ-4	74.2	25.0	14.7	7.90
AJ-5	1,060	222	160	34.7
AJ-6	1,720	173	146	62.0
AJ-7	1,700	260	142	14.6
AJ-8	556	38.6	19.8	-
AJ-9	3,470	451	290	32.7
AJ-10	3,360	595	465	140
AJ-11	2,240	485	313	87.1
AJ-12	3,690	795	496	37.2
AJ-13	110	18.2	1.63	-
AJ-14	386	51.0	32.7	6.60
AJ-15	533	96.4	74.7	31.0
AJ-16	204	36.7	25.0	5.78
AJ-17	224	26.7	18.4	1.37
AJ-18	372	124	102	29.3

[a] Normalizing values are 27 kph (17 mph), 38 Mg (42 tons), and 6.1 wheels.

[b] Blank entries denote net mass fluxes too small to be accurately sampled.

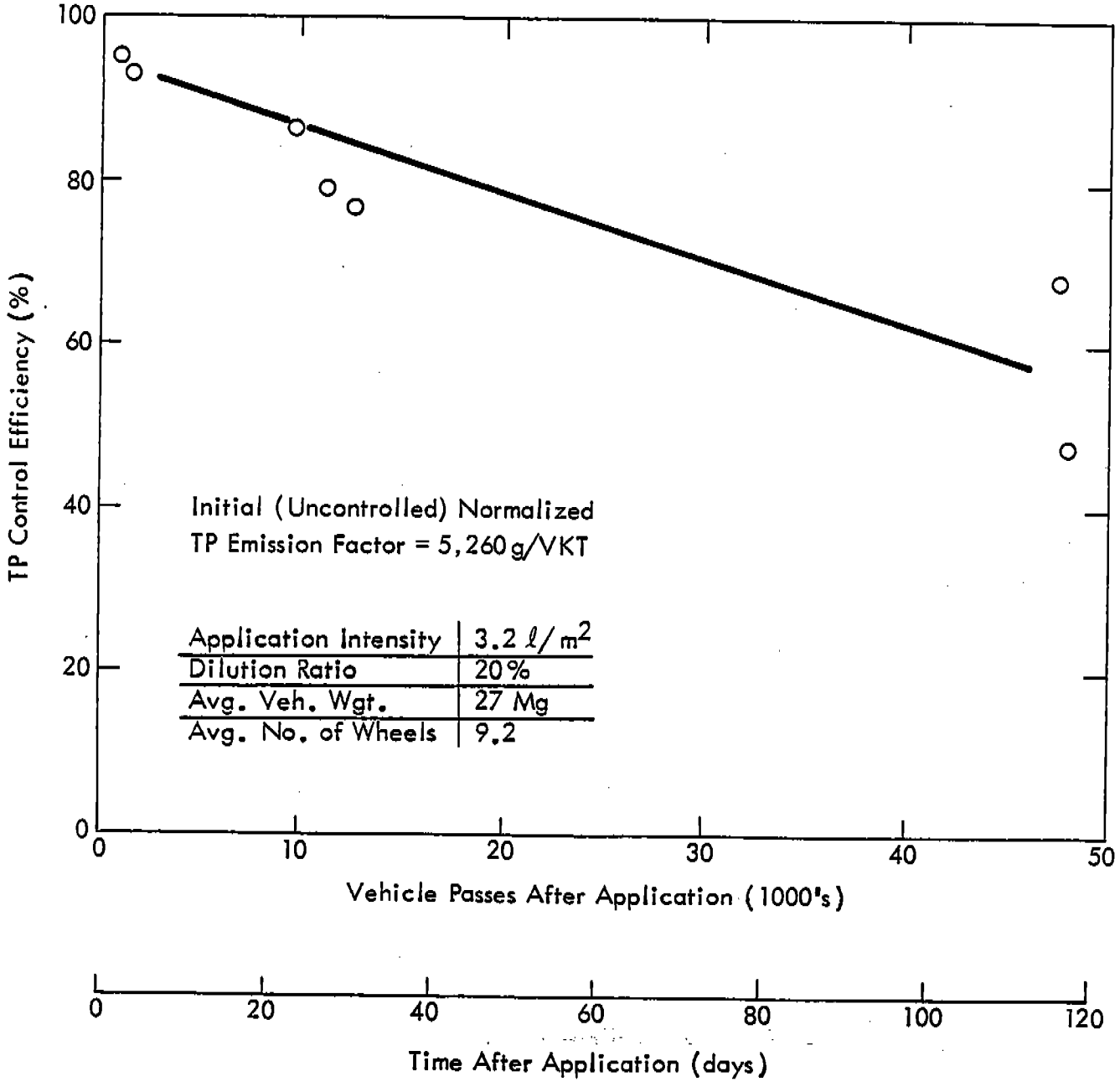

Figure 3-3. TP control efficiency decay for an initial application of Petro Tac.

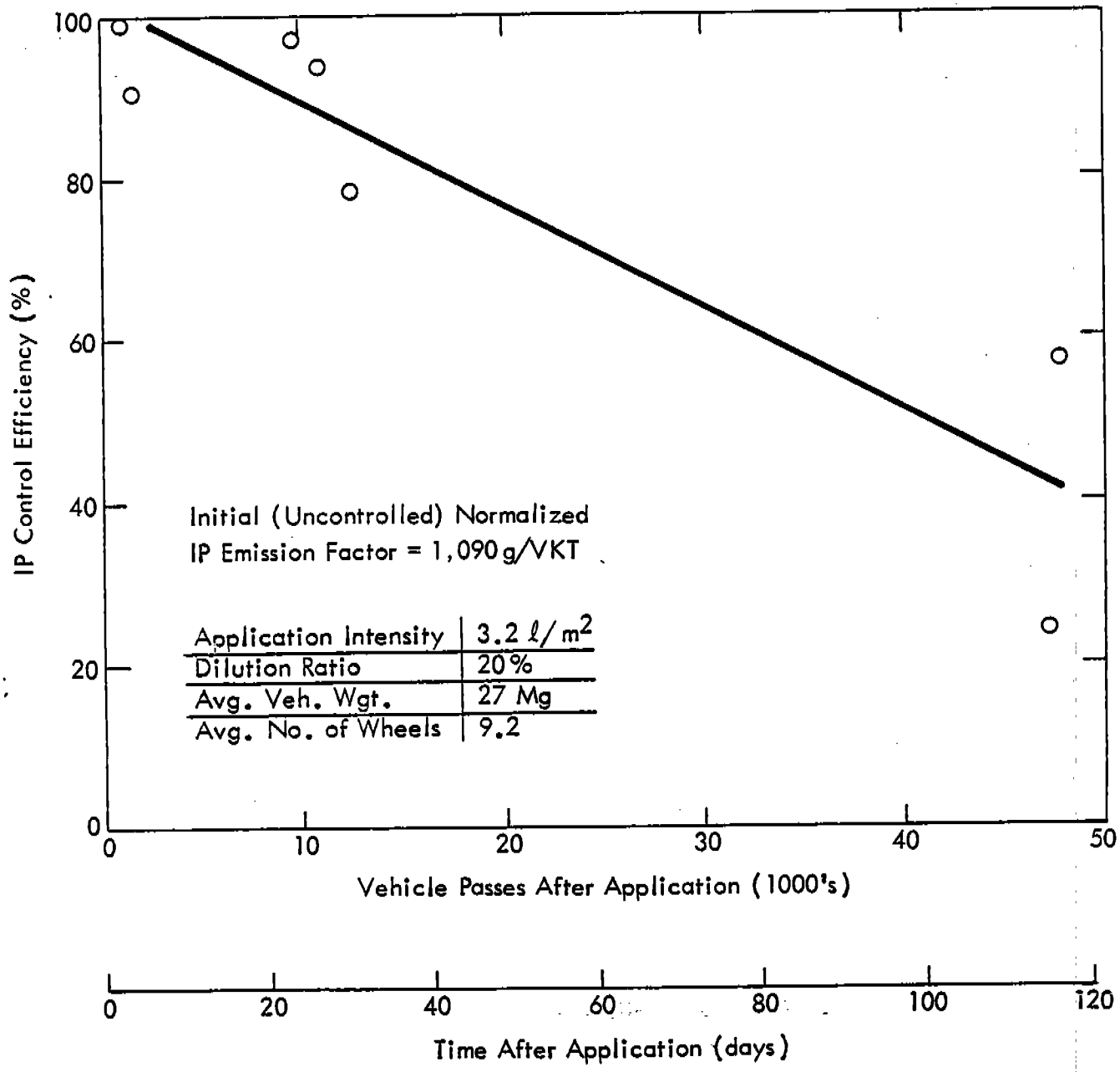

Figure 3-4. IP control efficiency decay for an initial application of Petro Tac.

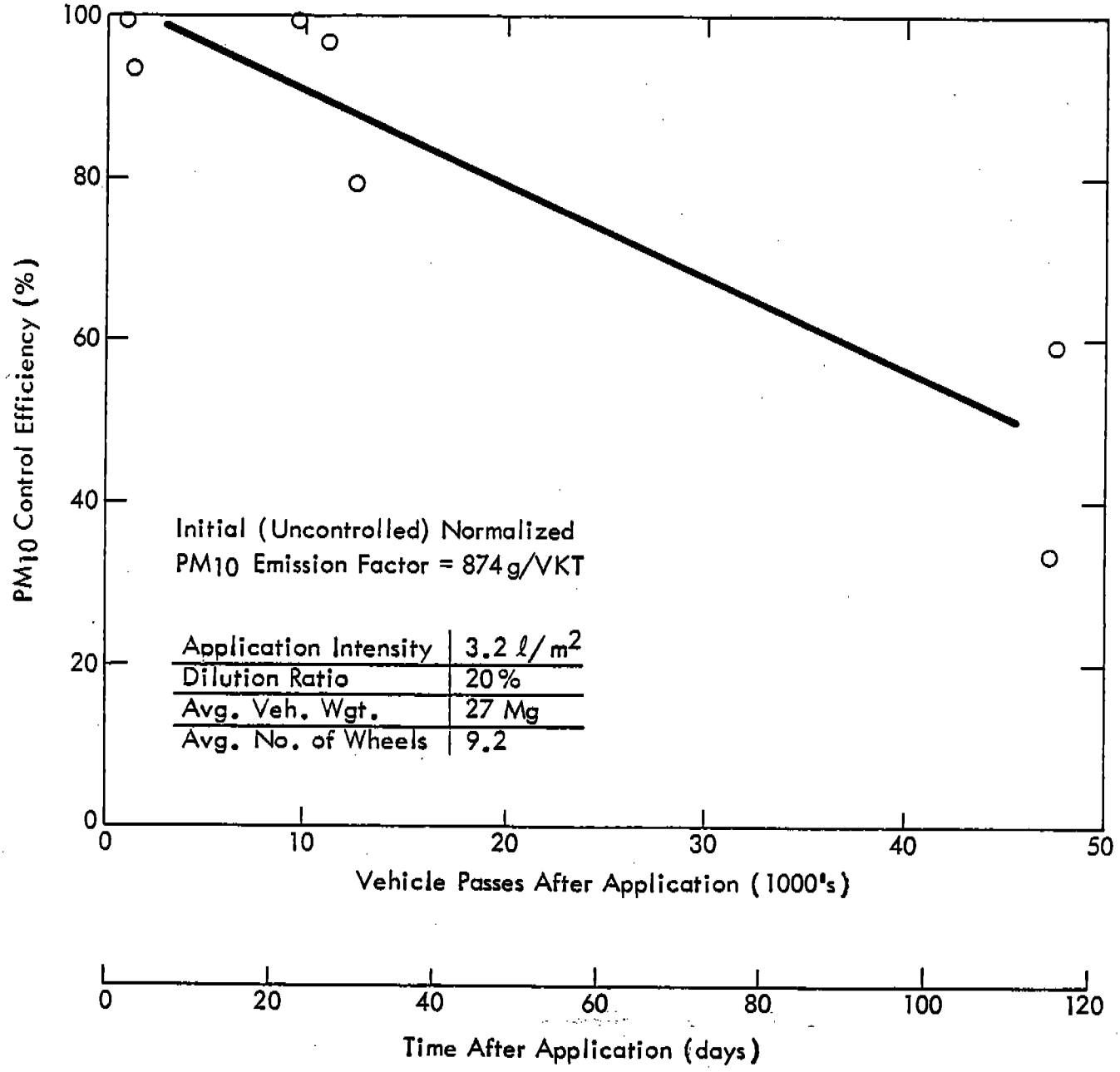

Figure 3-5. PM_{10} control efficiency decay for an initial application of Petro Tac.

Also shown in these figures are the least-squares fit of control efficiency versus vehicle passes and time after application. The control efficiency decay of any chemical dust suppressant is a function of vehicle passes and only indirectly a function of time. However, for watering, the effect of time (in terms of solar radiation) is more likely predominant. Tables 3-11 and 3-12 present the best fit equations for control efficiency as a function of vehicle passes and time, respectively. Also included are values which measure the goodness of fit of the equation to the measured data, and source/application parameters which affect control performance.

It is of interest to note that, for the linear control efficiency decay functions in Table 3-11, the time T (in days) between applications required to achieve an average control efficiency is

$$T = \frac{2}{mR_T} (a - C)$$

where

a = intercept of the decay curve (%)
m = decay constant (%/vehicle pass)
C = average control efficiency (%) $\geq$ 50%
R_T = traffic rate on road of interest (vehicle passes/day)

The asphalt emulsion provided a considerably higher level of control than was anticipated. TP emissions showed the lowest initial control efficiency, while the TP control efficiency at the end of 4 months was approximately 50%. Control efficiencies associated with particulate emissions in the smaller size ranges showed more rapid decay. Initial control was greater than for TP; however, the level of control at the end of testing was less than that for TP. The extreme case is illustrated in Figure 3-6 in which TP and FP control efficiency values are shown together. Note that a parabola has been used to characterize FP control efficiency decay. As can be seen from this figure, initial FP control was substantially greater than TP, but a sharp decrease in control occurred with the result that FP emissions nearly match the uncontrolled state at a time when TP emissions are still controlled at the 50% level.

The level of control efficiency on each side of the test road at Plant AG differed markedly. As mentioned, this is believed to be due to the larger friction forces associated with stop and go traffic on the south side. From the results presented in Table 3-9, the control efficiencies associated with north and south sides of the road were obtained and are presented in Table 3-13. Thus, the north side of the road exhibited control efficiencies which averaged about 85% over all size ranges 4 months after application. At the same time, the south side indicated efficiencies ranging from 40% down to roughly the uncontrolled level for FP emissions. It is of interest to note that the asphalt emulsion was applied at a 65% higher intensity on the south side than the north. Thus, there is reason to believe that average control efficiencies of approximately 90% over several months are achievable when Petro Tac is applied at 0.70 gal/yd^2 of 20% solution to a well constructed road without a significant amount of stop and go traffic.

TABLE 3-11. CONTROL EFFICIENCY AS A FUNCTION OF VEHICLE PASSES

Control measure	Time after application	Average No. of vehicle passes per day	Mean vehicle parameters: Weight (Mg)	Weight (tons)	No. of wheels	Particle size range	Least-squares fit of control efficiency[a] (%)	Correlation coefficient	Level of significance
Petro Tac- 3.2 ℓ/m² (0.70 gal/yd²) of 20% solution in water	2-116 days	410	27	30	9.2	TP	92.9-0.000800 V	-0.913	99%
						IP	102-0.00129 V	-0.915	99%
						PM_{10}	102-0.00113 V	-0.921	99%
						FP	100-3.54 (10^{-8}) V^2	-0.986	99.9%[b]
Coherex® - initial application 3.8 ℓ/m² (0.83 gal/yd²) of 20% solution in water	7-41 days	94	34	38	6.2	TP	79.1-0.0139 V	-0.717	< 90%
						IP	92.2-0.0144 V	-0.869	95%
						PM_{10}	94.9-0.0134 V	-0.892	98%
						FP	102-0.0127 V	-0.796	90%
Coherex® - reapplication 4.5 ℓ/m² (1.0 gal/yd²) of 12% solution in water	4-35 days	97	39	43	6.0	TP	97.0-0.00225 V	-0.648	< 90%
						IP	99.1-0.00375 V	-0.958	95%
						PM_{10}	100-0.00430 V	-0.960	95%
						FP	100-0.00568 V	-0.890	< 90%
Watering[c]	1.0-2.8 hr	1,200	44	49	6.0	TP	103-0.209 V	-0.958	N/A
						IP	102-0.187 V	-0.969	N/A
						PM_{10}	102-0.179 V	-0.963	N/A
						FP	101-0.156 V	-0.990	N/A

[a] V represents cumulative vehicle passes after application.
[b] Complete mitigation is assumed immediately after application. Because a parabola was used to characterize FP control efficiency decay, standard tests of significance are not strictly applicable.
[c] Run AJ-6 was not used in developing the equations for water.

TABLE 3-12. CONTROL EFFICIENCY AS A FUNCTION OF TIME

Control measure	Time after application	Average No. of vehicle passes per day	Mean vehicle parameters: Weight (Mg)	Weight (tons)	No. of wheels	Particle size range	Least-squares fit of control efficiency[a] (%)	Correlation coefficient	Level of significance
Petro Tac- 3.2 ℓ/m² (0.70 gal/yd²) of 20% solution in water	2-116 days	410	27	30	9.2	TP	92.9-0.328 t	-0.913	99%
						IP	102-0.528 t	-0.915	99%
						PM_{10}	102-0.464 t	-0.921	99%
						FP	100-0.00595 t^2	-0.986	99.9%[b]
Coherex® - initial application 3.8 ℓ/m² (0.83 gal/yd²) o 20% solution in water	7-41 days	94	34	38	6.2	TP	79.1-1.31 t	-0.717	< 90%
						IP	92.2-1.32 t	-0.869	95%
						PM_{10}	94.9-1.26 t	-0.892	98%
						FP	102-1.20 t	-0.796	90%
Coherex® - reapplication 4.5 ℓ/m² (1.0 gal/yd²) of 12% solution in water	4-35 days	97	39	43	6.0	TP	96.1-0.207 t	-0.594	< 90%
						IP	99.1-0.477 t	-0.986	95%
						PM_{10}	99.3-0.386 t	-0.946	95%
						FP	99.0-0.509 t	-0.869	< 90%
Watering[c]	1.0-2.8 hr	1,200	44	49	6.0	TP	103-218 t	-0.956	N/A
						IP	102-195 t	-0.968	N/A
						PM_{10}	102-187 t	-0.962	N/A
						FP	101-163 t	-0.990	N/A

[a] Time in days represented by t. Complete mitigation is assumed immediately after application.
[b] Because a parabola was used to characterize FP control efficiency decay, standard tests of significance are not strictly applicable.
[c] Run AJ-6 was not used in developing the equations for water.

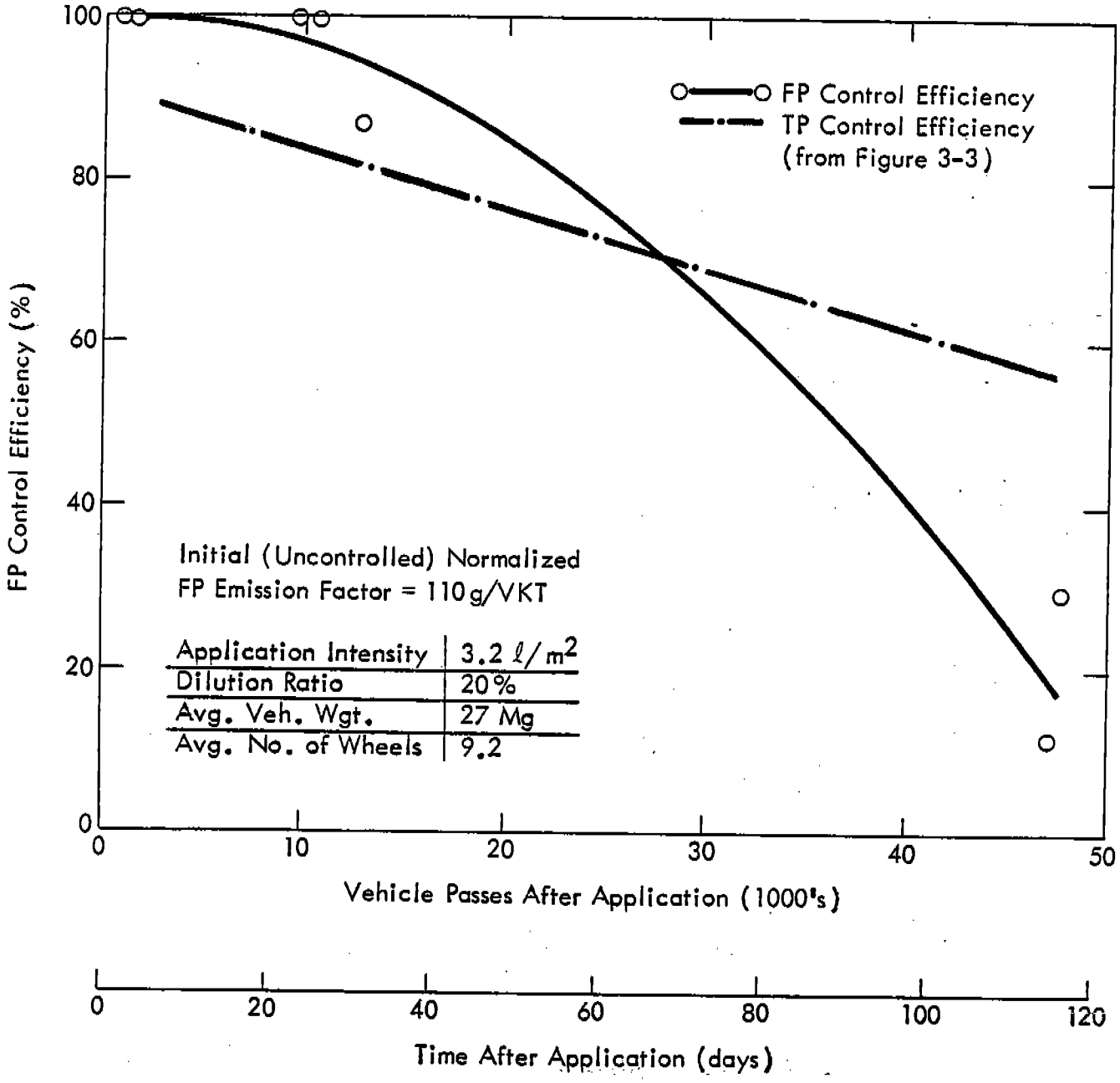

Figure 3-6. FP control efficiency decay for an initial application of Petro Tac compared to that for TP.

TABLE 3-13. CONTROL EFFICIENCY FOR THE TWO SIDES OF THE PLANT AG TEST ROAD

Run	Days after control application	Side	Control Efficiency (%) TP	IP	PM_{10}	FP
AG-6	23	North	99.8	100	100	N/A
		South	71.7	94.7	98.3	N/A
AG-7	26	North	99.5	99.9	99.9	N/A
		South	45.9	85.0	92.1	N/A
AG-8	30	North	97.5	97.9	98.0	98.7
		South	60.9	66.6	68.2	79.5
AG-9	115	North	94.3	86.7	88.6	84.7
		South	40.0	0	0	0
AG-10	116	North	84.7	87.5	88.6	80.1
		South	20.8	35.0	40.3	0
AG-11	116	North	76.3	83.6	85.4	94.6

Furthermore, attempts to modify existing traffic patterns where possible would extend a chemical control's lifetime, thus reducing the cost of a dust control program.

Watering as a control measure was tested during runs AJ-4 through AJ-6. It should be noted that, because of logistical problems, testing began fairly late in the day, with the result that testing continued after dusk. This fact, taken with the 9°C (16°F) temperature drop during testing, at least partially explains why the IP and PM_{10} control efficiency did not decrease from run AJ-5 to AJ-6, as shown in Table 3-14.

An earlier study by MRI indicated that the control efficiency of watering decays linearly with time.[3] The results obtained in this study for TP and FP also indicate such a decay. The following is a comparison of the results of the earlier study with those of AJ-4 and AJ-5:

	Reference 3	AJ-4, -5
Ambient air temperature	13-16°C	26-35°C
Application intensity	0.59 ℓ/m^2	1.9 ℓ/m^2
Average Vehicle weight	49 Mg	44 Mg
Decay rate (%/hr)		
TP	10.2	9.10
IP	11.8	8.14
PM_{10}	NA	7.79
FP	9.12	6.80

The above comparison assumes 100% efficiency immediately after application. As the comparison indicates, the rates of decay are similar for watering at two different plants, despite differences in ambient temperature and application intensity. There is reason to believe that a linear decay would have been observed for AJ-4 through AJ-6 for emissions in all size ranges had it been possible to begin testing earlier in the day. Best fit equations of watering control efficiency versus vehicle passes and time are presented in Tables 3-11 and 3-12, respectively.

Control efficiencies associated with an initial application of Coherex® are shown in Figures 3-7 through 3-10 for TP, IP, PM_{10}, and FP, respectively. Best fit equations of control efficiency for Coherex® versus vehicle passes and time are presented in Tables 3-11 and 3-12, respectively. Comparision with Figures 3-3 through 3-6 indicate that Coherex® exhibits a rate of decay an order of magnitude greater than that of Petro Tac. Undoubtedly much of this difference is attributable to the 30% greater vehicle weight at Plant AJ and to the fact that the road at Plant AJ was not as well compacted as Plant AG.

TABLE 3-14. CONTROL EFFICIENCY OF WATERING[a] UNPAVED ROADS

Time after application[b] (hr)	Control efficiency (%)			
	TP	IP	PM_{10}	FP
1.0	98.3	97.5	98.1	95.8
2.8	75.8	78.2	79.2	81.4
4.8[c]	60.9	83.0	81.1	66.8

[a] Application intensity of 1.9 ℓ/m^2 (0.43 gal/yd^2), with 72 ± 1.5 vehicle passes per hour during testing.

[b] At the midpoint of test.

[c] This test was conducted at approximately 8 p.m.

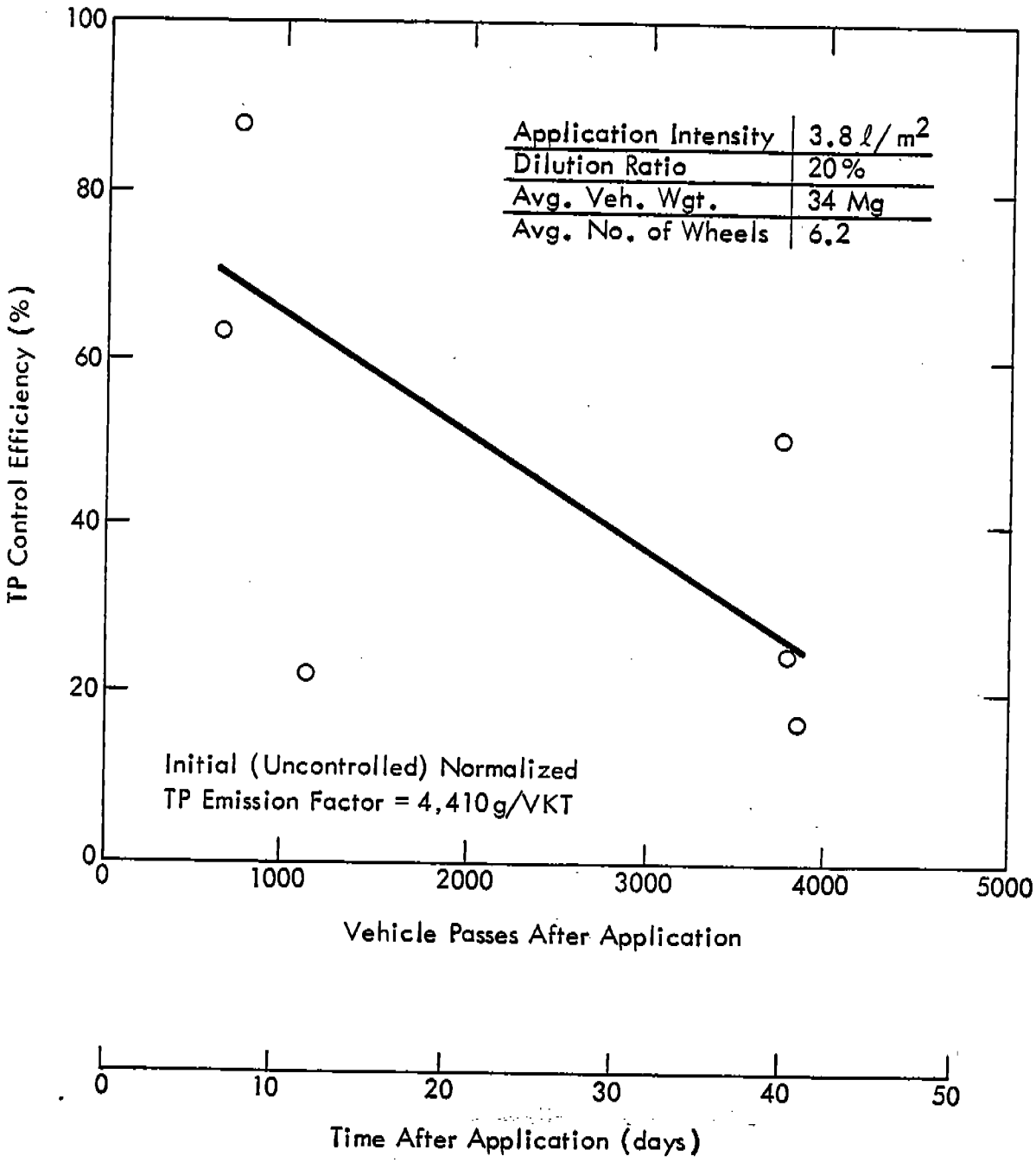

Figure 3-7. TP control efficiency decay for an initial application of Coherex®.

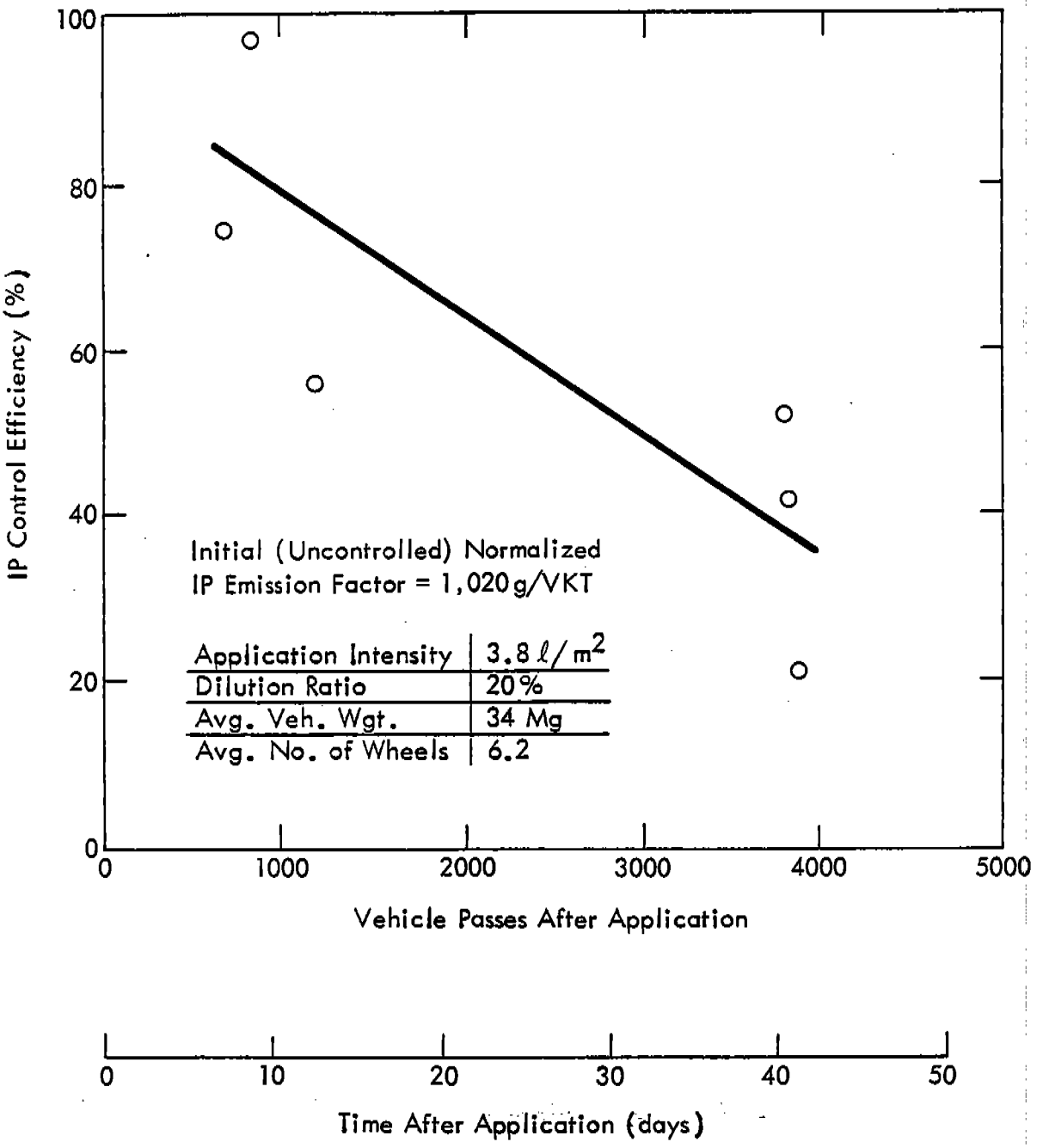

Figure 3-8. IP control efficiency decay for an initial application of Coherex®.

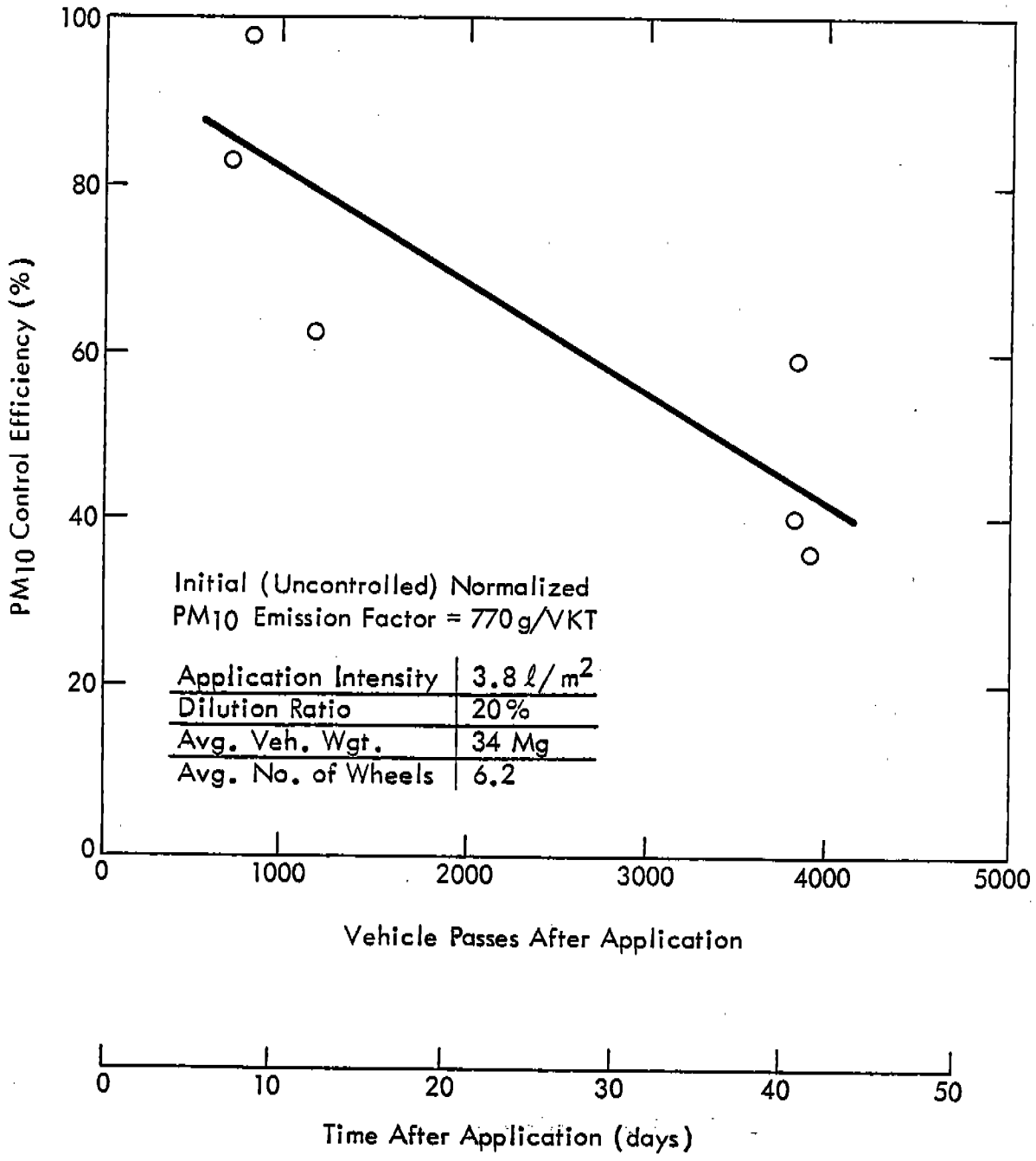

Figure 3-9. PM_{10} control efficiency decay for an initial application of Coherex®.

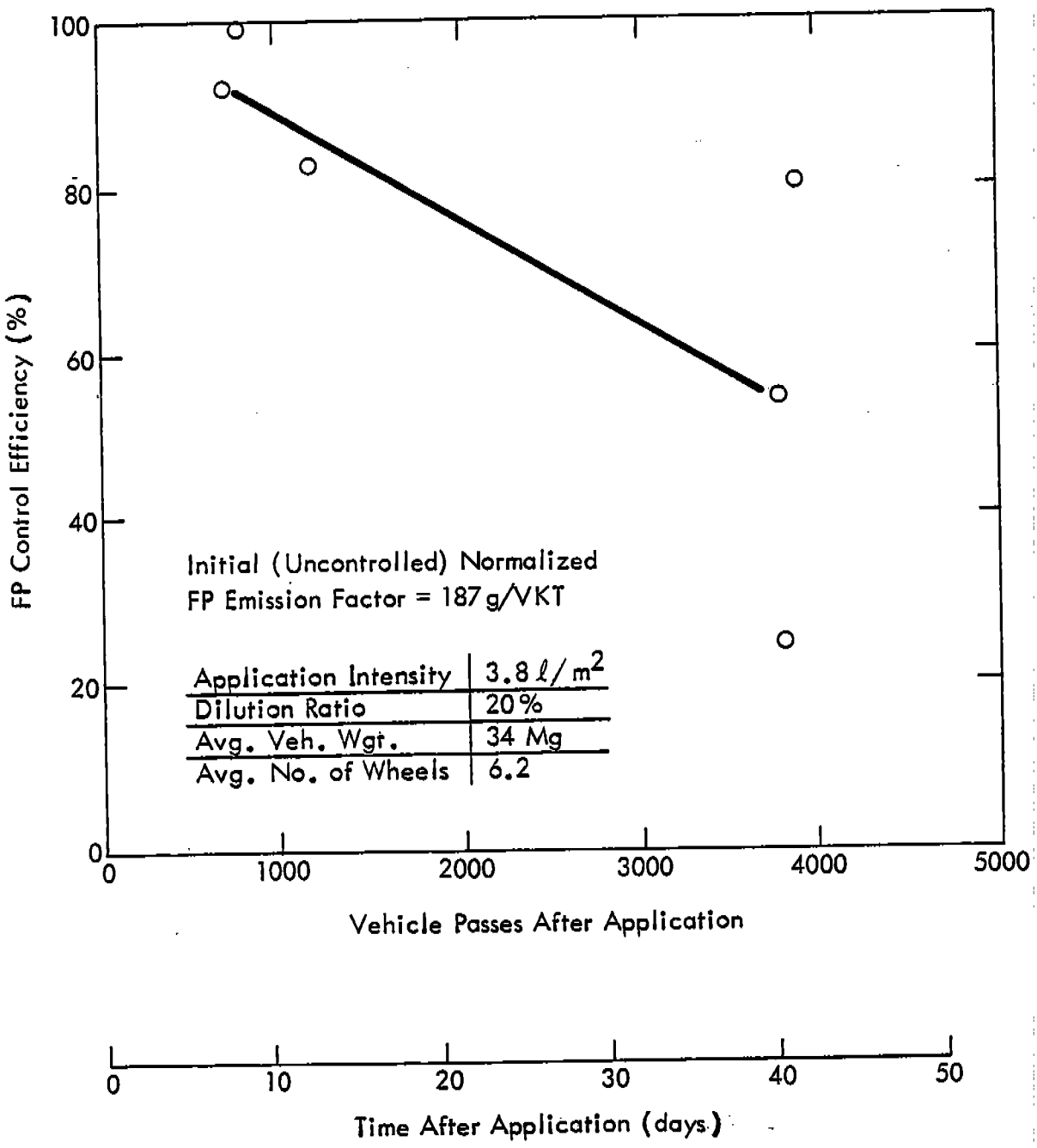

Figure 3-10. FP control efficiency decay for an initial application of Coherex®.

Unlike the asphalt emulsion evaluated at Plant AG, control efficiency curves for IP, PM_{10} and FP did not cross the curve for TP control efficiency during the span of testing. During each test, the control efficiency after a given number of vehicle passes increased as the particle size range decreased. Thus, as opposed to the tests of Petro Tac, Coherex®, when applied at 3.8 ℓ/m^2 of 20% solution appears to control particulate emissions of different size fractions in a fairly consistent manner throughout its lifetime. In other words, the decay rate for the initial application of Coherex® was nearly identical regardless of the particle size range. This can be seen by observing the slopes of the equations in Tables 3-11 and 3-12.

It should be noted that the results of Runs AJ-16 and AJ-17 were excluded in determining the control decay for Coherex®. This was done because the surface moisture contents measured for these late November and early December tests were substantially above those for either the uncontrolled or earlier tests of the Coherex®-treated road. The moisture contents for these two runs were actually closer to those measured during tests of watering as a control measure, as shown in Table 3-15. Because Runs AJ-16 and AJ-17 produced control efficiency values far above those indicated by the earlier tests, these results will be discussed in Section 5.4, under the effects of winter on unpaved road dust emissions.

Control efficiency values for a repeat application of Coherex® for TP, IP, PM_{10}, and FP emissions are presented in Figures 3-11 through 3-14, respectively. The best fit equations of the control efficiency decay functions versus vehicle passes and time are presented in Tables 3-11 and 3-12, respectively. It should be noted that the number of vehicle passes after application is shown explicitly on these figures because the traffic rate decreased during the testing period. Comparison with Figures 3-7 through 3-10 indicates that the decay rate for a repeat application of Coherex® is roughly an order of magnitude smaller than that associated with the original treatment. The data of Figures 3-11 to 3-14 suggest that the lifetime of the second Coherex® application would be approximately the same as that of the initial application of Petro Tac, although direct comparisons are difficult because of the greater traffic rate at Plant AG and the greater vehicle weight at Plant AJ.

Part of the lasting control associated with the repeat Coherex® application may be attributed to the strong bonding characteristics exhibited. As shown in Table 3-7, the surface aggregate material silt content measured during runs AJ-13 and AJ-14 was so small as to be undetectable. Table 3-16 compares the measured surface material size distributions before and after the reapplication. Because surface silt content (particles < 75 μm) has been shown to have a very strong, positive correlation with unpaved road emissions, the high level of control associated with the Coherex® reapplication is not surprising in light of the significant reduction in surface silt.

TABLE 3-15. COMPARISON OF SURFACE MOISTURE CONTENTS

Run	Control	Time since rainfall[a] or watering	Moisture content[b] (%)
AJ-4	Watering	1.0 hr	5.1
AJ-5	Watering	2.8 hr	2.0
AJ-16	Coherex®	3 days	3.7
AJ-17	Coherex®	4 days	3.0

[a] 0.1 in. or more.

[b] Sample taken after test.

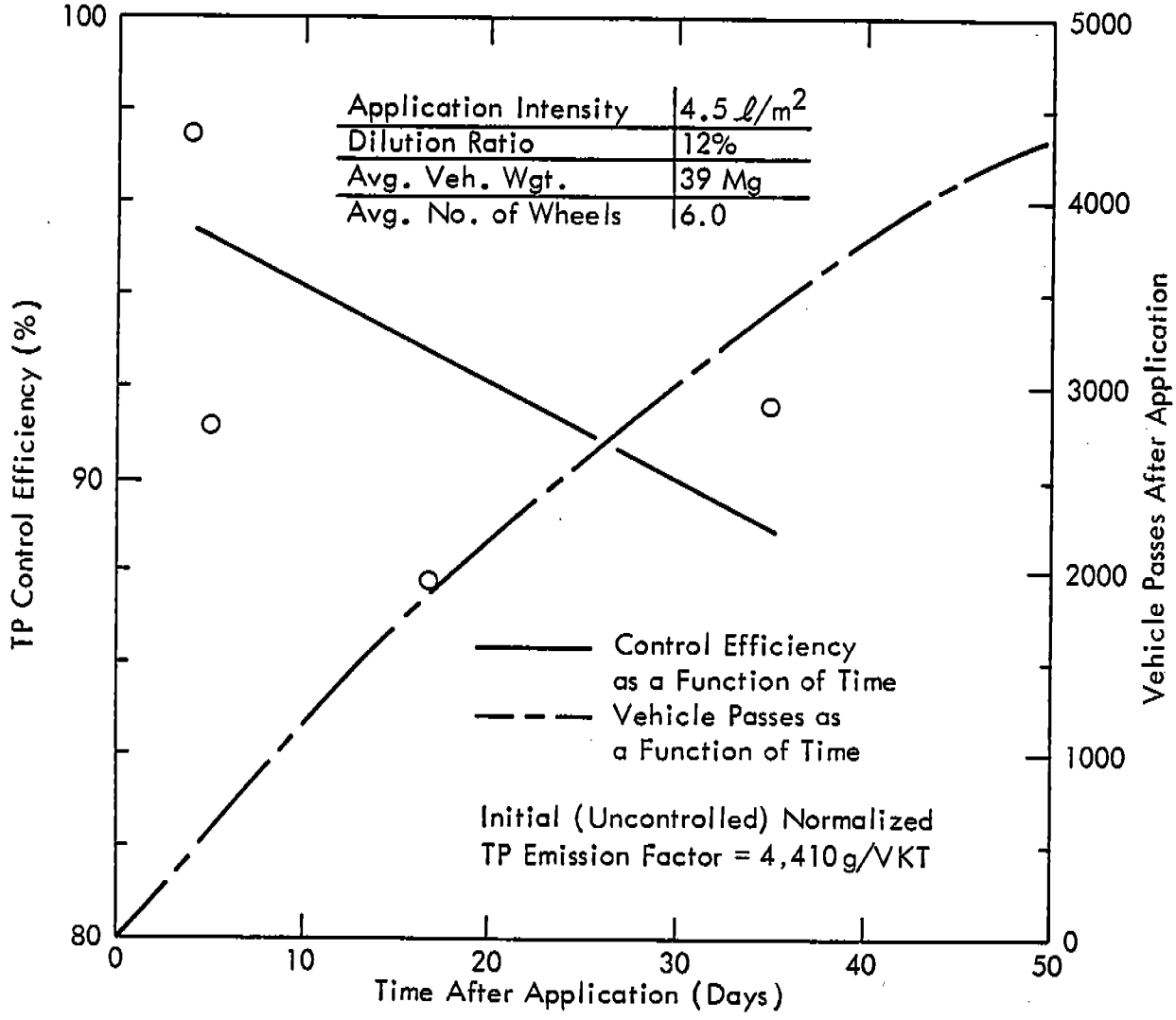

Figure 3-11. TP control efficiency decay for a reapplication of Coherex®.

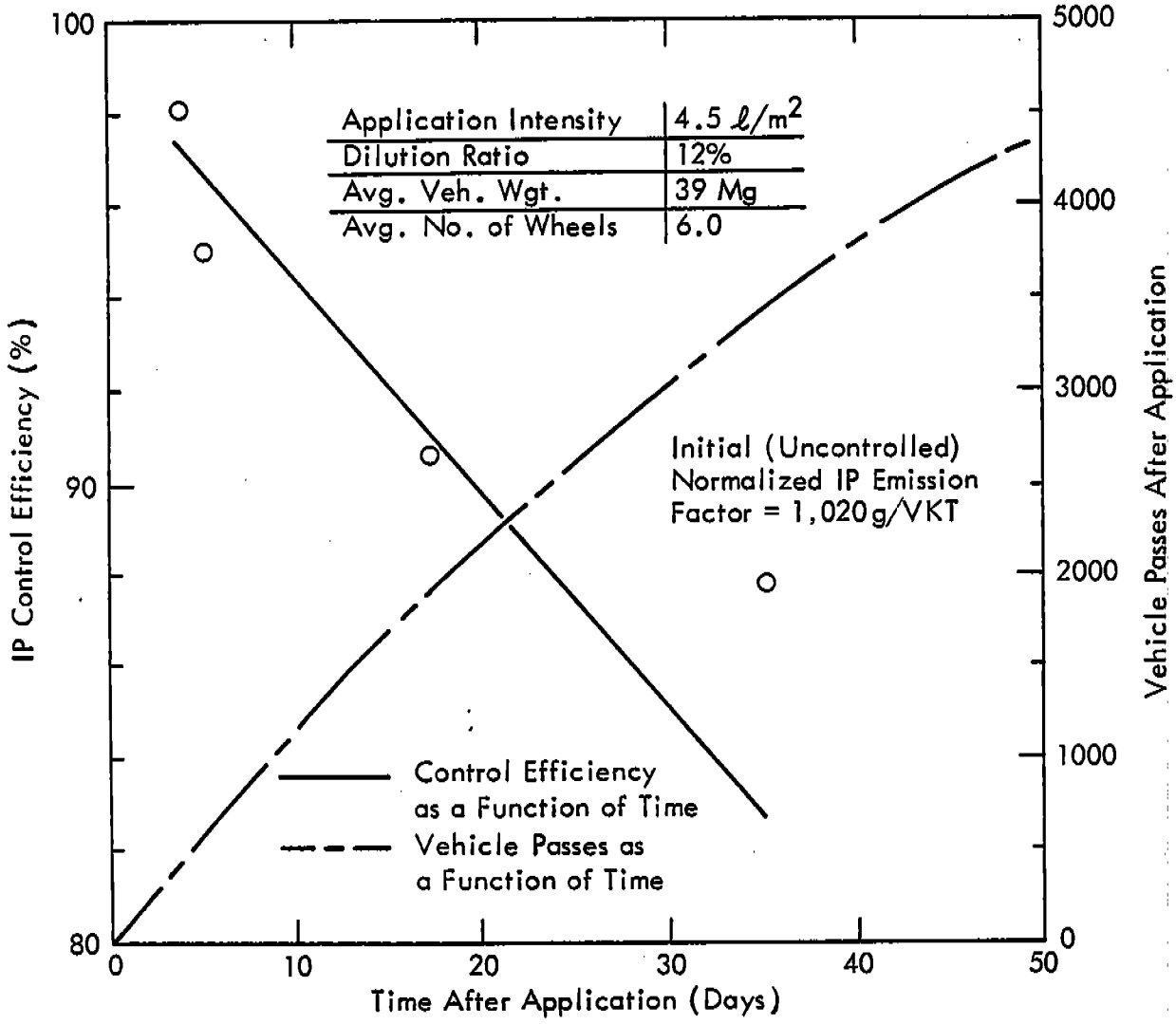

Figure 3-12. IP control efficiency decay for a reapplication of Coherex®.

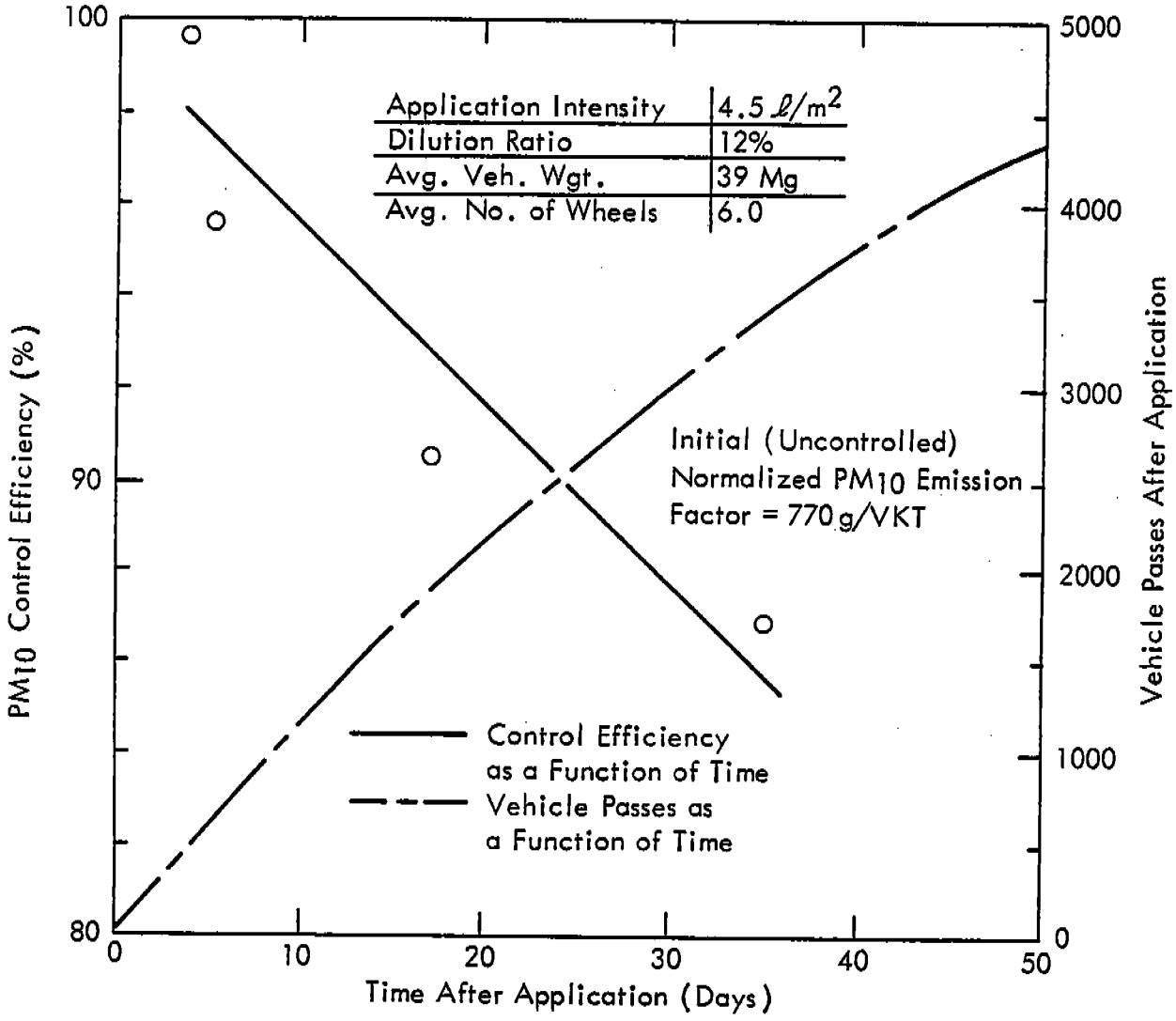

Figure 3-13. PM_{10} control efficiency decay for a reapplication of Coherex®.

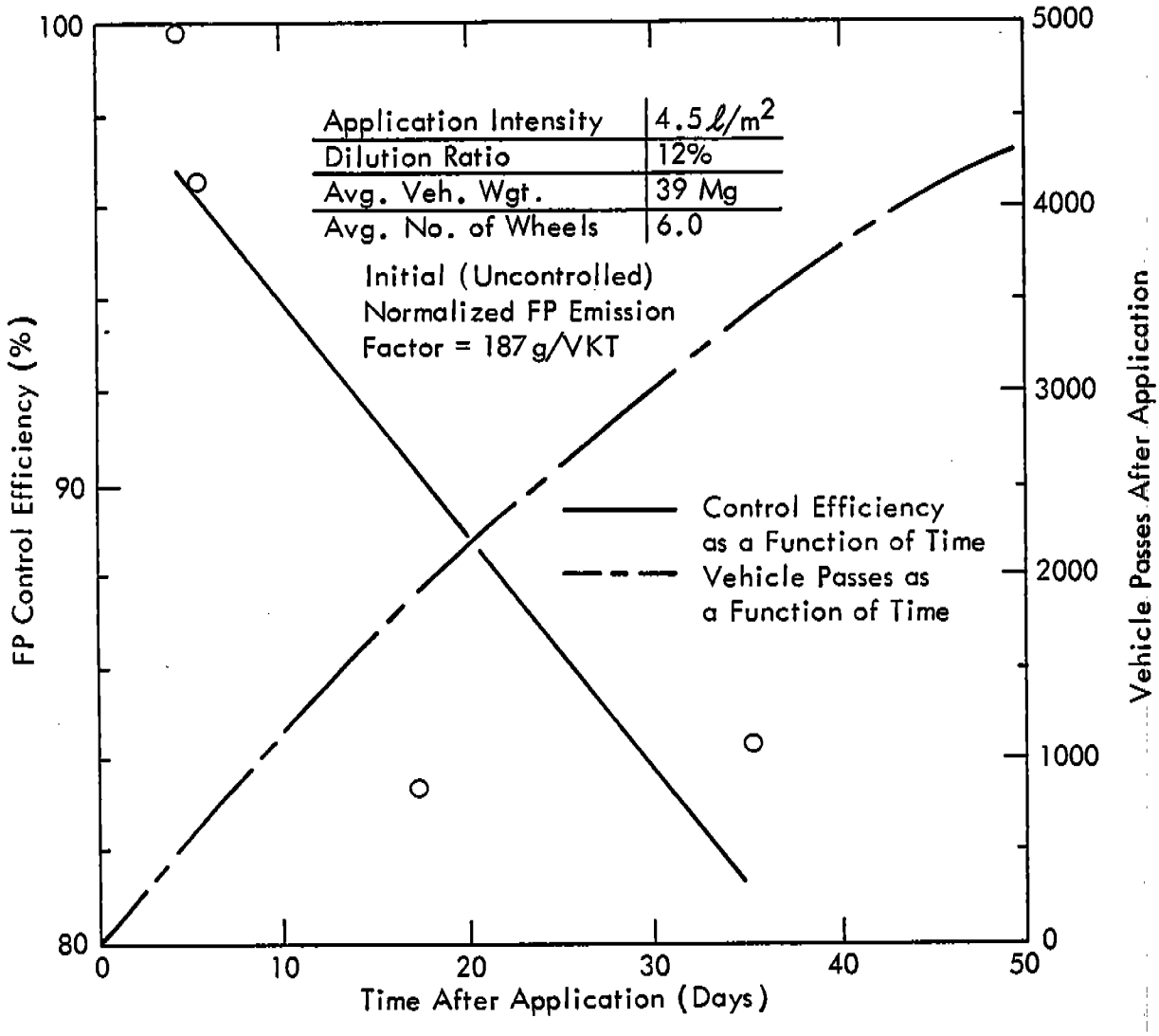

Figure 3-14. FP control efficiency decay for a reapplication of Coherex®.

TABLE 3-16. COMPARISON OF SURFACE SILT CONTENTS BEFORE AND AFTER COHEREX® REAPPLICATION

Physical Particle size (μm)	Mass fraction (%) less than stated size			
	Before re-application	After reapplication		
	AJ-12	AJ-13	AJ-14	AJ-15
2,000	77	30	35	60
830	55	4.1	13	35
420	35	0.069	4.4	19
250	23	0.0087	1.5	9.4
180	17	-	0.67	6.0
150	13	-	0.36	4.3
100	9.2	-	0.12	2.3
75	5.8	-	0.034	1.6

SECTION 4.0

COST-EFFECTIVENESS OF UNPAVED ROAD DUST CONTROLS

The purpose of this section is to develop the cost-effectiveness values for the unpaved road dust control techniques evaluated during this study. Cost effectiveness is defined as the cost of control divided by the reduction in mass emissions. Cost-effectiveness equations presented in a prior report[3] serve as the basis of these calculations. Cost-effectiveness values, like control efficiency values, are a function of particulate size. The analysis to follow will focus on the PM_{10} size fraction because this size is the most likely basis for the anticipated revision to the particulate NAAQS. This section: (a) reviews cost-effectiveness equations presented in a prior report; (b) develops new equations which facilitate interplant comparisons; (c) presents collected cost data and calculated cost-effectiveness values; and (d) contrasts and compares the cost-effectiveness of various dust suppressants applied at various plants.

4.1 COST-EFFECTIVENESS EQUATIONS ASSUMING LINEAR DECAY IN CONTROL EFFICIENCY WITH TIME

This section presents the cost-effectiveness equations resulting from a detailed development presented in a prior report.[3] Since the decay in PM_{10} control efficiency is linear with time (see Section 3.2), the control efficiency decay as a function of time after application can be written

$$CEF(t) = -bt + 1 \qquad (4\text{-}1)$$

where CEF = instantaneous control efficiency (fraction)
b = slope of decay function (days $^{-1}$)
t = time after control application (days)

The cost-effectiveness (CE) of an unpaved road dust control technique which exhibits a linear efficiency decay function, can be written

$$CE = \frac{D}{ER} = \frac{A\,(NT)}{EF \times SE\left(1 - \frac{b}{2}\frac{365}{NT}\right)} \qquad (4\text{-}2)$$

where CE = cost-effectiveness ($/lb)
D = annual cost of control technique ($/yr)
ER = annual emission reduction (lb of emissions reduced/yr)
A = unit cost of control ($/treatment)
NT = frequency of control application (treatments/year)
EF = uncontrolled emission factor (lb/VMT)
SE = annual source extent (VMT/year)

The above generalized expression for cost-effectiveness can be optimized to determine the number of treatments in a year that will produce the minimum value of CE. The optimized value of NT is[3]

$$NT_{opt} = 365b \qquad (4\text{-}3)$$

which indicates that the control efficiency should be allowed to decay to zero before reapplication, if the minimum value of cost-effectiveness is desired. However, for a linear decay in control efficiency, this produces an average reduction of 50% in emissions, which may or may not meet the needs of a particular plant. By substituting Equation 4-3 into Equation 4-2, the minimum cost-effectiveness can be written

$$CE_{min} = \frac{A \times 365 \times b}{\frac{1}{2} \times EF \times SE} \qquad (4\text{-}4)$$

If the control efficiency fraction at a specific plant must meet a required value (V) greater than 0.5, then the cost-effectiveness equation can be written

$$CE = \frac{A \times 365 \times b}{2 \times EF \times SE \times (V - V^2)} \qquad (4\text{-}5)$$

CE is a minimum for V = 0.5, and at V = 0.5, Equation 4-5 reduces to Equation 4-4.

The slope of the control efficiency fraction decay curve (b) can be viewed as the decay rate constant. It is the amount that the control efficiency fraction is reduced each day. For example, a decay rate of 0.1 day^{-1} implies that the instantaneous control efficiency fraction will be 0.9 at the end of day 1, 0.8 at the end of day 2, etc.

The decay rate constant for a given dust suppressant is dependent on the following source/control parameters: (a) the application intensity and dilution ratio; (b) the average annual traffic (vehicle passes per year); (c) vehicle characteristics such as average weight or number of wheels; and (d) road strength (as measured by the California Bearing Ratio (CBR)).

Because the decay rate constant is dependent on so many source/control parameters, it is difficult to apply the results of dust suppressant performance testing at one site to the prediction of performance at another site. In actuality, all four of the above source/control parameters must be the same at both sites in order for the measured decay rate to apply. Since this severely limits the applicability of performance test results, it becomes clear that the above source/control parameters should be quantified during all performance tests, and that the control efficiency and cost-effectiveness equations should be developed to account for these source/control parameters. The following section presents equations that account for variations in average daily traffic from plant to plant.

4.2 COST-EFFECTIVENESS EQUATIONS ASSUMING LINEAR DECAY IN CONTROL EFFICIENCY WITH VEHICLE PASSES

There are certain chemical dust suppressants, like Petro Tac and Coherex® which were tested in this study, for which the decay in control efficiency is not so much related to passage of time with the attendant weather changes, as it is related to the number of vehicles utilizing the treated road. Even for the suppressants tested in this study, there are exceptions to the above statement if the road subgrade is subjected to the freeze-thaw cycle. During this study, the exceptions were not a factor, and the control efficiency decay was well correlated linearly with vehicle passes as was shown in in Table 3-11 where the best-fit equations are presented.

The control efficiency decay as a function of vehicle passes after control application can be written

$$CEF(P) = -m\,P + 1 \qquad (4\text{-}6)$$

where $CEF(P)$ = instantaneous control efficiency (fraction)
m = decay constant (vehicle passes $^{-1}$)
P = number of vehicle passes after control application

Unlike b in Eq. 4-1, the decay constant m can be applied to sites other than those tested. The cost-effectiveness can then be written

$$CE = \frac{A \times \frac{AP}{N}}{EF \times SE\,(-\frac{m}{2} N + 1)} \qquad (4\text{-}7)$$

where AP = traffic rate (vehicle passes per year)
N = number of vehicle passes per treatment

The ratio AP/N actually represents the number of treatments per year.

The above generalized expression for cost-effectiveness (Equation 4-7) can be optimized to determine what number of passes per treatment will produce the minimum value of CE. The optimized value of N is

$$N_{opt} = \frac{1}{m} \qquad (4\text{-}8)$$

which implies that the control efficiency should be allowed to decay to zero before reapplying if one desires the minimum value of cost-effectiveness. Substituting the expression for N_{opt} into the equation for CE yields:

$$CE_{min} = \frac{A \times m \times AP}{1/2 \times EF \times SE} \qquad (4\text{-}9)$$

Let the entire length of road being treated be defined as ASE. If it is assumed that each vehicle pass travels the entire length of the road being treated, then the source extent can be written

$$SE = AP \times ASE \qquad (4\text{-}10)$$

The minimum cost-effectiveness can then be written

$$CE_{min} = \frac{\frac{A}{ASE} \times m}{\frac{1}{2} \times EF} \qquad (4\text{-}11)$$

The value A/ASE represents the cost per treated mile of road. The numerator of Equation (4-11) has units of dollars per vehicle mile traveled ($/VMT) while the denominator has units of pounds per vehicle mile traveled (lb/VMT). Equation (4-11) allows one to calculate the minimum cost-effectiveness value for a tested dust suppressant (i.e., where m is a known value) for any plant, providing that the cost per treated mile of road and the uncontrolled emission factor for the unpaved roads in that plant are known.

Equation (4-11) also yields the interesting conclusion that if A/ASE and EF are constant from plant to plant, then CE_{min} is also constant. This is true even if the second plant has many more vehicle passes per unit time than the first. This is because the increased cost at the other plant due to more frequent treatment is directly offset by the increase in the emission reduction.

4.3 QUANTIFICATION OF IMPORTANT VARIABLES IN THE COST-EFFECTIVENESS EQUATIONS

In this section, the variables in the cost-effectiveness equations (4-2, 4-4, 4-5, 4-7, 4-9, 4-11), are quantified for the dust suppressants tested at two plants in this study. Also, data from four plants made available through surveys are summarized in a format useful in the above equations. The variables of importance in the above equations are listed in Table 4-1 by the following categories: (a) cost related variables; (b) decay constants; (c) emission factor; (d) source extent variables; and (e) general variables selected by plant personnel. Table 4-1 also shows the other source/control parameters (where they exist) which can affect the value of each of the variables in the cost-effectiveness equations. When a variable is quantified in the field, the related source/control parameters should also be measured and reported.

4.3.1 Quantification of Cost-Related Variables

For the dust controls tested in this study, cost data were gathered in two ways. First, during testing, information needed to determine costs for chemical purchase and application as well as for burdened labor were recorded. Second, cost survey questionnaires were sent to two plants utilizing the chemical dust suppressants evaluated in this study in a large-scale program. A copy of the survey is presented in Appendix A.

A summary of the cost data collected during testing at J&L's Indiana Harbor Works and Armco's Kansas City Works is shown in Table 4-2. The Kansas City Works data are useful for intraplant comparison of different dust suppressants, but the costs should not be extrapolated to plant-wide suppressant application control programs since the economies of scale will significantly

TABLE 4-1. SOURCE/CONTROL PARAMETERS AFFECTING COST-EFFECTIVENESS VARIABLES

Variables			Source/Control Parameters
General Class	Symbol	Definition	Affecting Variable Value
Cost related	A	Cost per treatment ($/treatment)	. application intensity . dilution ratio . road length and width[a]
Decay constants	b	Decay rate constant (day^{-1})	. application intensity . dilution ratio . average annual traffic . average vehicle weight . average number of wheels . roadway CBR
	m	Decay constant ($vehicle\ passes^{-1}$)	. application intensity . dilution ratio . average vehicle weight . average number of wheels . roadway CBR
Emission factor	EF	Uncontrolled emission factor (lb/VMT)	. uncontrolled roadway silt content . average vehicle speed . average vehicle weight . average number of wheels
Source extent	SE	Annual source extent on treated roadway (VMT/yr)	. vehicle passes . length of treated roadway travelled
	AP	Annual number of vehicle passes (vehicle passes/yr)	
	ASE	Length of roadway treated per treatment (miles/treatment)	
General (selected by plant personnel)	NT	Number of treatments per year	
	N	Vehicle passes per treatment	

[a] The length and width of road treated along with the number of treatments per year aid in determining the economies of scale.

TABLE 4-2. SUMMARY OF TESTED UNPAVED ROAD DUST SUPPRESSANT COST DATA

Plant	Dust Suppressant	Cost Item	1982 Operation and maintenance costs ($)	Actual source extent Length (miles)	Actual source extent Width (ft)
J&L-Indiana Harbor Works	Petro Tac-Initial application: 0.7 gal/yd² of 20% solution	Chemical	670	0.093	60
		Application truck lease and labor	80		
Armco-Kansas City Works[a]	Coherex®-Initial application: 0.83 gal/yd² of 20% solution	Chemical	1,450[b]	0.27	30
		Application truck lease and labor	390		
		Forklift and driver	390[c]		
	Coherex® - Reapplication: 1.0 gal/yd² of 12% solution	Chemical	1,000[b]	0.23	30
		Application truck lease and labor	300		
		Forklift an driver	300[c]		
	Water: 0.43 gal/yd²	Application truck lease and labor	260[d]	0.25	30

[a] These data should not be extrapolated to plant-wide suppressant application control programs since the economies of scale will significantly lower these values.

[b] Coherex® was purchased in a lot size of thirty 55 gal. drums.

[c] Forklift needed to empty drums into application truck.

[d] Includes problems with lack of water pressure during filling of truck, broken hose repair, and excessive time spent waiting for trains. More typical cost could be a factor of two to four lower.

lower these values. Because there was no plant-wide open dust control program in progress at Armco's Kansas City Works, MRI had to purchase the chemical in a small lot size and negotiate with a contractor to apply this small lot. The chemical was purchased in drums and had to be emptied into the application truck with a forklift. As can be expected, the cost for chemical and application on this small scale necessitated extra cost per treatment and per mile of road treated.

At J&L's Indiana Harbor Works, there was already a plant-wide open dust control program in progress, so the chemical and application costs on Table 4-2 are at bulk handling prices. The cost for the storage tank at J&L is not shown in Table 4-2 since it was difficult to apportion the capital cost for the tanks over this small test application. The application truck lease and labor cost at J&L was at a rate negotiated by the plant with the contractor and based on bulk application. Because of the different situations at each plant, the cost data collected from testing should be compared between plants only with the greatest caution and realization of the impacts of economies of scale.

Table 4-3 displays the cost data of Table 4-2 in the units required for the cost-effectiveness equations. The other important source/control parameters affecting the cost per treatment (A) are also listed, including application intensity and dilution ratio, as well as length and width of road treated.

A summary of the cost data collected from the suppressant cost survey as related to unpaved roads is shown in Table 4-4. The two plants surveyed were J&L Indiana Harbor Works and Shenango, Inc., Neville Island Coke and Iron Works. Neither plant incurred any application truck purchase expense since application services were leased. J&L incurred some capital expense to upgrade two old, unused tanks to serve as Petro Tac storage tanks on the plant site. Shenango incurred no capital expenses for storage since the chemical application contractor owned the storage facility. Both plants purchased the chemical in bulk (3,000 to 6,000 gal. per order delivered in a tanker truck).

Table 4-5 displays the cost data of Table 4-4 in the units required for the cost-effectiveness equations. In addition to data from Table 4-4, Table 4-5 contains data from two plants surveyed in a previous study[3]: Armco-Middletown Works and Armco Houston Works. Comparison of the data from the two surveys should take into account cost escalation over the period 1980 to 1982.

4.3.2 Quantification of Decay Constants

Two important variables in the cost-effectiveness equations are the decay constants b and m. These constants quantify the decay in the control efficiency fraction as a function of time (b) and as a function of vehicle passes (m). Table 4-6 shows the values for b and m for the suppressants tested in this study. The value of m is more useful for interplant comparison of chemical dust suppressant performance.

TABLE 4-3. QUANTIFICATION OF COST-RELATED VARIABLES FOR SITES TESTED IN THIS STUDY

Plant	Dust suppressant	Cost per treatment (A) ($/treatment)	Length of road treated (ASE) (miles/treatment)	Average width of road treated (ft)
J&L - Indiana Harbor	Petro Tac - Initial Application: 0.70 gal/yd^2 of 20% solution	750[b]	0.093	60
Armco - Kansas City[a]	Coherex® initial application: 0.83 gal/yd^2 of 20% solution	1,840[c]	0.27	30
	Coherex® reapplication: 1.0 gal/yd^2 of 12% solution	1,300[c]	0.23	30
	Water: 0.43 gal/yd^2	260[d]	0.25	30

[a] These data should not be extrapolated to plant-wide suppressant application control programs since the economies of scale will significantly lower these values.

[b] Does not include any prorated cost for storage tanks; includes only chemical purchase, truck lease, and labor costs.

[c] Does not include cost of forklift or driver.

[d] Includes additional cost due to problems with lack of water pressure during filling of truck, broken hose, and excessive time spent waiting for trains. Also, it required two loads to treat 0.25 miles. More typical cost per treatment could be a factor of two to four lower.

TABLE 4-4. SUMMARY OF SURVEYED UNPAVED ROAD DUST SUPPRESSANT COST DATA

Plant	Dust Suppressant	Cost Item	Purchase and installation cost ($)	Year of purchase	Estimated lifetime (yrs)	Operation and maintenance costs ($)	1982 Treated source extent (miles)	Actual source extent	
								Length (miles)	Avg. width (ft)
J&L-Indiana Harbor Works	Petro Tac - each application: 0.5 gal/yd² of 20% solution followed by 0.5 gal/yd² of 12% solution	Modify existing tanks	10,800	1982	20		10	2	60
		Chemical				81,900			
		Application truck lease and labor				6,500			
Shenango, Inc.-Neville Island Plant	Coherex®-Initial application: 0.16 gal/yd² of 20% solution Coherex® -Reapplications: 0.16 gal/yd² of 8 to 20% solution	Storage tank	a	a	a		18.8	1.57	20
		Chemical				10,000			
		Application truck lease and labor				4,100			

[a] Shenango has no capital investment costs for storage since a contractor owns the 8,000 gal. storage tank

TABLE 4-5. QUANTIFICATION OF COST-RELATED VARIABLES FOR PLANTS SURVEYED

Plant	Dust suppressant	Cost per treatment (A) ($/treatment)	Year	Length of road treated (ASE) (miles/treatment)	Average width of road treated (ft)
Armco-Middletown Works	Coherex® initial application: 0.19 gal/yd² of 16.7% solution Coherex® reapplications: 0.28 gal/yd² of 11% solution	5,350[a]	1980	7.1	36
Armco-Houston Works	Water: 0.48 gal/yd²	157[b]	1980	4.3	36
J&L-Indiana Harbor Works	Petro Tac - each application: 0.5 gal/yd² of 20% solution followed by: 0.5 gal/yd² of 12% solution	18,000	1982	2	60
Shenango, Inc. Neville Island Plant	Coherex® initial application: 0.16 gal/yd² of 20% solution Coherex® reapplications: 0.16 gal/yd² of 8 to 20% solution	1,175[a]	1982	1.57	20

[a] Averaged over initial application and subsequent reapplications.

[b] Cost data were not sufficiently subivided to determine if all costs were accounted for. It is suspected that this value is low.

TABLE 4-6. DECAY CONSTANTS FOR TESTED SUPPRESSANTS[a]

Suppressant	Decay constant for PM_{10} b (day^{-1})	Decay constant for PM_{10} m (vehicle $passes^{-1}$)	Average traffic rate (vehicle passes per day)	Average vehicle characteristics: Weight (T)	Average vehicle characteristics: No. of wheels
Petro Tac 0.7 gal/yd^2 of 20% solution	4.6×10^{-3}	1.1×10^{-5}	410	30	9.2
Coherex Initial application 0.83 gal/yd^2 of 20% solution	1.3×10^{-2}	1.3×10^{-4}	94	38	6.2
Reapplication 1.0 gal/yd^2 of 12% solution	3.9×10^{-3}	4.3×10^{-5}	97	43	6.0
Water 0.43 gal/yd^2	1.9	1.8×10^{-3}	1,200	49	6.0

[a] The road strength as measured by the CBR is an important parameter that was not quantified.

However, the value of b may be more useful in comparing the performance of watering between plants. This is because the decay in watering performance in the absence of cloud cover is thought to be much more sensitive to accumulated solar heat input over time than to the number of vehicle passes and the attendant heat from these vehicles. This can be seen in the extreme where even with no vehicle traffic on a watered road, the decay in control efficiency on a day with little cloud cover will be relatively rapid.

In addition to the decay constants, Table 4-6 shows the other source/control parameters which effect the values of the decay constants for each suppressant. These parameters include application intensity and dilution ratio, average traffic rate, and average vehicle characteristics of weight and number of wheels.

4.3.3 Quantification of Uncontrolled Emission Factors

The uncontrolled emission factors measured during testing are important in the cost-effectiveness equations. Uncontrolled emission factors play a role in determining the mass of dust reduced by a given suppressant. From Table 3-6, one can see that the geometric average uncontrolled emission factor for PM_{10} at J&L's Indiana Harbor Works was 3.05 lb/VMT, while at Armco's Kansas City Works, it was 2.86 lb/VMT. The other important source/control parameters affecting the emission factor are also shown on Table 3-7.

4.4 CALCULATION OF COST-EFFECTIVENESS

In this section, the cost-effectiveness values for the suppressants tested in this study are presented. The cost-effectiveness values presented are the optimum (minimum) values corresponding to reapplication only after the control efficiency is allowed to decay to zero. Equation 4-11 was used to calculate CE_{min}, and the results are shown in Table 4-7. All the values in Table 4-7 represent an average control efficiency of 50%. If an average control efficiency greater than 50% were required, the values in Table 4-7 would increase by the same factor so that the ratios of the values would remain the same.

4.5 CONCLUSIONS

This section presents conclusions from the predictive equations presented in Sections 4.1 and 4.2, as well as conclusions based on comparisons of cost-effectiveness values calculated in Section 4.3.

4.5.1 Conclusions from the Predictive Equations

When cost-effectiveness values based on suppressant performance tests at one plant are applied at another plant, the predictive equations in Sections 4.1 and 4.2 along with Table 4-1 serve as useful tools. For example, Table 4-1 shows that the decay rate constant, b, is dependent on the traffic rate. Actually, the value of b varies directly with traffic rate. However, the source extent also varies directly with the traffic rate (see Eq. 4-10) so that the minimum cost-effectiveness value remains the same. What this

TABLE 4-7. CALCULATED VALUES OF MINIMUM COST-EFFECTIVENESS FOR TESTED SUPPRESSANTS

Suppressant	CE_{min}[a] ($/lb of PM_{10} reduced)
Petro Tac Initial application 0.7 gal/yd² of 20% solution	0.060
Coherex® Initial application 0.83 gal/yd² of 20% solution	0.64[b]
Reapplication 1.0 gal/yd² of 12% solution	0.16[b]
Water 0.43 gal/yd²	1.30[b,c]

[a] Petro Tac was applied to a road 60 ft wide while the other chemicals were applied to a road 30 ft wide.

[b] These data should not be extrapolated to plant-wide suppressant application control programs since the economies of scale will significantly lower these values.

[c] Includes additional cost due to problems with lack of water pressure during filling of truck, broken hose, and excessive time spent waiting for trains. More typical cost per treatment could be a factor of two to four lower.

result means physically is that while the cost of treatment is increased for a plant with a higher traffic rate, for example, the emission reduction is increased by the same factor. Therefore, the cost-effectiveness value will remain the same.

Another interesting point involves the effect of changing vehicle weight and number of wheels from plant to plant or even from road to road within a plant. Table 4-1 indicates that the decay rates, b and m, are both affected by the vehicle characteristics. However, Table 4-1 also shows that the uncontrolled emission factor is also effected by these variables. As vehicle weight and number of wheels increase, both the suppressant decay rates as well as the uncontrolled emission factor increases. While it is not known how b and m change as a function of vehicle weight and wheels, it is evident from the cost-effectiveness equations, that the effects are offset, at least partially, by the change in the emission factor. Consequently, the cost-effectiveness value is definitely less sensitive to changes in vehicle weight and number of wheels than are the decay rates or the emission factor individually.

Both of the above points tend to support the conclusion that cost-effectiveness values can be directly applied at plants other than those tested. However, any changes in applicaton intensities, dilution ratio, or road strength make this transferral of data less reliable.

4.5.2 Comparisons of Minimum Cost-Effectiveness

The comparisons of cost-effectiveness values that can be made with a minimum of caveats are those relating to Coherex® and water. Both of these dust suppressants were applied to the same road at the same plant by the same contractor. From Table 4-7, the initial application of Coherex® appears to be a factor of two more cost-effective than the water, while the reapplication of Coherex® appears to be a factor of eight more cost-effective than the water. This conclusion, however, is affected by the variation in other source/control parameters. The impact of these source/control parameters can be classified as either strengthening or weakening the conclusion.

If a change in the source/control parameters (shown in Table 4-1) between two sites and/or two chemicals being compared can be used to explain the difference in the cost-effectiveness values obtained, then the conclusion that one cost-effectiveness value is better than another is weakened. However, if a change in the source/control parameters between the two sides of the comparison allows one to reason that, were the parameters the same, the cost-effectiveness values would be even further apart, then the conclusion that one cost-effectiveness value is better than another is strengthened. The following is a list of source/control parameters affecting the conclusion that Coherex® is more cost-effective than water.and their impact:

1. The watering tests had a significantly higher vehicle weight than either the initial application or reapplication of the Coherex.® This weakens the conclusion.

2. The Coherex® purchase price was inflated due to the small lot purchased. This strengthens the conclusion when applied to a decision between water and Coherex® for a plant-wide control program.

3. There were significant atypical problems in the application of the water which increased the time and consequently the cost required to apply the water. This weakens the conclusion.

Another intraplant comparison of minimum cost-effectiveness values can be made between the Coherex® initial application and the reapplication. The reapplication appears to be a factor of four more cost-effective than the initial application. The following is a list of source/control parameters affecting the conclusion and their impact:

1. The vehicle traffic on the reapplied Coherex® was 13% heavier on the average than the traffic traveling on the initial application of Coherex®. This strengthen the conclusion.

2. The reapplication required 25% less Coherex® and therefore less cost than the initial application. This strengthens the conclusion since less Coherex® was used and yet a lower decay rate achieved, but weakens the conclusion since the cost was less.

One of the most probable explanations why the reapplication performed better is the residual effect from the initial application. It is not known whether more reapplications would have shown improved performance due to continued residual build-up from prior applications.

Two final comparisons can be made from Table 4-7, that is, the interplant comparisons between watering and Petro Tac and between Coherex® and Petro Tac. These comparisons are necessary heavily qualified due to the many differences between the two plants. Petro Tac appears from Table 4-7 to be a factor of 22 more cost-effective than watering. The following is a list of source/control parameters affecting the conclusion and their impact:

1. The vehicle traffic on the watered road was 63% heavier on the average than the traffic on the Petro Tac treated road. This weakens the conclusion.

2. The Petro Tac road was twice as wide as the watered road resulting in increased costs. This strengthens the conclusion.

3. The vehicle traffic on the Petro Tac treated road had 50% more wheels than on the water road. This strengthens the conclusion.

4. The economies of scale made the Petro Tac application costs per unit area treated much lower than the watering costs. This weakens the conclusion.

5. The watering costs were atypically high due to several problems. This weakens the conclusion.

In comparing Coherex® performance to Petro Tac performance, only the initial application of the Coherex® can be used since Petro Tac, had it been reapplied, might also have had a strong residual effect. It appears that the initial application of Petro Tac was 10 times more cost-effective than the initial application of Coherex®. The following is a list of source/control parameters affecting the conclusion and their impact:

1. The CBR on the road treated with Petro Tac, while not measured, is estimated to be higher than the CBR on the road treated with Coherex®. This weakens the conclusion.

2. The vehicle traffic on the road treated with Petro Tac was 27% lighter than on the road treated with Coherex®. This weakens the conclusion.

3. The vehicle traffic on the Petro Tac treated road had 50% more wheels than the traffic on the watered road. This strengthens the conclusion.

4. The Petro Tac road was twice as wide as the watered road resulting in increased application and chemical costs. This strengthens the conclusion.

5. The economies of scale made the Petro Tac application costs per unit area much lower than the watering costs. This weakens the conclusion.

6. The Petro Tac treated road was covered with 16% less chemical per unit area than the Coherex® treated road resulting in lower chemical purchase cost per unit area treated. This strengths the conclusion since a lower application intensity achieved a lower decay rate, but weakens the conclusion since a lower volume of chemical afforded a reduced cost.

SECTION 5.0

SPECIAL STUDIES

A number of studies were performed in addition to developing long-term control efficiencies associated with various techniques used to mitigate unpaved road dust emissions. Special studies were conducted to examine:

(a) Predicted versus actual uncontrolled emissions;

(b) Elemental chemical composition of particulate emissions in the iron and steel industry;

(c) Variation in emission factor values with uppermost profiler intake height; and

(d) Natural mitigation of emissions during winter months.

Each of the studies will be discussed separately.

5.1 COMPARISON OF PREDICTED AND ACTUAL UNCONTROLLED EMISSIONS

During the course of this field testing program, six tests of vehicular traffic on uncontrolled roads were performed. In addition to providing baseline emission data for control efficiency determination, these tests expanded the data base used in forming the MRI predictive emission factor equation for unpaved roads (Table 1-1)[2].

Although the primary purpose of this study was the measurement of control efficiency, the uncontrolled tests were included in the data base to determine how well the MRI equation predicts measured emission levels. This is of particular interest because MRI is currently in the process of refining the predictive equations by including recent test results from a variety of roads (industrial paved and unpaved, urban paved, and rural unpaved). This work is supported under EPA Contract No. 68-02-3158.

The results of the comparison of predicted and observed emissions are presented in Table 5-1, with the final six entries from the present study. The first 22 entries in the table are the tests used in developing the predictive equation.[2] The F series of runs represent the uncontrolled tests conducted during a prior study of unpaved road dust suppressant control performance in the iron and steel industry.[3] It should be noted that the AJ emission factors presented in Table 5-1 are identical to the values for TP in Table 3-6 because Table 3-4 indicates that the downwind largest particle is essentially the same as the cut-point for the predictive equation.

TABLE 5-1. PREDICTED VERSUS ACTUAL EMISSIONS

Run	Silt (%)	Average vehicle speed (km/hr)	Average vehicle speed (mph)	Average vehicle weight (Mg)	Average vehicle weight (tons)	Average No. of vehicle wheels	Emission factor[a] Predicted[b] (kg/VKT)	Emission factor[a] Predicted[b] (lb/VMT)	Emission factor[a] Actual (kg/VKT)	Emission factor[a] Actual (lb/VMT)	Predicted ÷ actual
R-1	12	48	30	3	3	4.0	1.7	5.9	1.7	6.0	0.98
R-2	13	48	30	3	3	4.0	1.8	6.4	1.9	6.8	0.94
R-3	13	64	40	3	3	4.0	2.4	8.5	2.2	7.9	1.08
R-8	20	48	30	3	3	4.5	2.9	10.4	2.3	8.1	1.29
R-10	5	64	40	3	3	4.0	0.93	3.3	1.1	3.9	0.85
R-13	68	48	30	3	3	4.0	9.3	33.0	9.0	32.0	1.03
A-14	4.8	48	30	64	70	4.0	6.0	21.4	6.0	21.5	1.00
A-15	4.8	48	30	64	70	4.0	6.0	21.4	6.5	23.0	0.93
E-1	8.7	23	14	31	34	9.4	4.7	16.7	3.8	13.6	1.23
E-2	8.7	26	16	31	34	8.3	5.1	18.0	3.4	12.2	1.47
E-3	8.7	26	16	21	23	6.4	3.4	12.0	4.1	14.5	0.83
F-21	9.0	24	15	3	3	4.0	0.62	2.2	0.84	3.0	0.73
F-22	9.0	24	15	3	3	4.0	0.62	2.2	0.48	1.7	1.29
F-23	9.0	24	15	4	4	4.1	0.76	2.7	0.65	2.3	1.19
G-27	5.3	35	22	15	17	11.0	3.0	10.7	3.4	12.0	0.89
G-28	5.3	37	23	11	12	9.5	2.3	8.1	2.0	7.2	1.13
G-29	5.3	39	24	8	9	7.8	1.8	6.3	1.6	5.6	1.12
G-30	4.3	40	25	13	14	8.5	2.1	7.5	2.4	8.7	0.87
G-31	4.3	47	29	7	8	6.2	1.4	6.1	1.4	5.1	0.99
G-32	4.3	35	22	27	30	13.0	3.9	14.0	4.5	16.0	0.88
I-3	4.7	24	15	61	67	6.0	3.5	12.4	4.1	14.5	0.86
I-5	4.7	24	15	142	157	6.0	6.4	22.6	7.0	25.0	0.90
F-28	10[c]	24	15	3	3	4.0	0.71	2.5	0.62	2.2	1.14
F-29	10[c]	24	15	3	3	4.0	0.71	2.5	2.0	7.3	0.34
F-30	10[c]	24	15	3	3	4.0	0.71	2.5	1.4	5.1	0.49
F-31	10[c]	24	15	3	3	4.0	0.71	2.5	1.8	6.4	0.39
F-68	14	32	20	20	29	5.9	8.3	29.6	14.5	51.3	0.58
F-69	15[c]	32	20	48	53	10.0	16.4	58.0	13.5	48.0	1.21
F-70	16	32	20	48	53	10.0	17.5	61.9	17.4	61.7	1.00
AG-1	7.5	24	15	24	27	9.8	3.8	13.4	1.6	5.7	2.34
AG-2	5.8	27	17	23	25	7.3	2.7	9.6	5.1	18.0	0.54
AG-3	7.2	26	16	25	28	6.6	2.9	10.4	3.8	13.6	0.76
AJ-1	6.3	24	15	49	54	6.0	4.0	14.3	3.9	13.8	1.04
AJ-2	7.4	24	15	47	52	6.0	4.6	16.4	6.0	21.4	0.77
AJ-3	7.7	24	15	45	50	7.1	5.1	18.1	4.2	14.8	1.22

[a] Particles smaller than 30 μm in Stokes diameter, based on actual density of silt particles.

[b] Based on revised MRI emission factor equation in Table 1-1.

[c] Estimated value.

The precision factors (as defined in the Glossary) for the predictive equation applied to the different data bases are shown below:

Data Base	Number of Tests	Precision Factor one-sigma	Precision Factor two-sigma
Reference 2	22	1.22	1.48
References 2 and 3	29	1.44	2.09
Reference 2 and Present Study	28	1.33	1.78
References 2 and 3 and Present Study	35	1.48	2.19

That the precision factor increases when predicting measurements in an expanded data base is indicative of the possible need to refine MRI's predictive equation. As mentioned above, this process is underway.

5.2 CHEMICAL ANALYSIS OF SELECTED SAMPLES

The objective of this study was to determine the elemental chemical composition of particulate emissions from uncontrolled unpaved roads within the iron and steel industry. Information of this type is of importance in credibly implementing the Bubble Policy. Because unpaved road dust emissions may be used to offset process emissions on a strict mass basis, it is important to identify concentration levels of specific toxic components in the road dust emissions.

Twenty-six samples comprised of 12 exposed filters and 14 road surface silt samples were analyzed for trace metals using inductively coupled plasma (ICP) emission spectroscopy. Both filter and surface samples consisted of two different size fractions, as shown in Table 5-2. In addition, five blank filters were analyzed. As can be seen from this table, the road surface aggregate from AG-2 was divided in two. One sample is comprised of material that was sieved only one-half the time of the other samples, as shown in Figure 5-1. This was done in order to determine possible contamination of the aggregate samples from the brass screens used in mechanical sieving or from the nickel-plated screens for sonic sieving.

Samples taken from Plant AG were prepared using the U.S. EPA reference method for acid leaching of lead from suspended particulate collected on glass fiber filters.[9] This preparation technique is summarized in Appendix B. The rates of recovery for a triplicate preparation of NBS Coal Fly Ash (Standard Reference Material 1633) indicate that, although this method possesses adequate reproducibility, it does not remove all of the nitric acid soluble metals in the reference material. The rates of recovery are presented in Table 5-3.

TABLE 5-2. SAMPLES SUBJECTED TO ICP ANALYSIS

Run	Surface material		Filters	
	20-75 μm[a]	< 20 μm[a]	Profiler[b]	Cyclone[c]
AG-1	1	1	1	1
AG-2	2	2	1	1
AG-3	1	1	1	1
AJ-1	1	1	1	1
AJ-2	1	1	1	1
AJ-3	1	1	1	1

[a] Physical diameter.

[b] Measures particulate less than 30-60 μm in aerodynamic diameter.

[c] Measures inhalable particulate.

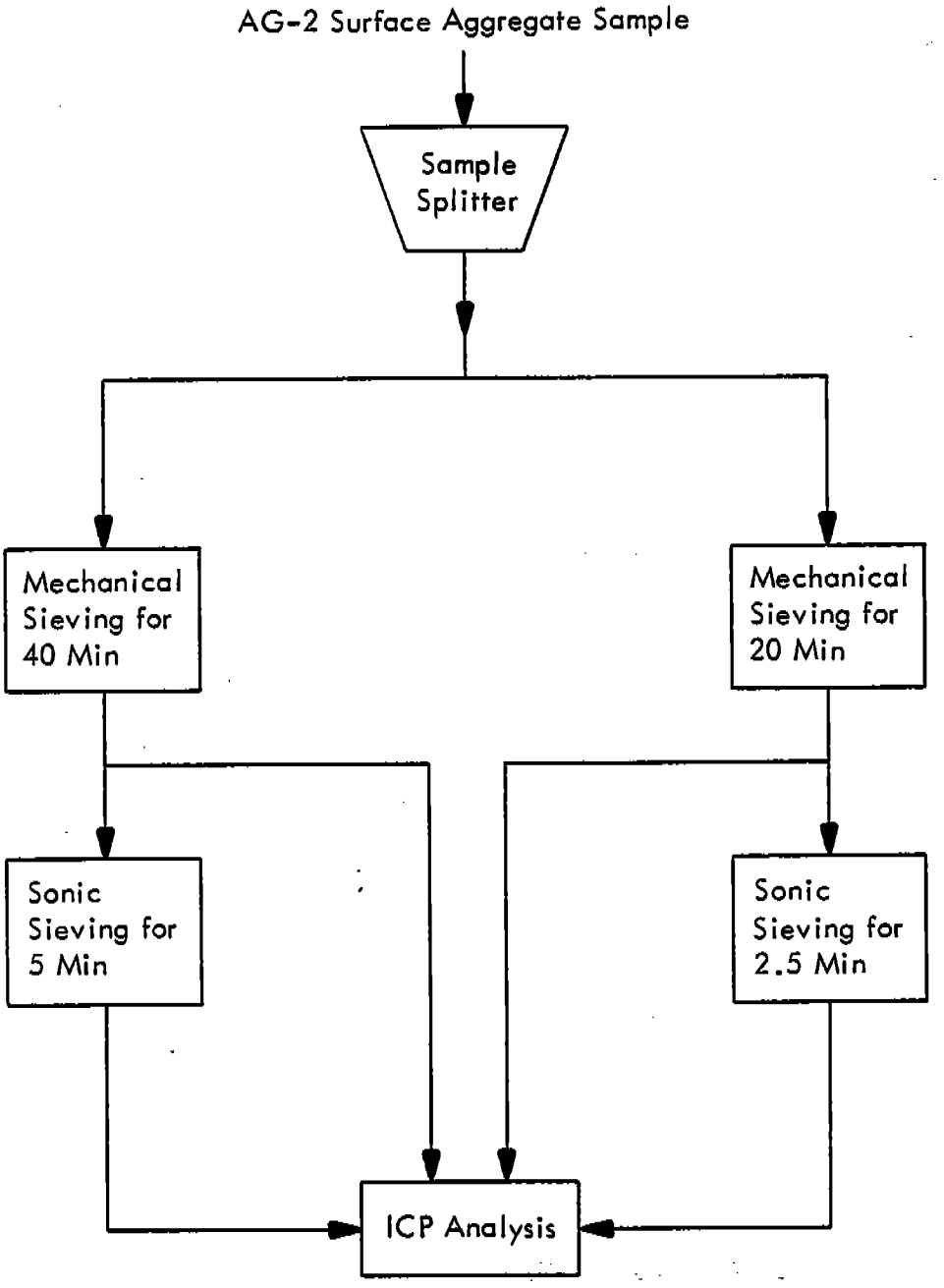

Figure 5-1. Preparation of AG-2 surface aggregate samples.

TABLE 5-3. COMPARISON OF RATES OF RECOVERY FOR REPLICATE REFERENCE MATERIAL SAMPLES (NBS COAL FLY ASH)

Analyte	Original preparation[a]		Modified preparation[b]	
	Mean recovery (%)	Relative standard deviation (%)	Mean recovery (%)	Relative standard deviation (%)
Al	-	-	94.8	1.79
As	44.5	16.5	-	-
Ba	-	-	90.4	0.580
Be	12.3	23.5	-	-
Ca	-	-	91.6	1.85
Cd	13.3	12.3	-	-
Co	26.7	15.5	-	-
Cr	21.8	19.1	127	0.425
Cu	25.8	27.0	45.4	0.486
Fe	-	-	94.7	0.247
K	6.21	22.1	98.0	1.26
Mg	-	-	76.0	1.75
Mn	57.7	23.4	100	2.72
Na	-	-	91.6	1.45
Ni	11.6	40.4	122	4.75
Pb	33.3	19.3	-	-
Ti	-	-	97.4	1.71
Y	-	-	95.6	0.910
Zn	21.4	25.3	107	1.26

[a] Based on the EPA reference nitric acid leaching method for digesting lead on glass fiber filters (Reference 9 and Section B.1).

[b] Nitric-hydrofluoric acid leaching method (Section B.2).

Because of the low recovery rates, samples taken from Plant AJ were prepared using a nitric-hydrofluoric acid solution instead of nitric acid alone. This modified preparation technique is summarized in Appendix B. The rates of recovery for replicate preparation of NBS Coal Fly Ash using the nitric-hydrofluoric acid solution are also shown in Table 5-3. Comparison of the results from the two preparations indicates that the nitric-hydrofluoric acid preparation produces recoveries much closer to unity while reducing variability in the recovery rates.

However, the modified acid leaching method caused some complications in the analysis. Because boric acid was added to neutralize excess fluorine ions, no reliable information on concentration levels of boron in the samples could be obtained. Secondly, the nitric-hydrofluoric acid digestion leached significant amounts of metals from the filters. Table 5-4 compares digestion concentrations for the major elements in both exposed and blank filters. As can be seen from this table, exposed and blank filters contain quite similar amounts of the major elements. Thus, more acceptable recovery rates were obtained at the cost of significant leaching of metals from the filters.

In order to provide quality assurance for the chemical analyses, a limit of detection (LOD) was defined as

$$LOD = 3\,\sigma_{bx}$$

where σ_{bx} = the standard deviation (μg) of the field blank masses for analyte x

No further calculations were made unless the blank-corrected mass (m_x) exceeded this operational definition of LOD:

$$m_x = M_x - M_{xb} \geqq LOD$$

where M_x = mass (μg) of analyte x
M_{xb} = average mass (μg) of analyte x as determined from the field blanks

In the above, the term "blank" is applied to the blank filters in the case of filter samples and to reagent blanks in the case of surface aggregate samples.

For metals detected above the LOD in each sample of a set of three (e.g., the profiler filters from Plant AG or the subsilt samples from Plant AJ) mean, blank-corrected mass concentrations were determined. Tables 5-5 and 5-6 present summary statistics for exposed filters and surface samples, respectively.

The values given for copper in Table 5-6 are to be considered suspect because of contamination from the brass screens used in mechanical sieving. Comparison of the split soil samples from run AG-2 indicated that the copper concentration of the sample sieved 40 min was 360% greater than that of the 20 min sample.

TABLE 5-4. COMPARISON OF DIGESTION CONCENTRATIONS FOR BLANK AND EXPOSED FILTERS

Run	Equipment used to sample particulate	Digestion concentration (μg analyte/g digest)						
		Al	Ca	Fe	K	Mg	Na	Zn
AJ-1	Profiler	21.6	32.0	0.720	3.30	13.7	73.2	0.798
	Cyclone	15.2	23.2	0.695	4.24	9.52	45.9	0.592
AJ-2	Profiler	26.1	38.3	1.51	3.91	16.1	82.0	0.998
	Cyclone	0.474	4.16	0.348	4.33	1.09	39.0	0.630
AJ-3	Profiler	30.2	44.6	1.49	3.52	19.0	97.9	1.12
	Cyclone	19.4	30.7	1.12	3.94	12.0	62.5	0.783
	Blank	20.2	30.9	0.292	4.68	13.3	51.2	0.835
	Blank	23.5	33.7	0.338	4.71	15.7	71.6	0.925
	Blank	21.8	36.5	0.331	3.48	13.8	82.5	1.04

TABLE 5-5. SUMMARY STATISTICS FOR ICP ANALYSIS OF AIRBORNE PARTICULATE FROM UNCONTROLLED, UNPAVED ROADS[a] (Concentrations in µg analyte/g particulate)

Analyte	Mean for Particulate Sampled by Profiler				Mean for Particulate Sampled by Cyclone			
	Plant AG[b]		Plant AJ		Plant AG[b]		Plant AJ	
Calcium	246,000	(25)	-	-	310,000	(26)	-	-
Iron	75,900	(29)	67,600	(22)	80,400	(34)	32,800	(61)
Magnesium	-	-	-	-	42,800	(37)	-	-
Manganese	9,930	(30)	6,790	(15)	10,500	(34)	-	-
Titanium	1,790	(31)	-	-	1,930	(31)	-	-
Copper	385	(82)	-	-	701	(46)	-	-
Chromium	688	(25)	-	-	729	(33)	-	-
Barium	-	-	-	-	-	-	29,600	(80)
Zinc	-	-	57,600	(50)	-	-	28,900	(41)

a Value in parentheses represents relative standard deviation (%).

b These concentrations have been scaled using the mean rate of recovery for NBS Coal Fly Ash for the particular analyte if available, or by the average recovery rate for all the analytes detected in the samples.

TABLE 5-6. SUMMARY STATISTICS FOR ICP ANALYSIS OF UNCONTROLLED, UNPAVED ROAD SURFACE AGGREGATE SAMPLES[a]
(Concentrations in µg analyte/g particulate)

Analyte	Mean Concentration for Silt (< 75 µm)				Mean Concentration for Subsilt (< 20 µm)			
	Plant AG[b]		Plant AJ		Plant AG[b]		Plant AJ	
Calcium	446,000	(7.9)	83,700	(38)	548,000	(6.3)	111,000	(8.2)
Iron	153,000	(16)	> 96,400	(NA)	250,000	(21)	66,100	(3.3)
Magnesium	75,900	(13)	13,900	(39)	94,300	(2.5)	12,000	(7.1)
Manganese	30,500	(15)	14,900	(16)	39,200	(16)	8,760	(5.4)
Aluminum	13,400	(7.6)	18,800	(51)	16,700	(5.2)	27,800	(8.6)
Potassium	-		6,290	(16)	-		8,370	(7.6)
Titanium	3,660	(17)	1,390	(9.4)	6,580	(8.5)	2,410	(6.2)
Sodium	1,190	(19)	2,300	(42)	1,680	(19)	3,560	(7.3)
Chromium	1,760	(17)	2,230	(14)	2,420	(24)	1,240	(3.5)
Zinc	645	(40)	1,730	(9.6)	1,050	(88)	1,920	(15)
Boron	159	(21)	-		196	(21)	-	
Lead	-		331	(29)	-		418	(8.5)
Barium	145	(7.6)	262	(64)	176	(5.3)	426	(7.9)
Copper[c]	121	(39)	115	(27)	872	(88)	160	(9.5)
Nickel	-		86.1	(17)	-		52.7	(17)
Yttrium	-		-		38.1	(17)	-	

[a] Value in parentheses represents relative standard deviation (%).

[b] Concentrations scaled in the same manner as in Table 5-5.

[c] There is evidence of copper contamination during mechanical sieving, as discussed in the text.

Tin concentrations also increased with sieving time. Thus, it appears that contamination of the sample occurs during mechanical sieving. Because nickel was not detected in any of the AG-2 surface aggregate samples, it is not known if there is contamination associated with sonic sieving.

It is interesting to note the enrichment factors suggested by Tables 5-5 and 5-6. The mass concentration of an analyte is generally greater for the sample containing the finer particles. Thus, most of the analytes appear to be concentrated in the smaller size particulate.

As can be seen from Tables 5-5 and 5-6, trace metal concentrations in the filter samples tend to increase with increases in the concentration in the surface sample. The two exceptions are zinc and barium. The concentrations in these metals in the filter samples are much greater than the concentrations in the surface sample.

With the exceptions of copper, zinc, and barium, it was found that an essentially linear relationship between downwind airborne and surface aggregate mass concentrations is indicated by the limited data available here:

$$C_a = k\,(C_s)^P$$

where C_a = airborne mass concentration (μg analyte/g particulate)
C_s^a = mass concentration of surface aggregate (μg analyte/g particulate)
k,P = regression parameters as follows

Sample		Regression Parameters		Numer of	Correlation
Air Sampler	Surface Aggregate	k	P	data points	Coefficient
Profiler	Silt	0.297	1.04	6	0.997
Cyclone	Subsilt	0.129	1.10	7	0.994

Because of these relationships, it appears possible to estimate airborne elemental mass concentrations by examining corresponding concentrations in the surface aggregate material. Not only would this provide an obviously more economical analysis because of the ease of collecting surface aggregate samples, but also these samples are easier to prepare and analyze.

5.3 VARIATION IN EMISSION FACTORS WITH PROFILER HEIGHT

During the course of field testing at Plant AJ, a 10 m isokinetic profiling tower was constructed. The purpose of including a higher sampling head was to determine the difference in measurement-based emission factors using a 10 m rather than a 6 m tower. The 10 m tower was deployed during runs AJ-3 through AJ-5. The measured concentrations for these tests are given in Table 5-7.

Note that the upwind data for AJ-4 and AJ-5 indicate that the background concentration initially increases with height. Similar increases with height

TABLE 5-7. PARTICULATE CONCENTRATIONS MEASURED USING A 10 m PROFILING TOWER

Run	Height (m)	Upwind/ downwind	Isokinetic TP concentration[a] (μg/m³)
AJ-3	1.5	D	12,600
	3.0	D	7,620
	4.5	D	4,310
	6.0	D	1,720
	10	D	205
	3	U	91
AJ-4	1.5	D	316
	3.0	D	208
	4.5	D	135
	6.0	D	172
	10	D	173
	1.5	U	90[b]
	4.5	U	129[b]
AJ-5	1.5	D	2,510
	3.0	D	1,560
	4.5	D	992
	6.0	D	480
	10	D	363
	1.5	U	90[b]
	4.5	U	129[b]

[a] Downwind concentrations from profiler, upwind from cyclones.

[b] The same upwind samplers were operated during AJ-4 and AJ-5.

were noted in two other tests at this plant. However, the background concentration cannot increase indefinitely with height. Furthermore, above some height the downwind and upwind concentration profiles should be identical because of negligible source contribution. In order to approximate the point above which the background is assumed invariant with height, least-squares fits of the downwind concentration data to a power function of height was obtained for AJ-4 and AJ-5. The point of intersection between this function and the linear extrapolation of upwind concentration was taken as the point above which the background concentration was constant. Figure 5-2 illustrates this procedure for AJ-4.

From Figure 5-2, it would appear that 7 to 7.5 m is a good approximation of the plume height for Run AJ-4. However, in order to provide an upper limit on the relative difference between the emission factors determined from the two tower heights, the following "worst case" approach was employed. The 10 m net concentration was found to be positive using the assumed background profile shown in Figure 5-2 even though this is well above the 7-7.5 m height that approximates the limit of the source contribution.

Net exposure values were obtained following the procedures described in Section 2.5.4 and are presented in Table 5-8. Because the purpose of this study was to provide an upper bound on the differences in measurement-based emission factors with varying tower heights, the 6 m results presented here are determined without reference to 10 m data.

The integrated exposures (which are proportional to the emission factors) obtained from the data in Table 5-8 are presented below:

Run	Plume height (m)		Integrated exposure ($m \cdot mg/cm^2$)		Worst-case percent difference in emission factor
	6 m tower	10 m tower	6 m tower	10 m tower	
AJ-3	6.94	10.3	20.8	23.0	9.56
AJ-4	6.00	10.9	0.627	0.760	17.5
AJ-5	6.94	11.0	7.77	9.18	15.4

As can be seen, there is at the worst a 10 to 17% difference in emission factors obtained from 6 m and 10 m profiling towers. Thus, a 6 m profiler samples at least 83 to 90% of the mass flux measured by a 10 m tower downwind of the road and, as such, should be considered more than adequate in characterizing particulate emissions at a 5 m distance from the edge of the road. Because there are such small differences between the 6 m and 10 m emission factor values (even in this comparison designed to provide a worst-case), the variation is within the experimental accuracy of the method. Therefore, the small additional mass flux sampled (which may be due to the lower background concentration assumed at 10 m) does not justify the difficulties in erecting and operating a 10 m tower at this distance from the road. Of course, if one deploys a profiler at a distance of more than 5 m from the road, then a taller tower is necessary. A taller tower may also be necessary if testing is performed at very low wind speeds or if vehicle speeds on the test road are much higher. Either of these conditions could cause a significantly higher plume.

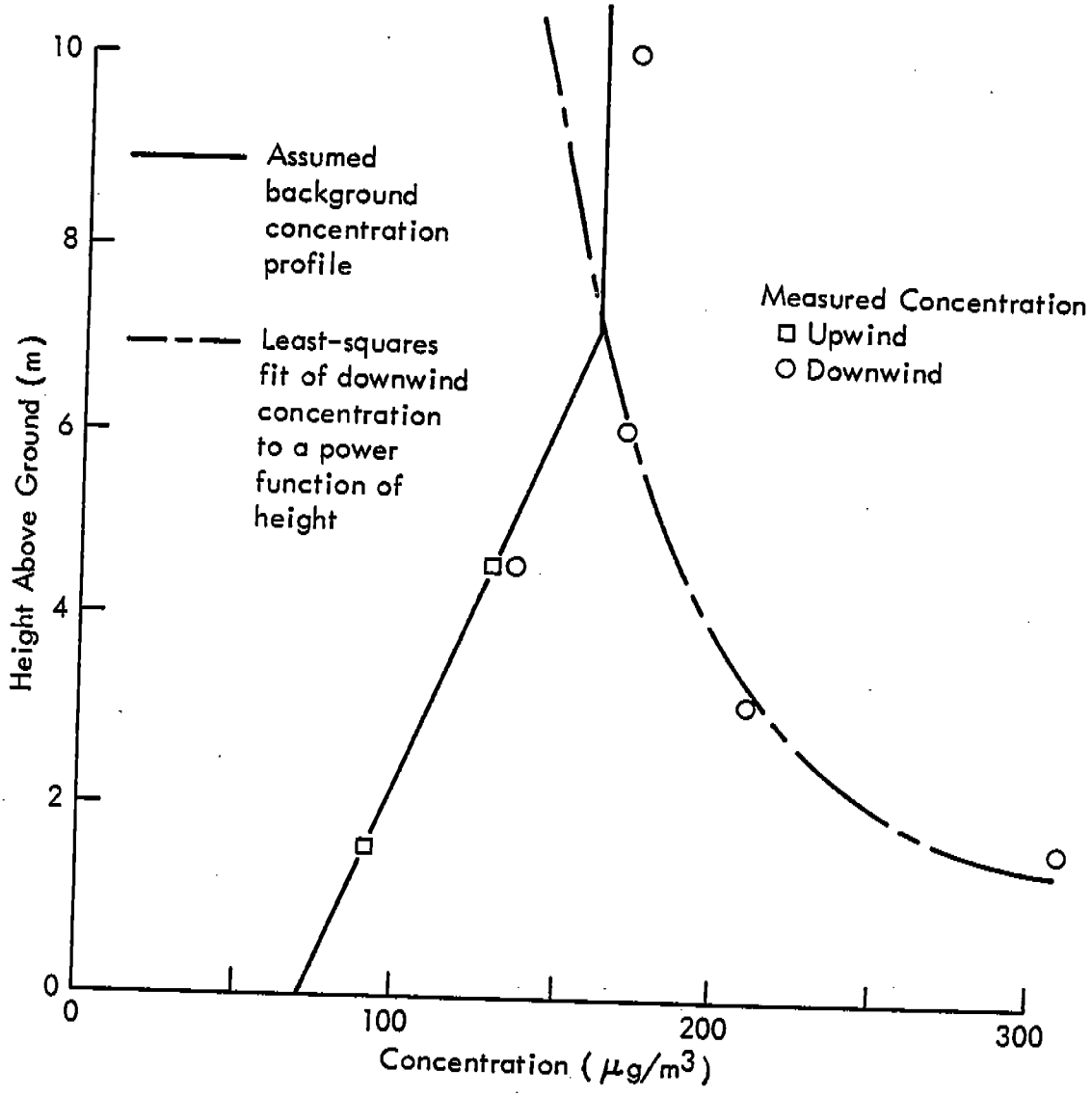

Figure 5-2. Determination of background concentration profile for AJ-4 for use in a worst-case comparison of emission factors.

TABLE 5-8. COMPARISON OF PLUME SAMPLING DATA FROM 6 M AND 10 M PROFILING TOWERS

Height (m)	Net TP exposure[a] (mg/cm²)					
	AJ-3		AJ-4		AJ-5	
	6 m	10 m	6 m	10 m	6 m	10 m
0	(3.48)	(3.48)	(0.209)	(0.209)	(1.46)	(1.46)
1.5	3.67	3.67	0.188	0.188	1.47	1.47
3.0	4.24	4.24	0.128	0.128	1.47	1.47
4.5	3.04	3.04	0.00948	0.00948	1.08	1.08
6.0	1.36	1.36	0.00	0.0427	0.474	0.474
7.5	0	(0.891)	0	(0.0307)	0	(0.402)
9.0	0	(0.426)	0	(0.0188)	0	(0.330)
10.0		0.117		0.0108		0.282
10.5		0		(0.00480)		(0.135)
12.0		0		0		0

[a] Values in parentheses are interpolated for use in the integration process.

5.4 WINTER TESTING

As mentioned in Section 3.0, runs AJ-16 and AJ-17 were excluded in determining the decay in control efficiency of an initial application of Coherex®. These tests indicate over 90% control of particulate emissions although Figures 3-7 through 3-10 would indicate the control efficiency due to the initial Coherex® application should have decayed to 20% or less at 76-77 days after application. Road surface moisture contents measured for these tests, however, were approximately 70% greater than those of the uncontrolled tests, and were, in fact, much closer to those values associated with the tests of watering as a control measure. The control efficiencies associated with AJ-16 and AJ-17 are presented in Table 5-9 together with efficiency values from the watering tests AJ-4 and AJ-5. As can be seen from this table, the control efficiencies associated with runs AJ-16 and AJ-17 are generally between those of the watering tests as are the moisture contents for the tests.

At the start of the field exercises on the days runs AJ-16 and AJ-17 were performed, the road was too damp from overnight condensation to begin testing immediately. On both mornings captive, heavy-duty traffic drove on the road the rest of the morning in order to dry it. Neither test began before noon, and both ended at roughly 3 p.m.

The testing for these two runs occurred during the hottest part of the day (temperature during tests averaged 60°F) when most plants would accelerate the watering schedule to compensate for increased evaporation. However, the results of runs AJ-16 and AJ-17 indicate that natural mitigation of particulate emissions from unpaved roads due to morning condensation during the cooler periods of the year can be significant, reducing the need for afternoon watering. Control at approximately the 90% level was observed with nearly all the control effectiveness attributable to natural moisture due to condensation (only 20% could be attributed to the decayed Coherex® treatment). The limited data available here suggest that an open dust control program developed with attention paid to seasonal variations in emission levels could provide a more cost-effective means of reducing particulate emissions.

TABLE 5-9. COMPARISON OF CONTROL EFFICIENCIES

Run	Moisture content[a] (%)	Control efficiency (%)			
		TP	IP	PM_{10}	FP
AJ-16[b]	3.7	95.4	96.4	96.8	96.9
AJ-17[b]	3.0	94.9	97.4	97.6	99.3
AJ-4[c]	5.1	98.3	97.5	98.1	95.8
AJ-5[c]	2.0	76.0	78.2	79.2	81.4

[a] Sample collected after test.

[b] Winter tests of a road treated with Coherex®.

[c] Tests performed 1 to 3 hrs after road was watered.

SECTION 6.0

REFERENCES

1. Bohn, R., T. Cuscino, Jr., and C. Cowherd, Jr. Fugitive Emissions from Integrated Iron and Steel Plants. EPA-600/2-78-050, U.S. Environmental Protection Agency, Research Triangle Park, North Carolina, March 1978.

2. Cowherd, C., Jr., R. Bohn, and T. Cuscino, Jr. Iron and Steel Plant Open Source Fugitive Emission Evaluation. EPA-600/2-79-103, U.S. Environmental Protection Agency, Research Triangle Park, North Carolina, May 1979. 139 pp.

3. Cuscino, T., Jr., G. E. Muleski, and C. Cowherd, Jr. Iron and Steel Plant Open Source Fugitive Emission Control Evaluation. Final Report, EPA Contract No. 68-02-3177, Task 4, U.S. Environmental Protection Agency, Research Triangle Park, North Carolina, August 1983. 181 pp.

4. Cowherd, C., Jr., C. M. Maxwell, and D. W. Nelson. Quantification of Dust Entrainment from Paved Roads. EPA-450/3-77-027, U.S. Environmental Protection Agency, Research Triangle Park, North Carolina, July 1977. 89 pp.

5. Cowherd, C., Jr., K. Axetell, Jr., C. M. Guenther (Maxwell), and G. Jutze. Development of Emission Factors for Fugitive Dust Sources. EPA-450/3-74-037, U.S. Environmental Protection Agency, Research Triangle Park, North Carolina, June 1974. 190 pp.

6. Cuscino, T., Jr. Taconite Mining Fugitive Emissions Study. Final Report, Midwest Research Institute for Minnesota Pollution Control Agency, June 7, 1979.

7. Bohn, R., T. Cuscino, Jr., D. Lane, F. Pendleton, and R. Hackney. Dust Control for Haul Roads. U.S. Bureau of Mines, Minneapolis, Minnesota, February 1981.

8. Davies, C. N. The Entry of Aerosols in Sampling Heads and Tubes. British Journal of Applied Physics, 2:921 (1968).

9. Federal Register, 43(194), October 5, 1978, pp. 46260-1.

SECTION 7.0

GLOSSARY

Activity Factor - Measure of the intensity of aggregate material disturbance by mechanical forces in relation to reference activity level defined as unity.

Application Frequency - Number of applications of a control measure to a specific source per unit time; equivalently, the inverse of time between two applications.

Application Intensity - Volume of water or chemical solution applied per unit area of the treated surface.

Control Efficiency, Average - Mean value of the (instantaneous) control efficiency function over a specified period of time.

Control Efficiency, (Instantaneous) - Percent decrease in controlled emissions at a given instant in time from the uncontrolled state.

Cost-Effectiveness - The cost of control per unit mass of reduced particulate emissions.

Decay Rate - The absolute value of the slope of the (instantaneous) control efficiency function.

Dilution Ratio - Ratio of the number of parts of chemical to the number of parts of solution, expressed in percent (e.g., one part of chemical to four parts of water corresponds to a 20% solution).

Dry Day - Day without measurable (0.01 in. or more) precipitation.

Dry Sieving - The sieving of oven-dried aggregate by passing it through a series of screens of descending opening size.

Duration of Storage - The average time that a unit of aggregate material remains in open storage, or the average pile turnover time. Calculated by dividing the average mass in the pile by the average pile throughput.

Dust Suppressant - Water or chemical solution which, when applied to an aggregate material, binds suspendable particulate into larger less suspendable particles.

Exposure - The point value of the flux (mass/area-time) of airborne particulate passing through the atmosphere, integrated over the time of measurement.

Exposure, Integrated - The result of mathematical integration of spatially distributed measurements of airborne particulate exposure downwind of a fugitive emissions source.

Exposure Profiling - Direct measurement of the total passage of airborne particulate immediately downwind of the source by means of simultaneous multipoint isokinetic sampling over the effective cross-section of the emissions plume.

Exposure Sampler - Directional particulate sampler with a fiberglass intake serving as a settling chamber followed by a backup filter. The sampler has variable flow control to provide for isokinetic sampling at wind speeds of 1.8 to 8.9 m/s (4 to 20 mph).

Fugitive Emissions - Emissions not originating from a stack, duct, or flue.

Load-in - The addition of material to a storage pile.

Load-out - The removal of material from a storage pile.

Moisture Content - The mass portion of an aggregate sample consisting of unbound surface moisture as determined from weight loss in oven drying.

Normalization - Procedure that ensures that emission reductions not attributable to a control measure are excluded in determining an efficiency of control.

Particle Diameter, Aerodynamic - The diameter of a hypothetical sphere of unit density (1 g/cm^3) having the same terminal settling velocity as the particle in question, regardless of its geometric size, shape and true density. Units used in the report are microns aerodynamic (μmA).

Particle Drift Distance - Horizontal distance from point of particle injection into the atmosphere to point of removal by contact with the ground surface.

Particulate, Fine - Airborne particulate smaller than 2.5 μm in aerodynamic diameter.

Particulate, Inhalable - Airborne particulate smaller than 15 μm in aerodynamic diameter.

Particulate, PM_{10} - Airborne particulate smaller than 10 μm in aerodynamic diameter.

Particulate, Total - All airborne particulate regardless of particle size.

Particulate, Total Suspended - Airborne particulate matter as measured by a standard high-volume (hi-vol) sampler.

Precipitation-Evaporation Index - A climatic factor equal to 10 times the sum of 12 consecutive monthly ratios of precipitation in inches over evaporation in inches, which is used as a measure of the annual average moisture of exposed material on a flat surface of compacted aggregate.

Precision Factor - The one-sigma precision factor (f) for an emission factor equation is defined such that the 68% confidence interval for a predicted emission factor value (P) extends from P/f to Pf; the precision factor is determined by exponentiating the standard deviation of the differences between the natural logarithms of the predicted and observed emission factors. The two-sigma precision factor defines the 95% confidence interval and is the square of the one-sigma value.

Road, Paved - A roadway constructed of rigid surface materials, such as asphalt, cement, concrete, and brick.

Road, Unpaved - A roadway constructed of nonrigid surface materials such as dirt, gravel (crushed stone or slag), and oil and chip surfaces.

Road Surface Dust Loading, Paved - The mass of loose surface dust on a paved roadway, per length of roadway, as determined by dry vacuuming preceded by broom sweeping, if necessary.

Road Surface Dust Loading, Unpaved - The mass of loose surface dust on an unpaved roadway, per unit area, as determined by broom sweeping.

Road Surface Material - Loose material present on the surface of an unpaved road.

Silt Content - The mass portion of an aggregate sample smaller than 75 micrometers in diameter as determined by dry sieving.

Source, Open Dust - Any source from which emissions are generated by the forces of wind and machinery acting on exposed aggregate materials.

Spray System - A device for applying a liquid dust suppressant in the form of droplets to an aggregate material for the purposes of controlling the generation of dust.

Storage Pile Activities - Processes associated with aggregate storage piles, specifically, load-in, vehicular traffic around storage piles, wind erosion from storage piles, and load-out.

Subsilt - The mass portion of an aggregate sample smaller than 20 micrometers as determined by sonic sifting.

Surface Erodibility - Potential for wind erosion losses from an unsheltered area, based on the percentage of erodible particles (smaller than 0.85 mm in diameter) in the surface material.

Vehicle, Heavy-Duty - A motor vehicle with a gross vehicle travelling weight exceeding 30 tons.

Vehicle, Light-Duty - A motor vehicle with a gross vehicle travelling weight of less than or equal to 3 tons.

Vehicle, Medium-Duty - A motor vehicle with a gross vehicle travelling weight of greater than 3 tons, but less than 30 tons.

SECTION 8.0

ENGLISH TO METRIC UNIT CONVERSION TABLE

English unit	Multiplied by	Metric unit
gal/yd^2	4.53	ℓ/m^2
lb/vehicle mile	0.282	kg/vehicle km
lb	0.454	kg
T	0.907	Mg
mph	0.447	m/s
mile	1.61	km
ft	0.305	m
gal	3.78	ℓ
yd^2	0.836	m^2

Example: 5 miles x 1.61 = 8 km.

APPENDIX A

IRON AND STEEL PLANT UNPAVED ROAD DUST CONTROL SURVEY

IRON AND STEEL PLANT UNPAVED ROAD DUST CONTROL SURVEY

I. GENERAL INFORMATION

Name of Company _____ Location of Plant _____

Total Length of Unpaved Roads in Plant _____ mi.

Length of Unpaved Roads Being Treated _____ mi.

Vehicle Miles Travelled (VMT) Annually on Treated Unpaved Roads _____ VMT/yr

Cumulative Length of Road Which Is Treated Annually _____ miles/yr
(Please attach supporting calculations)

Name of Party
Completing This Survey _____ (Name) _____ (Title) ( ) _____ (Telephone Number)

II. CONTROL TECHNOLOGY FOR UNPAVED ROADS

Please complete the following information for your facility where applicable. Please use a full year of data. If you use data for only a portion of a year, indicate the months being considered.

Treatment Method: Watering _____ Chemical Dust Suppressants _____ Other _____ (Specify)

Type(s) of Chemical(s) Used: (Check one or more as applicable)

Lignin Sulfonate ___ Petroleum Resins ___ Salts ___ Wetting Agents _____
Other _____ (specify)

Trade or Chemical Name(s) of Dust Suppressant(s) Used (if any) _____

Name, Address and Phone Number of Dust Suppressant Supplier _____

_____

Date of Initial Application _____

Initial Application Rate _____ gal. of Solution per yd^2 of Surface Treated

Initial Dilution Ratio _____ Parts of Chemical to _____ Parts of _____ (type of diluent, e.g., water)

Follow-up Application Rate _____ gal. of Solution Per yd^2 of Surface Treated

Follow-up Dilution Ratio _____ Parts of Chemical to _____ Parts of _____ (type of diluent, e.g., water)

Concentration of Chemical Suppressant as Received _____% by _____ (weight or volume)

Frequency of Application _____

Basis for Frequency of Application _____

Method of Application (e.g., pressure spray or gravity feed distributor truck) _____

Total Capacity of On-Site Chemical Storage _____ gal.
No. and Capacity of each Storage Tank _____

Cost of Concentrated Chemical Dust Suppressant(s) Delivered to Your Plant

$_____/gal. in _____ (Chemical)
(year)

$_____/gal. in _____ (Freight)
(year)

Gallons of Chemical Delivered Per Shipment _____ gal.

Mode of Delivery (e.g., rail tanker car, tanker truck) _____

Gallons of Chemical Delivered Per Year _____ gal. in _____
(year)

Capital Cost for Storage Tanks $_____ in _____ dollars
(year of purchase)

Line Items Included In Capital Cost for Storage Tanks:

$ _____ for tanks

$ _____ for installation labor

$ _____ for accessories

$ _____ for other

Construction Material for Storage Tanks (e.g., concrete or metal) _____

Estimated Useful Life of Storage Tanks _____ yrs.

Is Storage Tank Above or Below Ground _____

Is the Tank Heated _____

Capital Equipment Cost for Application Equipment (e.g., distributor truck)
$ _____

If Application Equipment is Leased, List the Lease Cost Per Application $ _____
and the Number of Applications Per Year _____

Capacity of Distributor Truck _____ gallons

Estimated Useful Life of Distributor Truck _____ yrs.

Annual Operating and Maintenance Cost of Storage and Application Equipment $ _____
in _____ dollars
(year)

(Please attach supporting calculation for operating and maintenance costs)

List Major Maintenance Problems Encountered _____

APPENDIX B

TRACE METAL ANALYSIS SAMPLE PREPARATION PROCEDURES

This appendix describes the two procedures used to prepare filter and surface aggregate samples for the ICP analysis described in Section 5.2. As discussed in that section, the first field samples were leached with nitric acid following an adapted form of the EPA reference method for lead in atmospheric suspended particulate. This method resulted in low, yet reproducible, rates of recovery for NBS coal fly ash. Because of the low recovery rates, the second batch of field samples were prepared with a nitric-hydrofluoric acid solution.

B.1. ORIGINAL (NITRIC ACID) PREPARATION

B.1.1 Analytical Methods

B.1.1.1 Container Cleaning

To minimize sample contamination due to unwanted elemental metals to lowest possible level, all glassware and plastic were cleaned as follows:

1. Soaked overnight in fresh reagent-grade 8 N HNO_3.
2. Thoroughly rinsed with Milli-Q® high purity (18 megaohm/cm) deionized water.
3. Filled with 0.5 N Baker Ultrex® HNO_3 in Milli-Q® water for 2 hr.
4. Beakers used for the acid leaching sample preparation were then partially filled with 3 N Baker Ultrex® HNO_3 that was refluxed 1 hr.
5. Thoroughly rinsed again with Milli-Q® water.
6. Excess water was shaken out and the containers placed in clean plastic bags until used.

B.1.1.2 Whatman #2 Filter Cleaning

The Whatman #2 filters used for filtering leached field samples were first acid cleaned as follows:

1. Placed in cleaned plastic funnel.
2. 100 ml of Baker Ultrex® 1% v/v HNO_3 was passed through the filter.
3. 150 ml of Milli-Q® water was then passed through the filter.
4. Each filter/funnel unit was placed intact in a clean plastic bag until used.

B.1.1.3 Field Sample Acid Leaching

Two types of field samples were leached for trace metal content:

1. Eight-inch by 10-in. fiber filters loaded with particulates.

2. Surface aggregate (silt and subsilt).

The metals in these samples were prepared for chemical analysis using a modified form of the U.S. EPA reference method for lead in atmospheric suspended particulates, Federal Register, Vol. 43, No. 194, October 5, 1978. This method consisted of the following steps:

1. Folded the filters by hand using clean plastic disposal gloves and placed them in the bottom of 600 ml glass beakers with watch glass covers.

2. Weighed the surface aggregate on a five-place analytical balance and placed them in 50 ml glass beakers with water glass covers.

3. Added enough 3 N Baker Ultrex® HNO_3 to completely soak the filter or surface aggregate materials.

4. Slowly heated the acid solutions to near boiling.

5. Cooled for 30 min, and decanted the acid into clean plastic bottles.

6. Filled the sample preparation beakers with equal volumes of Milli-Q® water rinsing the interior beaker walls and watch glass face.

7. Poured the Milli-Q® water rinses through cleaned Whatman #2 filter/funnel assemblies into the respective plastic sample bottles.

B.1.1.4 ICP-AES Quantitative Analysis

The sample acid leachates were analyzed for trace metals by the Jarrell-Ash Model 1155A 30-channel direct-reading ICP-AES instrument system.

The instrument operating parameters were:

Forward Power: 1.1 kw	Coolant Gas Flow: 18 liters/min
Reflected Power: 1 w	Sample Gas Flow: 0.5 liters/min
Observation Height: 18 mm	Solution Uptake: 1.6 ml/min
Nebulizer Type: fixed crossflow	Peristaltic Pump Used

The spectrometer was set up and calibrated according to the Jarrell-Ash operating manual. Each analyte channel was calibrated using a reagent blank and a 10 ppm mixed calibration standard.

B.1.2 Internal Quality Control

B.1.2.1 Sample Preparation Quality Control

For the filter sample batch, the following QC samples were prepared and analyzed:

1. Two preparation reagent blanks.

2. Two fortified preparation reagent blanks.

3. Two method blank filters taken into the field.

4. One method blank filter taken into the field and fortified in the lab prior to preparation.

For the surface aggregate sample batch, the following QC samples were prepared and analyzed:

1. Two preparation reagent blanks.

2. Two fortified preparation reagent blanks.

3. Two duplicate preparations of field samples.

4. Three replicate preparations of Natural Bureau of Standard Coal Fly Ash, SRM 1633.

B.1.2.2 ICP-AES Analysis Quality Control

The samples were analyzed in manner consistent with the requirements of U.S. EPA Interim Method 200.7, "Inductively Coupled Plasma-Atomic Emission Spectrometric Method for Trace Element Analysis of Water and Wastes," EMSL-Cincinnati, November 1980.

This method requires the following analytical quality control (AQC) measures:

1. Close matching of the acid matrix composition of the samples with the calibration standards: A 10% HNO_3 matrix was used.

2. Validation of the accuracy of the instrument calibration using the following criteria:

   - Initial and repeated analysis of the calibration reagent blank every 10th sample must be within ± 2 standard deviations of its mean concentration values.

   - Initial and repeated analysis every 10th sample of independent AQC standards must be within ± 5% of the true concentration values. Two U.S. EPA reference standards, "ICAP-3" and "ICAP-23" were used in this study.

3. Validation of the accuracy of the spectral interference corrections performed by the computer using the following criteria:

   - Initial analysis on interference check standard should produce measured values for target elements which must be within ± 5% of the true concentration values.

B.2 MODIFIED (NITRIC-HYDROFLUORIC ACID) PREPARATION

B.2.1 Analytical Methods

B.2.1.1 Container Cleaning

To minimize sample contamination due to unwanted elemental metals to lowest possible level, all glassware and plastic were cleaned as follows:

1. Soaked overnight in fresh reagent-grade 8 N HNO_3.
2. Thoroughly rinsed with Milli-Q® high purity (18 megaohm/cm) deionized water.
3. Filled with 0.1 N Baker Ultrex® HNO_3 in Milli-Q® water for 2 hr.
4. Thoroughly rinsed again with Milli-Q® water.
5. Excess water was shaken out and the containers placed in clean plastic bags until used.

B.2.1.2 Teflon® Reaction Vessels

Teflon® 4-oz reaction bottles were cleaned as follows:

1. Rinsed thoroughly with building deionized water.
2. Partially filled with 8 N reagent grade HNO_3 and refluxed at 125°C for 3 hr.
3. Rinsed thoroughly with Milli-Q® water.
4. Filled partially with 0.1 N Ultrex® HNO_3, capped, shaken well, and emptied.
5. Rinsed thoroughly with Milli-Q® water.
6. Excess water shaken out and used immediately for the next sample preparation.

B.2.1.3 Field Sample Acid Digestion

Two types of field samples were prepared for trace metals content:

1. Fiber filters (8 in. x 10 in.) loaded with particulates.
2. Road surface aggregate (silt and subsilt) collected by grab sampling and sieved.

It was observed that the EPA reference method using a mild 3 N HNO_3 acid leaching did not fully dissolve the particulates nor totally solubilize minor trace metals in NBS Standard Coal Fly Ash SRM 1633.

Therefore, MRI developed a more rigorous HNO_3:HF high temperature digestion to totally dissolve airborne particulates. Initial studies with NBS SRM 1633 were good enough that the following modified version of the preparation was utilized for the Plant AJ samples:

1. The samples, either filters or surface aggregate particulates, were placed in a cleaned, 4-oz Teflon® reaction bottle.

2. Enough of a 1:1 mixture of concentrated Baker Ultrex® HNO_3 and Ultrex® HF was added to completely soak the sample.

3. The bottles were tightly capped and heated at 125°C in an oven for 2 hr.

4. The bottles were cooled briefly and the caps loosened while the bottles were still hot. This had to be done because tightly capped bottles developed a very strong vacuum when allowed to fully cool, preventing their opening.

5. The contents were inspected, and it was found that all of the particulate material had not dissolved.

6. More 1:1 HNO_3 and HF Ultrex® acid mixture was added, the caps tightened, and the bottles heated at 150°C fo 2 hr.

7. The bottles were cooled, uncapped, and approximately 0.5 g of H_3BO_3 per 4 g of HNO_3:HF mixture added.

8. The bottles were recapped and heated at 90°C for 60 min.

9. The bottles were cooled, uncapped, and the contents filtered through precleaned Whatman No. 2 filter paper into tared 30-ml or 125-ml polyethylene bottles. Filters were prepared as described in Section B.1.1.2.

10. Teflon® reaction vessels were thoroughly rinsed with Milli-Q® water. The rinses were added to the appropriate sample digest polyethylene bottle.

11. The final wet sample digestion mass was recorded on the SAMPLE PREPARATION sheet.

B.2.2 ICP-AES Quantitative Analysis

The Jarrell-Ash ICP-AES instrument was calibrated and operated in the manner described in Section B.1.2.

B.2.3 Internal Quality Control

B.2.3.1 Sample Preparation Quality Control

For the filter sample batch, the following QC samples were prepared and analyzed:

1. Two preparation reagent blanks.
2. Two fortified preparation reagent blanks.
3. Three method blank filters taken into the field.
4. One method blank filter taken into the field and fortified in the lab prior to preparation.

For surface aggregate samples, the following QC samples were prepared and analyzed:

1. Two preparation reagent blanks.
2. Two fortified preparation reagent blanks.
3. Two replicate preparations of National Bureau of Standard Coal Fly Ash, SRM 1633.

B.2.3.2 ICP-AES Analysis Quality Control

The samples were analyzed in the same manner described in Section B.1.3.2.

APPENDIX C

TECHNIQUES FOR REDUCING THE EFFECTS OF FUGITIVE DUST PARTICLE BOUNCE IN CASCADE IMPACTORS

TECHNIQUES FOR REDUCING THE EFFECTS OF FUGITIVE DUST PARTICLE BOUNCE IN CASCADE IMPACTORS

Determination of the size distribution of airborne fugitive dust emissions presents a formidable task in field testing. During its 10 years of work in the fugitive emissions area, MRI has recognized the need for and the problems associated with particle sizing, and this work has been accompanied by continued refinement in sizing techniques. Table C-1 presents a chronological listing of significant developments in this regard, focusing on the use of inertial sizing devices for determination of fugitive dust particle size distribution.

Inertial sizing devices that classify particles in situ provide the advantage of direct measurement of particle size distribution by mass in response to aerodynamic forces. However, the performance curves for such sizing devices are frequently based on calibration using monodisperse aerosols of materials with properties considerably different from fugitive dust, and also under flow conditions far more uniform (still air or rectilinear flow) than those encountered in the field.

Abnormal particle pass-through in cascade impactors presents the most serious drawback in inertial sizing of dry particulate such as fugitive dust. Briefly put, a particle may bounce through a sizing device (e.g., impactor stage) designed to capture the particle, or it may be captured initially but then be reintroduced into the flow. In either case the particle can then continue through the impactor until final capture on the backup filter.

Both MRI and others[C-1, C-2] have obtained experimental evidence indicating particle bounce. In the first MRI tests of fugitive dust sources using cascade impactors in 1973, almost all the catch was found on the backup filter. This yielded an apparent mass median diameter (MMD) of less than 1 μm, which seemed implausible for fugitive dust. In an effort to reduce the number of large particles passing through the impactor, the cyclone preseparator was developed as a joint effort with Sierra Instruments. In subsequent tests performed in 1976 with collocated high-volume cascade impactors, backup filter concentrations measured by the cascade impactor with the cyclone averaged a factor of 10 smaller than the concentrations measured by the cascade impactor without the cyclone.

In an attempt to further reduce bounce-through effects, the cyclone/impactor flow rate was reduced from 40 cfm to 20 cfm, beginning with tests performed in 1977. Although the reduction in flow rate allows a greater proportion of large particles to enter the impactor by increasing the 50% cut-off diameter of the cyclone preseparator, the momentum of particles approaching the impaction surfaces is reduced by a factor of two at the lower flow rate.

TABLE C-1. SIGNIFICANT DEVELOPMENTS IN IMPACTOR USE AT MRI

1973	MRI performs first fugitive dust study. (EPA-450/3-74-037)
1975	MRI asks Sierra to develop a cyclone preseparator for a high-volume cascade impactor (40 cfm) which is first used for paved road tests. (EPA-450/3-77-027)
1976	Collocated hi-vol cascade impactors are tested downwind of unpaved roads in suburban Kansas City (40 cfm). Back-up filter concentrations ranged from three to 15 times greater without cyclone precollector. (EPA-450/3-77-027)
1976	MRI develops a mathematical particle bounce correction technique for use with cascade impactors.
1977	In an effort to reduce residual bounce, cyclone/impactor combinations are operated at 20 cfm for the first Iron and Steel study. (EPA-600/2-78-050)
1980	SSI/impactor combination (40 cfm) with greased substrates is used for the first time in testing of paved roads. (EPA Contract 68-02-1403, Task 25)
1981	Collocated cyclone/impactors with greased/ungreased substrates are tested downwind of paved roads in Kansas City. (EPA Contract 68-02-2814, W.A. 32)
1982	Cyclone cut point is calibrated in the laboratory for 10, 20, 40 cfm. Data for 40 cfm used to check only prior calibration by Sierra. (EPA Contract 68-02-3158, T.D. 12)
1983	MRI performs microscopic analysis of back-up filters for cyclone/impactors run at 20 cfm downwind of uncontrolled unpaved roads, with ungreased substrates. (EPA Contract 68-02-3177, W.A. 14)

To assess whether particle bounce-through was still occurring for the cascade impactor operated at 20 cfm with a cyclone preseparator, representative backup filters were recently examined by optical microscopy. Backup filters (20 x 25 cm) from two tests (G-1 and G-3) of an untreated unpaved road performed at Inland Steel in 1978 were selected for this purpose. During these tests the cyclone/impactors were located 5 m downwind of the road and at a height of 2 m. A blank filter taken to the field was also analyzed. Particles ranging up to 180 μm in equivalent physical diameter were observed on the exposed filters while the blank had no particles larger than 36 μm. Even larger particles might have been observed on the exposed filters had they not been prevented from reaching the backup filter due to the 190-μm slot width on stage 5.

Even though extremely large particles were observed on the backup filter, the question still remained as to whether they comprised an abnormal mass. Therefore, a full size analysis of particles visible under the optical microscope was performed on a 2.3 cm by 4.0 cm section of one filter (G-3) centered 2.5 cm from the middle of the filter along the 25 cm axis. Four hundred and fourteen particles were sized via a stratified count into six categories using a Porton graticule. Figure C-1 presents the cumulative particle size distribution by mass for this sample. A mass mean aerodynamic diameter of approximately 6 μmA was obtained, using a shape factor of 0.17 for conversion of projected particle area to equivalent aerodynamic diameter. Because stage 5 has a 50% cut point of 0.73 μmA at 20 ACFM, the MMD of particles on the backup filter should be less than 0.73 μmA, in the absence of particle bounce effects. However, particles smaller than about 0.2-0.3 μm cannot be distinguished under the optical microscope. Therefore unobservable fine particles may have been present on the backup filter which would in effect shift the MMD to a lower value.

There are three possible sources of fine particles on the backup filter: background particulate, road dust, and vehicle exhaust. The contribution of background particulate downwind of an uncontrolled unpaved road is usually negligible; however, for treated unpaved roads or for paved roads the contribution of background particulate may be appreciable. The contribution of fine road dust to the backup filter should be limited to about 5% of the total mass of the road dust emissions, because of the difficulty of generating submicron particles by grinding. A conservative (high) estimate of the particulate mass on the backup filter attributable to vehicle exhaust was developed as described in the following paragraph.

The mass of vehicle exhaust particulate generated by a single vehicle pass was determined by using the highest exhaust particulate emission factor (1.3 g/mile) presented in AP-42. Because of the small size of this type of particulate, the emissions were considered to be uniformly mixed in a one-mile long mixing cell with a 4.5 m by 6 m cross-section. The mass of exhaust particulate due to the number of vehicle passes occurring during a test was considered to be captured entirely on the backup filter. This mass was then compared to backup filter catches for cyclone/impactors operated at 20 CFM with intakes located at heights of 1 m and 3 m and at a horizontal distance of 5 m downwind of controlled paved and unpaved roads at Armco Middletown Works (Tests F-36 to F-44). In this comparison, it was found

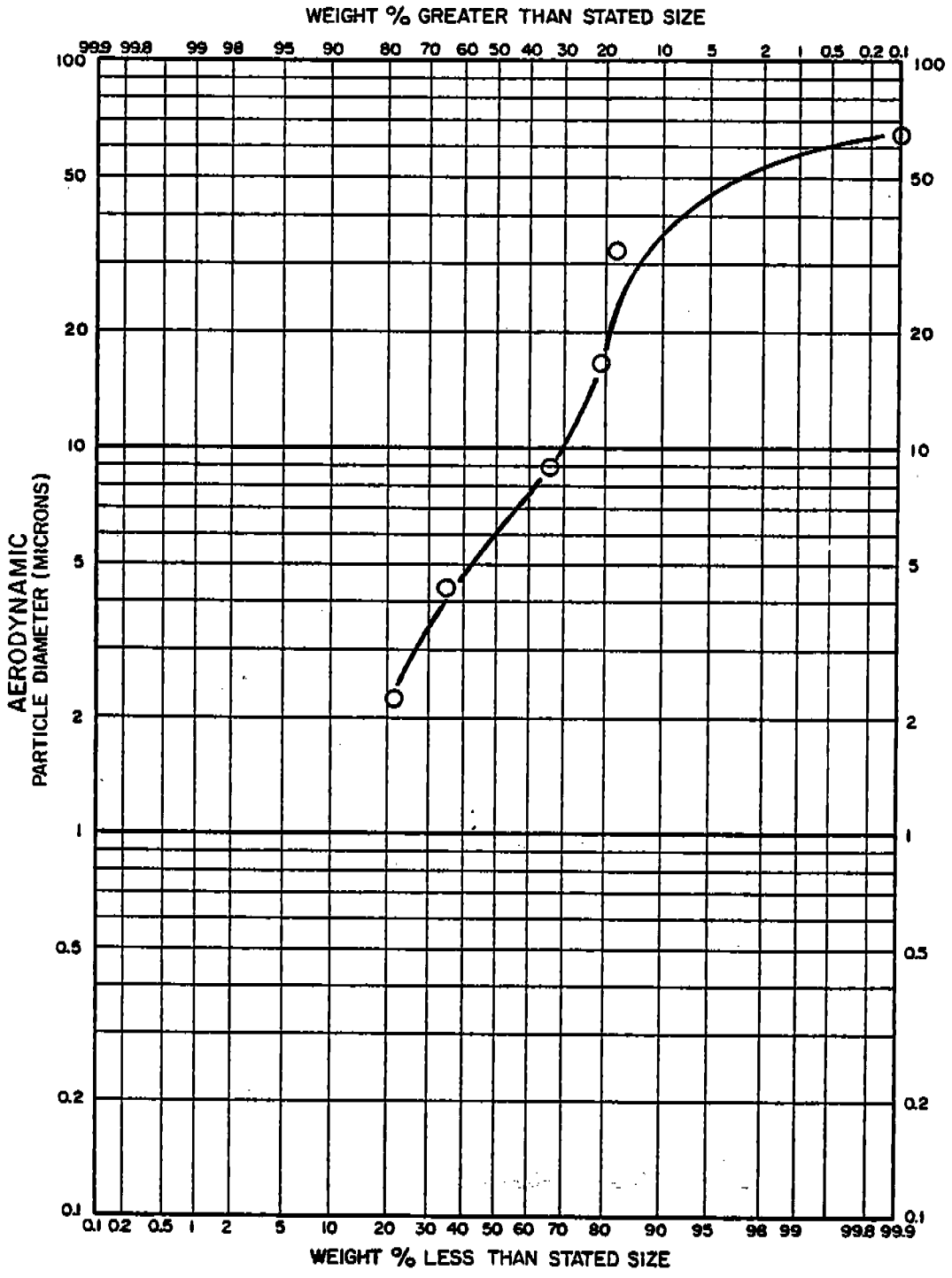

Figure C-1. Microscopically determined mass/size distribution of particulate on a backup filter under a 20 cfm cyclone/impactor with ungreased substrates operated 5 m downwind of an unpaved road.

that exhaust particulate contributes approximately 5% of the mass on the backup filter. Because of the conservative approach employed, 5% represents an upper bound on the contribution of vehicle exhaust to backup filter mass.

Four tests of paved roads, F-36 through F-39, were selected to illustrate the estimated contributions of the amount of particulate mass on the backup filter, background particulate, road dust, and vehicle exhaust. The contribution due to background particulate was estimated using TSP and IP (< 15 μmA) concentrations measured upwind during these tests. The IP/TSP mass fraction was used in conjunction with average geometric standard deviations reported by Lundgren and Paulus[C-3] for ambient concentrations measured in an industrial park. The contribution due to road dust was estimated conservatively by assuming that 5% of the net TP concentration on the backup filter is composed of road dust particles smaller than 0.73 μmA (the 50% cut-point for the fifth stage). Finally, the contribution due to vehicle exhaust was estimated using the technique described earlier.

The relative contributions of these three sources to the backup filter concentrations for Runs F-36 through F-39 are presented in Figure C-2. On the average, roughly 60% of the mass on the backup filter is not explained by the three sources and is thus attributable to particle bounce. It is of interest to note that the amount of particulate mass effectively removed by the MRI bounce correction reasonably matches the unexplained portion of mass:

Run	Percent Mass Unexplained	Percent Mass Effectively Removed
F-36	62	87
F-37	60	83
F-38	42	32
F-39	74	86

A further attempt to reduce particle bounce during sampling was the greasing of the impactor substrates beginning in 1980. A comparison of collocated SSI/impactors (40 cfm) with greased and ungreased substrates downwind of paved roads in Kansas City indicated that backup filter concentrations were reduced by roughly half when greasing was employed. Figure C-3 is typical of the size distributions of IP found for the greased versus ungreased substrates. The similarity in mass fractions for the first stage of the greased impactor and the last stage of the ungreased impactor suggests that the greased substrates are very effective in impeding particles from bouncing through the entire impactor.

To provide corroborative evidence that the particles observed under the microscope account for most of the actual particulate mass collected on the backup filter, the particle size distribution on the filter from Test F-68, as determined by optical microscopy, was converted to an equivalent integrated mass. Even though greased substrates were used in this test

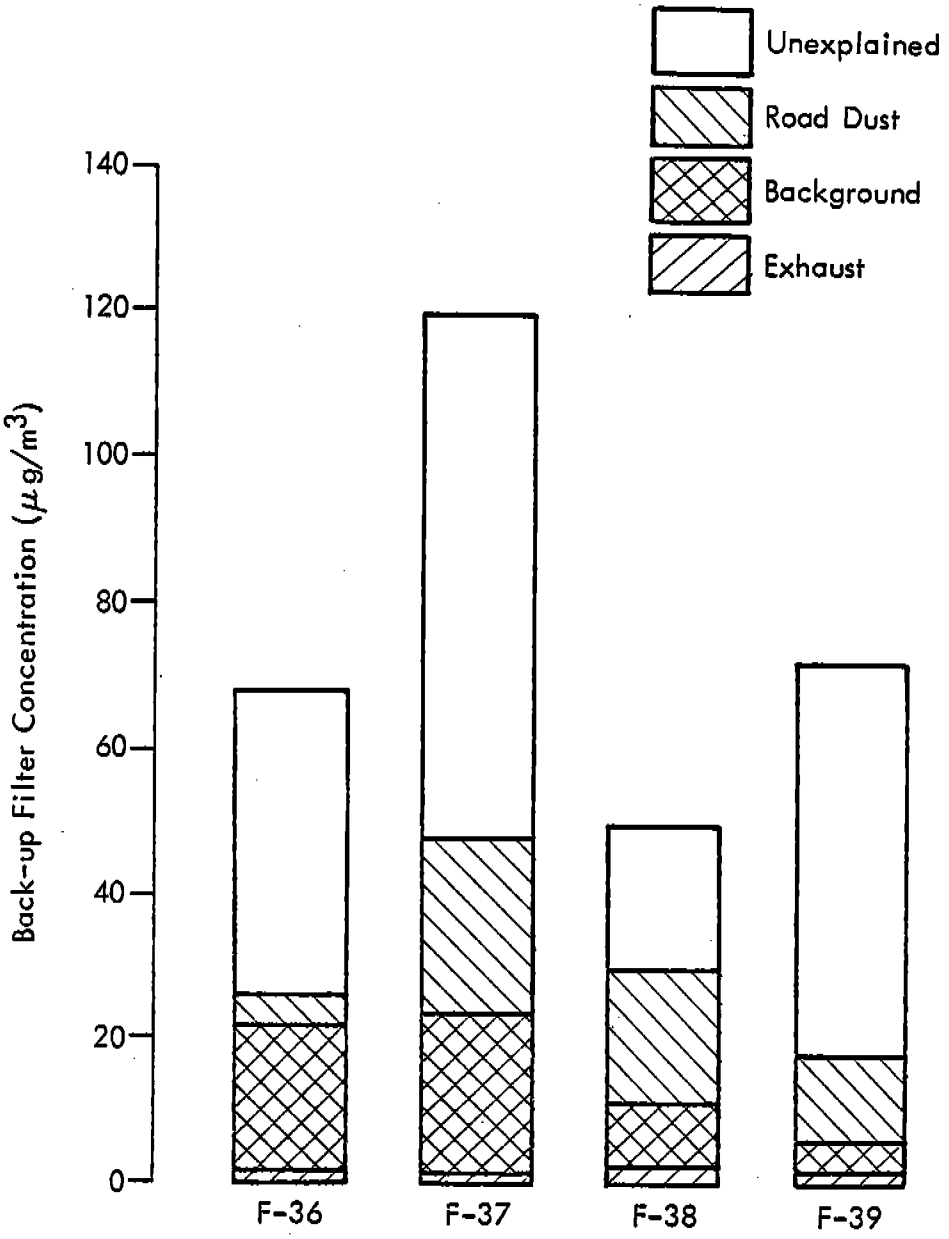

Figure C-2. Estimated contributions to backup filter concentrations from road dust, background concentration, and vehicle exhaust for Runs F-36 through F-39.

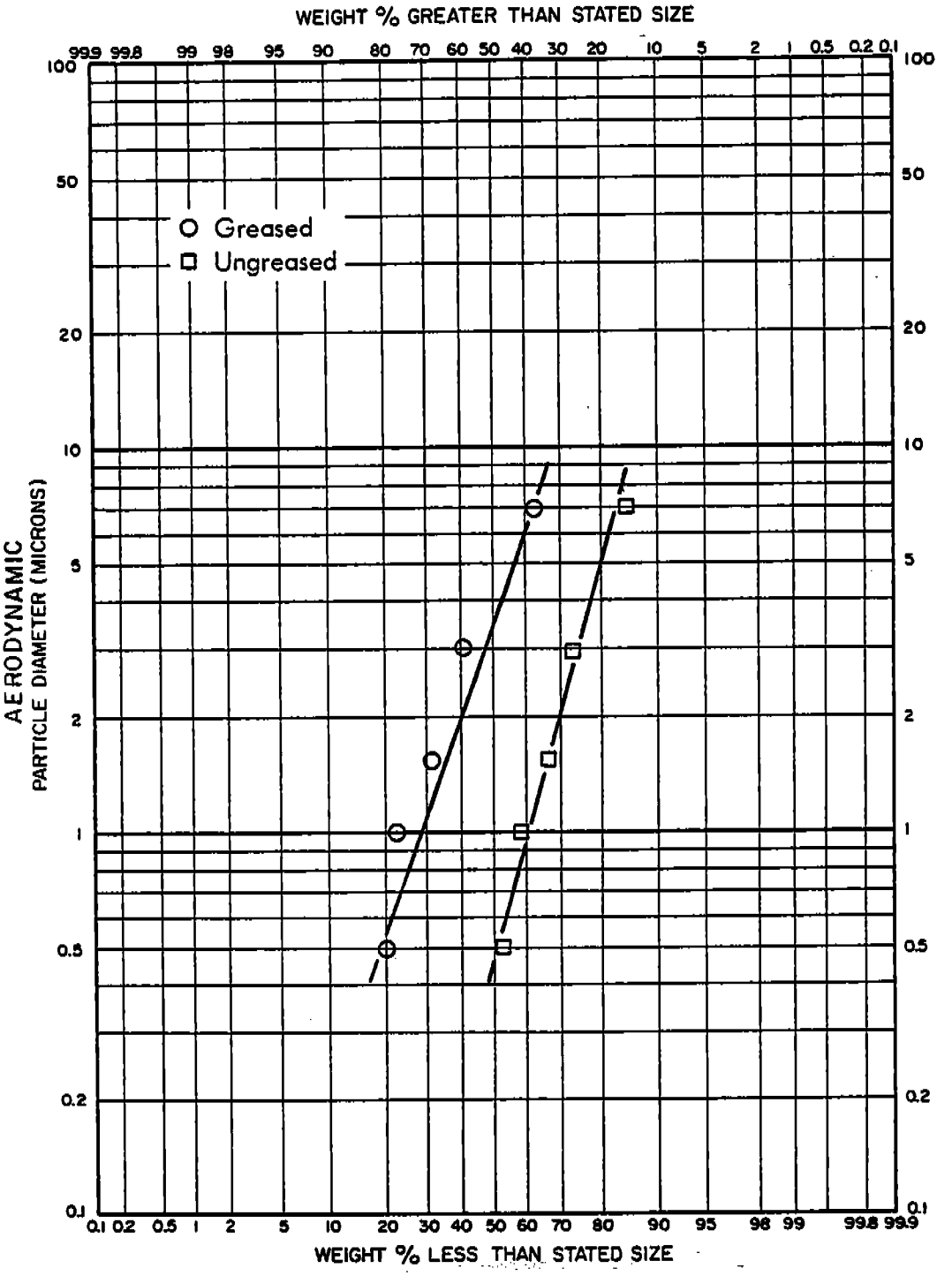

Figure C-3. Comparison of particle size distributions determined by collocated 40 cfm SSI/impactors with and without greased substrates operated 5 m downwind of a paved road.

of an uncontrolled unpaved road at Armco-Middletown, the high rate of emissions overloaded the substrates resulting in an even larger MMD value for particles observed on the backup filter. To obtain agreement between the calculated mass and the actual mass collected on the backup filter, an unusually small shape factor of 0.07 had to be assumed. In other words, for more typical shape factors, the observed particles accounted for more than the actual mass collected on the backup filter.

As detailed in the previous paragraphs, convincing evidence has been obtained to show that a very considerable portion of mass collected on the backup filter can be attributed to large particles which have been subject to particle bounce. The significant reduction in backup filter concentration resulting from use of a cyclone pre-collector and greased substrates clearly demonstrates the existence of particle bounce phenomena. This is further confirmed by microscopic analysis of representative backup filters.

Since 1976, a mathematical procedure has been used by MRI to correct the measured particle size distribution for the effects of residual particle bounce. Rather than to to completely ignore all the catch on the backup filter, which can distort the particle size distribution, the MRI correction procedure is based on the premise that the particle size is log-normally distributed. This procedure is as follows:

1. The calibrated cutoff diameter for the cyclone preseparator is used to fix the upper end of the particle-size distribution.

2. The lower end of the particle size distribution is fixed by the cutoff diameter of the last stage used and the measured (or corrected, if necessary) mass fraction collected on the backup filter. The corrected fraction collected on the backup filter is calculated as the average of the fractions measured on the two preceding stages. The lower of the measured and averaged fractions is used.

When a corrected mass on the backup filter is required, excess particulate mass is effectively removed from the backup filter. However, because no clear procedure exists for apportioning the excess mass back onto the impaction stages, the size distribution determined from tests with particle bounce problems is constructed using the log-normal assumption and two points--the mass fraction collected in the cyclone and the corrected mass faction collected on the backup filter.

Use of a log-normal distribution is predicated on the fact that the size of particles generated by a grinding process (such as tires rolling on an unpaved road surface) are customarily described by this distribution.[C-4] This type of particulate is predominant at 5 m downwind of a road. The only other source of particulate emissions from the road that could alter this log-normal distribution is that from vehicle exhaust, which has been shown to be a minor component.

In order to examine the effect of applying a bounce correction in the present study, Table C-2 compares mass fractions for certain particle size ranges of interest. Cyclone/impactors were operated at 20 cfm at heights of

TABLE C-2. EFFECTS OF CORRECTING FOR RESIDUAL PARTICLE BOUNCE ON UNPAVED ROAD TESTS

Plant code-Run No.	Surface	Height	% Mass removed from back-up	Mass fractions[a]	
				% < 10 μm	% < 2.5 μm
AG-3	Uncontrolled	1.5 m	28	24/27	9/14
		4.5 m	27	21/22	8/10
AG-7	Controlled by an asphalt emulsion	1.5 m	47	9/10	3/5
		4.5 m	60	9/10	4/7
AJ-14[b]	Controlled by a petroleum resin	1.5 m	10	11/11	4/4
		4.5 m	36	14/15	5/6

[a] First number represents value from corrected distribution; second from raw data.

[b] None of the uncontrolled tests at plant AJ required correction.

1.5 m and 4.5 m and at a distance of 5 m downwind of controlled and uncontrolled unpaved roads at J&L's Indiana Harbor Works (Plant AG) and Armco's Kansas City Works (Plant AJ).

Because 15 μmA is the point about which the curve is effectively rotated, those mass fractions are unaffected by the particle bounce correction. For the mass fractions less than 10 μmA, only a minimal change is found despite the effective removal of 1/4 to 1/2 the backup filter catch. The results for mass fractions less than 2.5 μmA show a greater change as would be expected because this is further from the "pivot" point.

In conclusion, there is compelling evidence that particle bounce occurs in cascade impactors when sampling fugitive dust downwind of roads. Although the magnitude of this effect is reduced substantially through the use of cyclone preseparators, residual particle bounce persists. Because of the bias this introduces, a correction should be applied. However, as noted earlier, ignoring the backup filter catch entirely can result in a serious underestimation of the mass fraction associated with the cut point of the preseparator. The correction scheme used by MRI attempts to avoid such complications while employing a physically acceptable particle distribution for interpolation purposes.

The greasing of substrates has been found to reduce the problem of particle bounce. However, once the substrate becomes loaded, greasing loses some of its effectiveness because the chance of a particle-particle collision increases.

Finally, as can be seen in this historical review, considerable development work has been carried out by MRI in characterizing the problems associated with particle bounce. The majority of this work has been initiated by MRI in an attempt to eliminate the fine particle bias (overestimation) resulting from particle bounce. Although the series of actions documented here have reduced bounce problems, there is a great deal of work still to be done in accurately determining the mass fraction of fine particulate in fugitive dust emissions.

REFERENCES

C-1. Willeke, K. Performance of the Slotted Impactor. American Industrial Hygiene Association Journal, 683-691, September 1975.

C-2. Dzubay, T. G., L. E. Hines and R. K. Stevens. Particle Bounce Errors in Cascade Impactors. Atomospheric Environment, 2, 229 (1976).

C-3. Lundgren, D. A., and H. J. Paulus. The Mass Distribution of Large Atmospheric Particles. Paper presented at the 66th Annual Meeting of the Air Pollution Control Association, Chicago, 1973.

C-4. Meyer, P. L. Introductory Probability and Statistical Applications. Addison-Wesley, Reading, Massachusetts, 1972.